Control of the motion of nonholonomic systems

by

Petrus Daniël Kemp

Submitted in partial fulfilment of the requirements for the degree

Master of Science (Applied Science)

in the

Faculty of Engineering

UNIVERSITY OF PRETORIA

September 2000

Abstract

This dissertation deals with the control, guidance and stabilisation of nonlinear, nonholonomic systems. It is shown that the kinematics of the system can be separated from the dynamics of the system by using successively two inverse dynamics type of transformations. This leads to a linear decoupled kinematical system, control strategies can then be developed that directly control the motion of the system. The method is applied to a system which is composed of a disk rolling on a plane, a controlled slender rod that is pivoted through its center of mass about the disk's center and two overhead rotors with their axes fixed in the upper part of the rod. Control strategies are designed under which the disk's inclination is stabilised about its vertical position and the disk's motion is able to asymptotically track any given smooth ground trajectory. The control strategy is shown to be stable in the presence parametric uncertainties. It was furthermore shown that the system is path controllable. Finally an extended inverse dynamics control law is introduced which deals directly with underactuated systems. An example of an articulated crane is solved using extended inverse dynamics control. Feasible control is used to ensure that the internal dynamics of the system remains bounded and that the crane reach its desired final position in a given time interval $[0, t_f]$.

Keywords: nonlinear systems, nonholonomic systems, rolling disk, inverse dynamics control, path controllability, stabilisation, feasible control.

Uittreksel

Hierdie proefskrif gee aandag aan die beheer, bestuur en stabilisering van nie-lineêre, nie-holonomiese stelsels. Dit word aangetoon dat die kinematika van die stelsel geskei kan work van die dinamika deur van twee opeenvolgende inverse dinamiese transformasies gebruik te maak. Hierdie metode lei tot 'n ontkoppelde lineêre kinematiese stelsel wat gebruik kan word in die ontwerp van beheerstelsels wat direk die beweging van die stelsel beheer. Die metode is toegepas op 'n stelsel wat bestaan uit 'n skyf wat rol op 'n plat vlak, 'n beheerde staaf wat verbind is deur sy massa middelpunt rondom die middel van die skyf en twee oorhoofse rotors met asse wat vas is aan die boonste deel van die staaf. Beheerstelsels is ontwerp wat die beweging van die skyf stabiliseer om sy vertikale posisie en die skyf instaatstel om enige nominaaltrajek te volg. Daar word aangetoon dat die beheerstelsel stabiel is tydens parametriese variasies. Daar word verder gewys dat die stelsel baanbeheerbaar is. Die konsep van inverse dinamiese beheer word uitgebrei om onder-geakstueerde stelsels in te sluit. 'n Voorbeeld van 'n hyskraan word opgelos en uitvoerbare beheer word toegepas om te verseker dat die interne dinamika van die stelsel gebonde bly terwyl die hyskraan sy finale posisie bereik in 'n gegewe tydsinterval $[0, t_f]$.

Sleutelwoorde: nie-lineêre stelsels, nie-holonomiese stelsels, rollende skyf, inverse dinamiese beheer, baan-beheerbaarheid, stabilisasie, uitvoerbare beheer.

Acknowledgements

- Prof. Yaakov Yavin for his help and guidance.
- Polina Burdukova for her love, patience and support.
- My parents for their continued love and support.

Contents

Chapter 1

Introduction

This work deals with the analysis and design of nonlinear and nonholonomic control systems. The first four sections of this chapter provide an overview of control systems in general and in particular it discusses the behaviour and importance of nonlinear and nonholonomic systems. The final two sections introduce the specific problems dealt with in this work and provide an overview of the organization of the dissertation.

1.1 Nonlinear systems

The control systems treated in this work are nonlinear multivariable systems with dynamics which can be represented in state space by a system of ordinary differential equations of the form

$$\frac{d\boldsymbol{x}}{dt} = \boldsymbol{f}(\boldsymbol{x}) + \sum_{i=1}^{m} \boldsymbol{g}_i(\boldsymbol{x}) u_i \,, \tag{1.1}$$

where $\boldsymbol{x} = (x_1 \,, \ldots \,, x_n)^T$ is the state vector of the system , $\boldsymbol{x} \in D$ where D is an open set in $\mathbb{R}^n$, $\boldsymbol{f}$ and $\boldsymbol{g}_i$, $i = 1 \,, \ldots \,, m$ are vector functions $D \to \mathbb{R}^n$. The system is assumed here to have m inputs $u_1 \,, \ldots \,, u_m$ which will be referred to as the control

vector $\boldsymbol{u} = (u_1 , \ldots , u_m)^T$.

The class of systems described by equation (1.1) is sufficiently large that most physical systems of practical interest are included. The class of linear systems are obviously also included and are obtained when $\boldsymbol{f}(\boldsymbol{x})$ is a linear function of $\boldsymbol{x}$ and $\boldsymbol{g}_1(\boldsymbol{x}) , \ldots , \boldsymbol{g}_m(\boldsymbol{x})$ are constant functions. Linear control theory is a mature field which has been proven successful in industrial applications with many methods available for the analysis and design of linear control systems, see for example [1] and [2].

Most systems encountered in practical engineering problems are nonlinear in nature. The application of linear control theory to nonlinear systems has been traditionally based on the following assumptions:

1. The system is linearisable.
2. The system will remain within a small operation range about the operating point around which the linearisation was performed.

However, if both these conditions do not hold then a high performance control system can only be obtained by applying nonlinear control techniques. Some of these techniques will be discussed in more detail in section 1.3 .

1.2 Nonholonomic systems

In practice a system described by equation (1.1) will be subject to various constraints placed on the system which depends on the particular problem under consideration. The discussion in this section is restricted to constraints on the dynamical model of the system, as opposed to constraints which arise from control objectives. The following notation will be used here and throughout the rest of the work. Denote by $\boldsymbol{q} = (q_1 , \ldots , q_n)^T$ the vector of generalized coordinates and let $\boldsymbol{p} = (\dot{q}_1 , \ldots , \dot{q}_n)^T$. In

the notation of the previous section the vectors $\boldsymbol{q}$ and $\boldsymbol{p}$ together form the state vector $\boldsymbol{x}$. The generalized coordinates are defined as the smallest number of coordinates needed to completely describe the position of all the constituents of the system, i.e. the generalized coordinates q_1 , ... , q_n are independent for an unconstrained system.

A constraint is called holonomic [3] if the constraint can be expressed by an equation of the form

$$f(q_1 , \ldots , q_n , t) = 0 . \tag{1.2}$$

If a constraint cannot be written in the form of equation (1.2) then the constraint is called nonholonomic. From the general form (1.2) of holonomic constraints it follows that each holonomic constraint imposed on the system can be used to eliminate one of the generalized coordinates, with the remaining coordinates still being independent.

The class of nonholonomic constraints dealt with in this work are kinematic constraints (differential constraints) [3, 4] of the following form

$$a_{j0}\, dt + \sum_{i=1}^{n} a_{ji}\, dq_i = 0 \quad , \quad j = 1, \ldots , r , \tag{1.3}$$

where

$$a_{ji} \equiv a_{ji}\,(\boldsymbol{q} , t) \quad , \quad i = 0, \ldots , n \quad , \quad j = 1, \ldots , r ,$$

where it is assumed that r kinematic constraints are present. If it is possible to integrate any of the nonholonomic constraints given by equation (1.3) a holonomic constraint will result, integrable kinematic constraints are therefore holonomic constraints. The set of r nonholonomic constraints imposed on the system is assumed here to be independent and non integrable.

Kinematical constraints commonly arise in finite dimensional mechanical systems such as a wheel rolling without slipping [5] , a sphere rolling without slipping [6] , wheeled

vehicles including a tractor with trailers [7]. See also [8] and the references cited therein for more examples of nonholonomic systems.

Kinematic constraints are in effect a condition placed upon the velocities of the system, and not on the coordinates. The number of generalized coordinates can therefore not be reduced in the presence of kinematic constraints. However, the set of constraints given by equation (1.3) introduces a dependence between the generalized coordinates. An arbitrary infinitesimal displacement is no longer possible in the presence of nonholonomic constraints, and as a result, an arbitrary path in state space is no longer possible since the path the system follows in state space must also satisfy the r kinematic constraints placed on the system. The difficulties these conditions introduce on the control of nonholonomic systems are discussed in section 1.4 .

1.3 Nonlinear control strategies

It is very difficult, often impossible, to deal with nonlinear systems directly due to the intuitively complex and varied behavior caused by the nonlinearities in the system. For these reasons it is desirable to simplify the form the system's model is described by. The desired form for the system model is usually linear since well established control strategies exist for the control of linear control systems.

A typical approach of linear control theory has been to linearise the dynamical model around a desired operating point making use of Jacobian linearisation to obtain an approximate linear model of the system. The approximate model can then be analyzed and controlled via linear control theory, [9] . As already stated in section 1.1 this approach has the disadvantage that the model, and therefore the controller, only perform properly in a small region around the operating point. One method of overcoming the problem of a small operating region has been to use gain scheduling, [10], in which the model is linearised around a number of operating points and linear controllers are

designed for each linearisation. Gain scheduling refers to the interpolation between the different controllers. This method, although intuitively simple, is difficult to verify theoretically and is computationally expensive to implement, [10] .

Modern nonlinear control theory has for the most part followed the approach of simplifying the system dynamics by using exact state transformations and feedback. The resultant form of the system model is therefore equivalent to the original system model and is not an approximation. Many different methods have been developed which transforms a nonlinear system into a linear system. In [11] necessary and sufficient conditions are given under which a coordinate transformation can be used to transform a nonlinear system into a linear system. A fundamental result which derives sufficient conditions under which a nonlinear system can be transformed to a linear system using a global transformation is given in [12]. The analysis and control of nonlinear systems is discussed in detail in [13] and [14]. Related work using an alternative approach has been given for example in [15] in which a nonlinear system is transformed to a linearised model around a set of operating points and in [16] an extension to gain scheduling is made using dynamic feedback.

The use of Lyapunov functions in the design of nonlinear control laws has recently experienced renewed interest. A number of algorithms and universal formulas are now available for the construction of control laws using Lyapunov functions. In [17] the computational complexity for Lyapunov stability analysis is examined for systems which are nonlinear in only a few variables.

The class of systems dealt with in the above mentioned methods is restrictive and excludes many problems encountered in practice. The above mentioned works make heavy use of differential geometric techniques. The computation of the Lie algebraic structure for nonlinear systems of high order is difficult and time consuming. Furthermore most of the theory deals only with the controllability of nonlinear systems and are difficult to use in the design of practical controllers. The theory is also not applicable to constrained control problems.

The approach of this work, as will discussed later in this chapter, is to use a kind of inverse dynamics control. Decoupling theory, see for example [13], also deals with similar problems and does not use differential geometric techniques. It could therefore also be applied to the problems dealt with in this work. Inverse dynamics control was chosen because it is naturally suitable to be directly applied to the form and structure of dynamical models which result from using the Lagrangian method. Decoupling theory (problem of noninteracting control) are not used in this work nor are its similarities with inverse dynamics control discussed.

1.4 Nonholonomic control strategies

Nonholonomic control systems have been researched extensively (see [8] and references therein) in resent years, largely due to the importance of nonholonomic systems in a variety of practical problems. Linear control theory and standard transformation methods do not apply well to nonholonomic systems and fundamentally nonlinear methods are necessary to solve nonholonomic problems.

The theoretical framework for dealing with nonholonomic control systems is dealt with for example in [18]. The algorithm presented in [18] for the calculation of control laws makes extensive use of differential geometric techniques which is used to rewrite the dynamics of the system. The nonholonomic constraints are subsequently used to obtain reduced-order state equations. The procedure is restricted to the class of nonholonomic systems for which $m \geq n-r$ where m is the number of control inputs, n is the number of generalized coordinates and r is the number of nonholonomic constraints.

Recently there has been interest in the control of chain form systems and power form systems. See for example [19] which deals with the calculation of both open loop and closed loop control laws for chain form systems. In [20] an exponentially convergent control law is designed for power form systems. Both papers makes use of differen-

tial geometric techniques to obtain the desired form and subsequently makes use of Lyapunov control design to obtain the desired control strategy. There are however computational difficulties in transforming a system to chain or power form.

Mobile car-like robots have been studied extensively largely due to the practical applicability of such systems. Reeds and Shepp showed in [21] that the shortest unobstucted path between two points for a car that goes both forwards and backwards consists of line segments and arcs of circles with the minimal turning radius of the car. This type of optimal path has been used by other authors, in [22] an algorithm is given to calculate a near optimal path when obstructions are present. First, a collision free path ignoring the nonholonomic constraints are calculated, the path is then divided into discrete points which is connected by paths of the Reeds and Shepp type. An exponential tracking control law for a car-like robot is developed in [23] which also assumes that the desired path is a Reeds and Shepp type path. Car-like mobile robots are however a highly restricted and low dimensional example of nonholonomic systems and the methods mentioned here cannot be applied in their current form to nonholonomic systems in general.

In order to obtain a general theory of nonholonomic control systems attempts have been made to redefine the fundamental dynamics of nonholonomic systems in terms of topologies instead of treating them as Lagrangian systems, see for example [24]. Although the resulting structure appears to be more natural in this form the computational difficulties imposed does not make it suited for solving realistic problems.

1.5 Nonholonomic control problems

This work deals with the control of nonholonomic systems. The theory and methods used are presented by means of two examples, namely a disk with two overhead rotors, and an articulated crane. The methods used to solve these control problems are appli-

cable to a large variety of control problems dealing with systems which are subject to kinematical constraints.

The main part of this work deals with the control of a disk with two overhead rotors. The system is composed of a disk rolling on a horizontal plane, a controlled slender rod pivoted through its center of mass about the center of the disk and two overhead rotors attached to the rod with their axis fixed in the upper part of the rod (see figures 1.1 and 1.2). The rod is controlled in such a manner that it is always aligned along the line OC where O is the center of the disk and C is the point of contact between the disk and the surface. The rotors are attached in such a manner that they are rotating in mutually perpendicular planes, perpendicular to the plane of the disk, the upper rotor rotates in the plane spanned by the axis of the disk and the rod, whereas the lower rotor rotates in a plane that is perpendicular to the rod (see figures 1.1 and 1.2).

The control and guidance of a disk rolling on a horizontal plane, controlled by a tilting moment, a directional moment and a pedalling moment is dealt with in [5] and [25]. In [26] a single rotor is mounted on the upper end of a rod pivoted through its center of mass about a disk's center, and in [27] a rotor is placed on the axis of the disk. In both cases it was shown that the applied torque to the rotor induces a "side inclination" moment or a "tilting moment" on the motion of the disk. In [28] a similar configuration as in [26] is used but the rotor is mounted perpendicular the setup used there, and subsequently it was shown in [28] that the rotor induces a "directional moment" on the motion of the disk.

It is assumed in this work that the disk is rolling without slipping on the horizontal (X, Y) - plane. This condition leads to the presence of nonholonomic constraints, [4], on the motion of the disk. It will be shown in the chapter 2 that the system has 7 independent coordinates, 2 nonholonomic constraints, and 3 control inputs. Most of the methods discussed in section 1.4 can therefore not be applied.

A kind of inverse dynamics control was chosen as the basis for the control system design

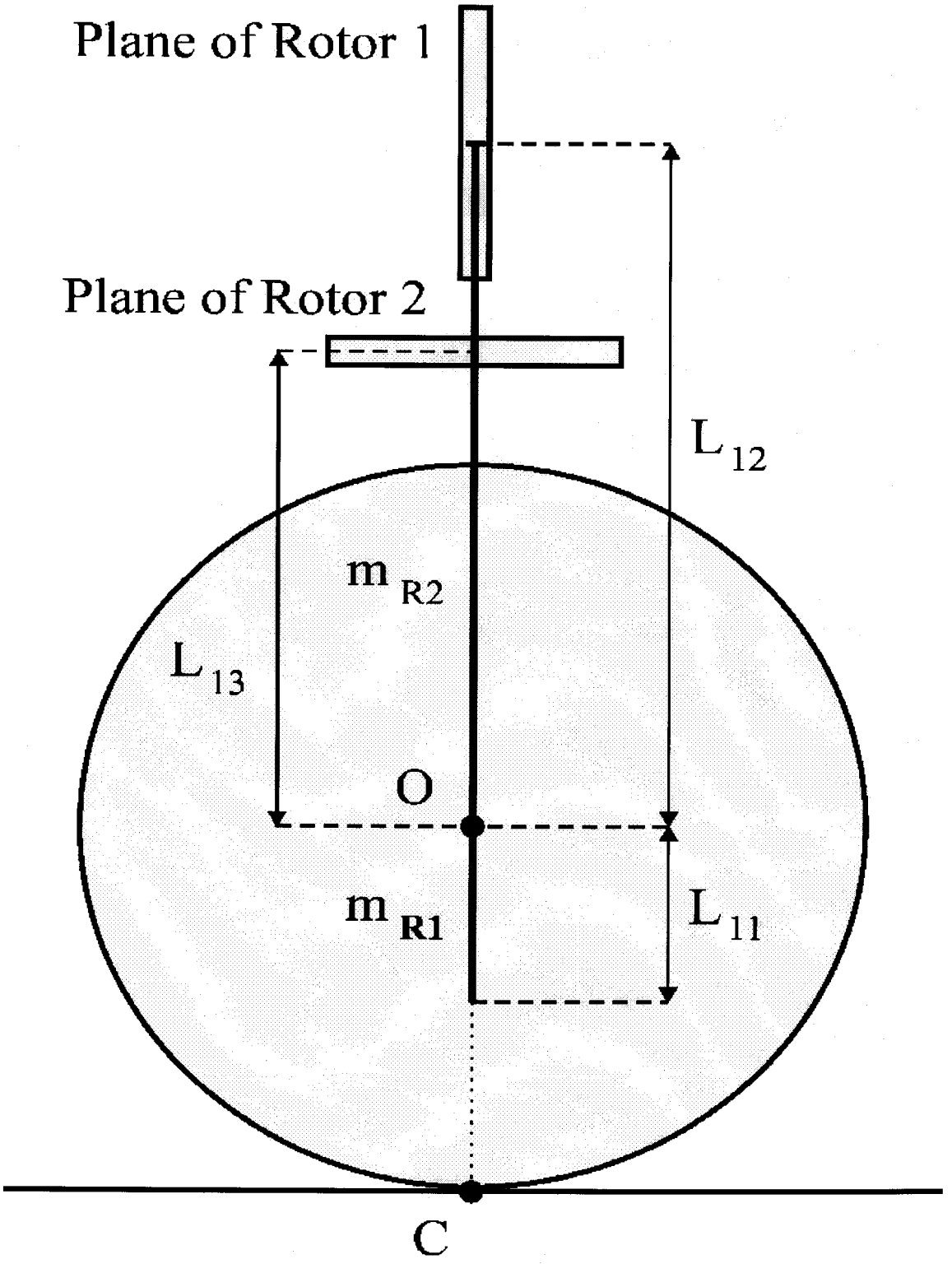

Figure 1.1: Side view of the system

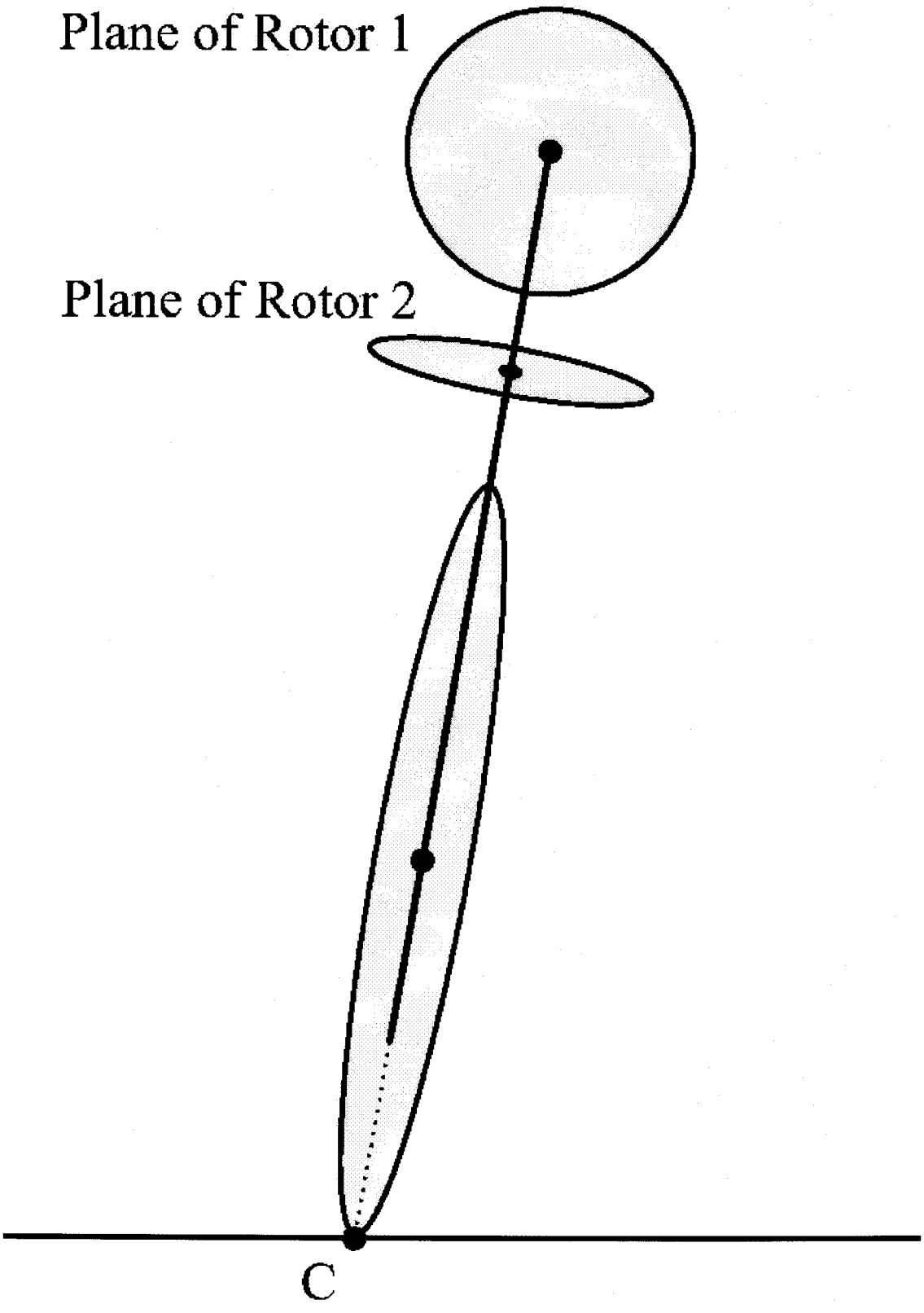

Figure 1.2: Front view of the system

for the above mentioned system. Inverse dynamics control is capable of dealing with the nonlinear and nonholonomic nature of the system and leads directly to a control strategy. It also surcumvents dealing with the Lie algebraic structure of the system. Different control strategies for the disk-rod-rotors system is designed in this work using inverse dynamics control as basis.

The disk with two overhead rotors was solved by using a kind of inverse dynamics control. An extension to the basic theory of inverse dynamics control is introduced which deals directly with underactuated systems. Feasible control is introduced as a means of solving constrained nonholonomic control problems. An example involving an articulated two dimensional crane is described and solved in chapter 6 using extended inverse dynamics control together with feasible control.

1.6 Organization

Chapter 2: The dynamical model of the disk-rod-rotors system is derived using the Lagrangian method. The equations of motion and the nonholonomic constraints of the system are given.

Chapter 3: A kind of inverse dynamics control is used to design a feedback control law for the disk-rod-rotors system such that the disk will be able to asymptotically track any given smooth ground trajectory.

Chapter 4: Deals with a stabilisation and guidance problem of the disk-rod-rotors system. It is shown using a kind of inverse dynamics control that the system is path controllable.

Chapter 5: The robustness of the feedback controller designed in chapter 3 is examined under parameter variations.

Chapter 6: The theory of inverse dynamics control is extended to include a larger class of problems. Extended inverse dynamics control is subsequently used to

solve a constrained control problem dealing with an articulated crane.

Chapter 7: Conclusion

Chapter 2

Dynamical Model

2.1 Introduction

A dynamical model is derived in this chapter for the system given by figures 1.1 and 1.2 with applied torques acting on the rotors and a pedalling torque acting directly on the disk. The effects of motor dynamics on the system is ignored here (see for example [29] for the effects of motor dynamics on the dynamical model) and it is assumed that the torques are controlled directly. It is also shown that the torque applied to the upper rotor (rotor 1) induces a "tilting moment" on the motion of the disk, whereas the torque applied to the lower rotor (rotor 2) induces a "directional moment" on the motion of the disk. The stabilisation, control and guidance of this system is dealt with in the following chapters.

Note that in this work it is assumed that the disk is rolling without slipping on the horizontal (X, Y) - plane. This condition leads to the presence of nonholonomic contraints, [4], on the motion of the disk.

Nomenclature

$(\mathbf{I}, \mathbf{J}, \mathbf{K})$ = unit vectors along the inertial (X, Y, Z) - coordinate system

(x, y, z) = coordinates of the center of mass of both the disk and the rod

θ = leaning angle of disk

ϕ = direction of disk

ψ_1 = angle of rotation of the disk about its axis

ψ_2 = angle of rotation of the rod about the center of the disk

α_1 = angle of rotation of rotor 1 about its own axis

α_2 = angle of rotation of rotor 2 about its own axis

$\mathbf{k}$ = unit vector along the axis of the disk

$\mathbf{i}_1, \mathbf{j}_1$ = unit vectors in the plane of the disk

$(\mathbf{i}_1, \mathbf{j}_1, \mathbf{k})$ = body fixed coordinate system used to describe the disk

$\mathbf{k}_{o1}$ = unit vector along rotor 1

$\mathbf{j}_{o1}$ = unit vector in plane of rotation of rotor 1 perpendicular to $\mathbf{k}_{o1}$

$\mathbf{r}_1$ = center of mass of rotor 1

I_{Dj} = moment of inertia of the disk about the $(\mathbf{i}_1, \mathbf{j}_1, \mathbf{k})$ axes respectively $(j = 1, 2, 3)$

$I_{Oj}^{(1)}$ = moment of inertia of rotor 1 about the $(\mathbf{j}_{o1}, -\mathbf{i}_\phi, \mathbf{k}_{o1})$ axes respectively $(j = 1, 2, 3)$

m_D = mass of the disk

m_R = mass of the rod

m_{O1} = mass of rotor 1

m_{O2} = mass of rotor 2

L_{12} = distance between the center of mass of the disk and the center of mass of rotor 1

L_{13} = distance between the center of mass of the disk and the center of mass of rotor 2

L_{11} = length of rod below its center of mass

L_{Oi} = length of rotor i, $(i = 1, 2)$

a = radius of the disk

$\mathbf{i}_\theta$ = unit vector in the plane of the disk

$\mathbf{i}_\phi$ = unit vector in the plane of the disk perpendicular to $\mathbf{i}_\theta$ and $\mathbf{k}$

$\mathbf{i}_2, \mathbf{j}_2$ = unit vectors in the plane of the disk

$(\mathbf{i}_2, \mathbf{j}_2, \mathbf{k})$ = body fixed coordinate system used to describe the rod

$\mathbf{k}_{o2}$ = unit vector along rotor 2

$\mathbf{j}_{o2}$ = unit vector in plane of rotation of rotor 2 perpendicular to $\mathbf{k}_{o2}$

$\mathbf{r}_2$ = center of mass of rotor 2

I_{Rj} = moment of inertia of the rod about the $(\mathbf{i}_2, \mathbf{j}_2, \mathbf{k})$ axes respectively $(j = 1, 2, 3)$

$I_{Oj}^{(2)}$ = moment of inertia of rotor 2 about the $(-\mathbf{i}_\theta, \mathbf{k}_{o2}, \mathbf{j}_{o2})$ axes respectively $(j = 1, 2, 3)$

2.2 Body coordinate system

Denote by $\boldsymbol{k}$

$$\boldsymbol{k} = \sin\theta\cos\phi\,\boldsymbol{I} + \sin\theta\sin\phi\,\boldsymbol{J} + \cos\theta\,\boldsymbol{K}\ , \tag{2.1}$$

a unit vector along the axis of the disk. Furthermore, the vector $\boldsymbol{k}$ describes here the orientation of the disk's axis, and by this the vector $\boldsymbol{k}$ defines the orientation of the disk in the $(X\ ,\ Y\ ,\ Z)$ - space. The unit vectors $\boldsymbol{i}_\theta$ and $\boldsymbol{i}_\phi$, given by $\boldsymbol{i}_\theta = \partial\boldsymbol{k}/\partial\theta$ and $\boldsymbol{i}_\phi = (1/\sin\theta)\,\partial\boldsymbol{k}/\partial\phi$, are always in plane of the disk, that is, $\boldsymbol{i}_\theta$, $\boldsymbol{i}_\phi$ and $\boldsymbol{k}$ are orthonormal and as a result constitute a basis in $\mathbb{R}^3$. Note that this basis is chosen with the attached rod along the vector $-\,\boldsymbol{i}_\theta$, which according to the configuration described in the previous chapter implies that the axis of rotor 1 is aligned along $-\,\boldsymbol{i}_\phi$ whereas the axis of rotor 2 is aligned along $-\,\boldsymbol{i}_\theta$. Thus $(\boldsymbol{k}\ ,\ \boldsymbol{i}_\theta\ ,\ \boldsymbol{i}_\phi)$ is the body fixed coordinate system which will be used here for describing the disk.

Define the the following vectors $\boldsymbol{i}_\nu$ and $\boldsymbol{j}_\nu$, $\nu = 1, 2$

$$\boldsymbol{i}_\nu = \cos\psi_\nu\,\boldsymbol{i}_\theta + \sin\psi_\nu\,\boldsymbol{i}_\phi\ , \quad \nu = 1\ ,\ 2\ , \tag{2.2}$$

$$\boldsymbol{j}_\nu = -\sin\psi_\nu\,\boldsymbol{i}_\theta + \cos\psi_\nu\,\boldsymbol{i}_\phi\ , \quad \nu = 1\ ,\ 2\ , \tag{2.3}$$

which are always in the plane of the disk. Also, let

$$\boldsymbol{k}_{o1} = \cos\alpha_1(-\boldsymbol{i}_\theta) + \sin\alpha_1\boldsymbol{k}\ , \tag{2.4}$$

be a unit vector along rotor 1 (the upper rotor), and let

$$\boldsymbol{j}_{o1} = \sin\alpha_1(-\boldsymbol{i}_\theta) - \cos\alpha_1\boldsymbol{k}\ , \tag{2.5}$$

be a unit vector perpendicular to $\boldsymbol{k}_{o1}$, both of them in the $(-\boldsymbol{i}_\theta\ ,\ \boldsymbol{k})$ - plane. Thus, it is assumed that rotor 1 rotates in the $(-\boldsymbol{i}_\theta\ ,\ \boldsymbol{k})$ - plane, with its axis always aligned along

the $-\boldsymbol{i}_\phi$ direction, with the center of mass of rotor 1 fixed at a point denoted here by the vector $\boldsymbol{r}_1$,

$$\boldsymbol{r}_1 = x\,\boldsymbol{I} + y\,\boldsymbol{J} + z\,\boldsymbol{K} - L_{12}\,\boldsymbol{i}_\theta \,, \tag{2.6}$$

In the same manner as above, denote by

$$\boldsymbol{k}_{o2} = \cos\alpha_2\,\boldsymbol{i}_\phi + \sin\alpha_2\,\boldsymbol{k} \,, \tag{2.7}$$

a unit vector along rotor 2 (the lower rotor), and let

$$\boldsymbol{j}_{o2} = -\sin\alpha_2\,\boldsymbol{i}_\phi + \cos\alpha_2\,\boldsymbol{k} \,, \tag{2.8}$$

be a unit vector perpendicular to $\boldsymbol{k}_{o2}$, both of them in the $(\boldsymbol{i}_\phi\,,\,\boldsymbol{k})$ - plane. Thus, it is assumed that rotor 2 rotates in the $(\boldsymbol{i}_\phi\,,\,\boldsymbol{k})$ - plane, with its axis always aligned along the $-\boldsymbol{i}_\theta$ direction, with the center of mass of rotor 2 fixed at a point denoted here by the vector $\boldsymbol{r}_2$,

$$\boldsymbol{r}_2 = x\,\boldsymbol{I} + y\,\boldsymbol{J} + z\,\boldsymbol{K} - L_{13}\,\boldsymbol{i}_\theta \,, \tag{2.9}$$

Thus, θ , ϕ , ψ_1 , ψ_2 , α_1 and α_2 have the following roles here: θ is the leaning angle of the disk, that is, the angle between the axis of the disk and the Z - axis where for $\theta = \pi/2$ the plane of the disk is perpendicular to the $(X\,,\,Y)$ - plane; $-\,\boldsymbol{i}_\phi$ is a vector in the $(X\,,\,Y)$ - plane which represents the direction of the disk, $\phi = 0$ indicates that the motion of the disk is in the direction of $-\boldsymbol{J}$ and $\phi = \pi/2$ indicates a motion in the direction of $\boldsymbol{I}$. In this work it is assumed that the rod is controlled in such a manner that it is always aligned along $-\,\boldsymbol{i}_\theta$, that is, $\psi_2(t) = \pi/2$ and $d\,\psi_2(t)/dt = 0$, for all $t \geq 0$. This control problem is dealt with in [30].

2.3 Angular velocities

The problem considered here has four angular velocity vectors involved in the motion of the system which are given by:

$$\boldsymbol{\omega}_D = \omega_{D1}\,\boldsymbol{i}_1 + \omega_{D2}\,\boldsymbol{j}_1 + \omega_{D3}\,\boldsymbol{k} = \omega_{Dx}\,\boldsymbol{I} + \omega_{Dy}\,\boldsymbol{J} + \omega_{Dz}\,\boldsymbol{K}\ , \tag{2.10}$$

which is the angular velocity of the disk,

$$\boldsymbol{\omega}_R = \omega_{R1}\,\boldsymbol{i}_2 + \omega_{R2}\,\boldsymbol{j}_2 + \omega_{R3}\,\boldsymbol{k} = \omega_{Rx}\,\boldsymbol{I} + \omega_{Ry}\,\boldsymbol{J} + \omega_{Rz}\,\boldsymbol{K}\ , \tag{2.11}$$

which is the angular velocity of the rod,

$$\boldsymbol{\omega}_o^{(1)} = \omega_{o1}^{(1)}\,\boldsymbol{j}_{o1} + \omega_{o2}^{(1)}\,(-\boldsymbol{i}_\phi) + \omega_{o3}^{(1)}\,\boldsymbol{k}_{o1}\ , \tag{2.12}$$

which is the angular velocity of rotor 1, and

$$\boldsymbol{\omega}_o^{(2)} = \omega_{o1}^{(2)}\,(-\boldsymbol{i}_\theta) + \omega_{o2}^{(2)}\,\boldsymbol{k}_{o2} + \omega_{o3}^{(2)}\,\boldsymbol{j}_{o2}\ , \tag{2.13}$$

which is the angular velocity of rotor 2.

The vectors $\boldsymbol{\omega}_D$ and $\boldsymbol{\omega}_R$ can be calculated, in the body fixed coordinate system, using the following procedure . Denote by ω_{aj} , $j = 1, 2, 3$ the components of $\boldsymbol{\omega}_D$ and $\boldsymbol{\omega}_R$ in the $(\boldsymbol{i}_\nu\ ,\ \boldsymbol{j}_\nu\ ,\ \boldsymbol{k})$ - coordinate system, where $a = D$ implies $\nu = 1$ and $a = R$ implies $\nu = 2$ and also $\psi_2(t) = \pi/2$ and $d\,\psi_2(t)/dt = 0$ for all $t \geq 0$. This notation will be used throughout the rest of the section.

Firstly, the rate of change of a given vector in a rotating coordinate system, see for example [4] and [3], is given by the cross-product of the angular velocity of the base vectors of the coordinate system with the given vector, i.e.

$$\begin{aligned}\frac{d\boldsymbol{i}_\nu}{dt} &= \boldsymbol{\omega}_a \times \boldsymbol{i}_\nu \\ &= \begin{vmatrix} \boldsymbol{i}_\nu & \boldsymbol{j}_\nu & \boldsymbol{k} \\ \omega_{a1} & \omega_{a2} & \omega_{a3} \\ 1 & 0 & 0 \end{vmatrix} \\ &= \omega_{a3}\,\boldsymbol{j}_\nu - \omega_{a2}\,\boldsymbol{k}\,,\end{aligned} \tag{2.14}$$

and similarly

$$\frac{d\boldsymbol{j}_\nu}{dt} = -\,\omega_{a3}\,\boldsymbol{i}_\nu + \omega_{a1}\,\boldsymbol{k}\,. \tag{2.15}$$

Secondly, from equation (2.1) and the definition of $\boldsymbol{i}_\theta$ and $\boldsymbol{i}_\phi$ it follows that

$$\boldsymbol{i}_\theta = \cos\theta\cos\phi\,\boldsymbol{I} + \cos\theta\sin\phi\,\boldsymbol{J} - \sin\theta\,\boldsymbol{K}\,, \tag{2.16}$$

$$\boldsymbol{i}_\phi = -\sin\phi\,\boldsymbol{I} + \cos\phi\,\boldsymbol{J}\,. \tag{2.17}$$

By taking the derivatives of $\boldsymbol{i}_\theta$ and $\boldsymbol{i}_\phi$ with respect to time we obtain

$$\begin{aligned}\frac{d\boldsymbol{i}_\theta}{dt} &= \frac{\partial \boldsymbol{i}_\theta}{\partial\theta}\frac{d\theta}{dt} + \frac{\partial \boldsymbol{i}_\theta}{\partial\phi}\frac{d\phi}{dt} \\ &= -\frac{d\theta}{dt}\,\boldsymbol{k} + \frac{d\phi}{dt}\cos\theta\,\boldsymbol{i}_\phi\,,\end{aligned} \tag{2.18}$$

$$\frac{d\boldsymbol{i}_\phi}{dt} = -\frac{d\phi}{dt}\sin\theta\,\boldsymbol{k} - \frac{d\phi}{dt}\cos\theta\,\boldsymbol{i}_\theta\,. \tag{2.19}$$

The time derivatives of equations (2.2) and (2.3) can be calculated directly. Substituting equations (2.18) and (2.19) yields

$$\begin{aligned}\frac{d\boldsymbol{i}_\nu}{dt} &= \left(\frac{d\psi_\nu}{dt} + \frac{d\phi}{dt}\cos\theta\right)\boldsymbol{j}_\nu \\ &\quad - \left(\frac{d\theta}{dt}\cos\psi_\nu + \frac{d\phi}{dt}\sin\theta\sin\psi_\nu\right)\boldsymbol{k}\,,\end{aligned} \tag{2.20}$$

$$\begin{aligned}\frac{d\boldsymbol{j}_\nu}{dt} &= -\left(\frac{d\psi_\nu}{dt} + \frac{d\phi}{dt}\cos\theta\right)\boldsymbol{i}_\nu \\ &\quad + \left(\frac{d\theta}{dt}\sin\psi_\nu - \frac{d\phi}{dt}\sin\theta\cos\psi_\nu\right)\boldsymbol{k}\ .\end{aligned} \tag{2.21}$$

Finally, the components of the angular velocity vectors in the body fixed coordinate system are found by comparing (2.20) with (2.14) and (2.21) with (2.15) and observing that the vectors $\boldsymbol{i}_\nu$, $\boldsymbol{j}_\nu$ and $\boldsymbol{k}$ are orthonormal ($\nu = 1\ ,\ 2$) . The components are given by

$$\omega_{a1} = \frac{d\theta}{dt}\sin\psi_\nu - \frac{d\phi}{dt}\sin\theta\cos\psi_\nu\ , \tag{2.22}$$

$$\omega_{a2} = \frac{d\theta}{dt}\cos\psi_\nu + \frac{d\phi}{dt}\sin\theta\sin\psi_\nu\ , \tag{2.23}$$

$$\omega_{a3} = \frac{d\psi_\nu}{dt} + \frac{d\phi}{dt}\cos\theta\ . \tag{2.24}$$

In order to obtain the representations (ω_{Dx} , ω_{Dy} , ω_{Dz}) and (ω_{Rx} , ω_{Ry} , ω_{Rz}) of the vectors $\boldsymbol{\omega}_D$ and $\boldsymbol{\omega}_R$ in the orthonormal inertial basis ($\boldsymbol{I}$, $\boldsymbol{J}$, $\boldsymbol{K}$) , the transformation between the ($\boldsymbol{i}_\nu$, $\boldsymbol{j}_\nu$, $\boldsymbol{k}$) basis and the ($\boldsymbol{I}$, $\boldsymbol{J}$, $\boldsymbol{K}$) basis is used. Since the ($\boldsymbol{i}_\nu$, $\boldsymbol{j}_\nu$, $\boldsymbol{k}$) basis and the ($\boldsymbol{I}$, $\boldsymbol{J}$, $\boldsymbol{K}$) basis are both orthonormal the transformation can simply be given as a rotation.

From (2.1) , (2.2) and (2.3) it follows directly (see for example [5]) that

$$\begin{pmatrix}\boldsymbol{i}_\nu \\ \boldsymbol{j}_\nu \\ \boldsymbol{k}\end{pmatrix} = \boldsymbol{E}_\nu\,(\theta\ ,\ \phi\ ,\ \psi_\nu)\begin{pmatrix}\boldsymbol{I} \\ \boldsymbol{J} \\ \boldsymbol{K}\end{pmatrix}\ , \tag{2.25}$$

where

$$\boldsymbol{E}_\nu = \begin{pmatrix} \cos\theta\cos\phi\cos\psi_\nu & \cos\theta\sin\phi\cos\psi_\nu & -\sin\theta\cos\psi_\nu \\ -\sin\phi\sin\psi_\nu & +\cos\phi\sin\psi_\nu & \\ -\cos\theta\cos\phi\sin\psi_\nu & -\cos\theta\sin\phi\sin\psi_\nu & \sin\theta\sin\psi_\nu \\ -\sin\phi\cos\psi_\nu & +\cos\phi\cos\psi_\nu & \\ \sin\theta\cos\phi & \sin\theta\sin\phi & \cos\theta \end{pmatrix} . \tag{2.26}$$

$\boldsymbol{E}_\nu = \boldsymbol{E}_\nu(\theta\,,\,\phi\,,\,\psi_\nu)$ is the matrix representation of the Euler angle transformation, [4, 31]. Above and in the remainder of the derivation, ν can take on the values 1 and 2, where $\boldsymbol{E}_1(\theta\,,\,\phi\,,\,\psi_1)$ denotes the transformation between $(\boldsymbol{i}_1\,,\,\boldsymbol{j}_1\,,\,\boldsymbol{k})$ basis and the $(\boldsymbol{I}\,,\,\boldsymbol{J}\,,\,\boldsymbol{K})$ basis and $\boldsymbol{E}_2(\theta\,,\,\phi\,,\,\psi_2)$ denotes the transformation between $(\boldsymbol{i}_2\,,\,\boldsymbol{j}_2\,,\,\boldsymbol{k})$ basis and the $(\boldsymbol{I}\,,\,\boldsymbol{J}\,,\,\boldsymbol{K})$ basis.

The Euler matrix $\boldsymbol{E}_\nu$ can be used to transform any given vector in $\mathbb{R}^3$ from its representation $\boldsymbol{r}$ in the $(\boldsymbol{I}\,,\,\boldsymbol{J}\,,\,\boldsymbol{K})$ basis to its representation $\boldsymbol{r}'$ in the $(\boldsymbol{i}_\nu\,,\,\boldsymbol{j}_\nu\,,\,\boldsymbol{k})$ basis. This can be written as

$$\boldsymbol{r}' = \boldsymbol{E}_\nu\boldsymbol{r}\,. \tag{2.27}$$

It should be noted that the view taken here is that of a coordinate transformation in $\mathbb{R}^3$ between two orthonormal coordinate systems. Thus, $\boldsymbol{r}$ and $\boldsymbol{r}'$ are different representations in different coordinate systems of the same vector in $\mathbb{R}^3$. The Euler matrix can however, given a coordinate system in $\mathbb{R}^3$, transform one vector into a different vector via a rotation defined by the Euler angles. In such a case only one coordinate system is used but the vectors are no longer the same - this type of transformation is not used in this work.

Furthermore the matrix $\boldsymbol{E}_\nu$ is orthogonal $(\boldsymbol{E}_\nu^T = \boldsymbol{E}_\nu^{-1})$, [31] , which implies that the inverse of equation (2.27) is given by

$$\boldsymbol{r} = \boldsymbol{E}_\nu^T\boldsymbol{r}'\,, \tag{2.28}$$

and in the case of the angular velocities of the disk and the rod it reduces to

$$\begin{pmatrix} \omega_{Ax} \\ \omega_{Ay} \\ \omega_{Az} \end{pmatrix} = \boldsymbol{E}_{\nu}^{T} \begin{pmatrix} \omega_{A1} \\ \omega_{A2} \\ \omega_{A3} \end{pmatrix} . \tag{2.29}$$

Finally the individual components are given by

$$\omega_{Ax} = \frac{d\psi_{\nu}}{dt} \sin\theta \cos\phi - \frac{d\theta}{dt} \sin\phi \, , \tag{2.30}$$

$$\omega_{Ay} = \frac{d\psi_{\nu}}{dt} \sin\theta \sin\phi + \frac{d\theta}{dt} \cos\phi \, , \tag{2.31}$$

$$\omega_{Az} = \frac{d\phi}{dt} + \frac{d\psi_{\nu}}{dt} \cos\theta \, , \tag{2.32}$$

where, as above, $A = D$ implies $\nu = 1$ and $A = R$ implies $\nu = 2$ and also $\psi_2(t) = \pi/2$ and $d\psi_2(t)/dt = 0$ for all $t \geq 0$.

The angular velocities of the rotors can be calculated as the sum between the rotor's rotation around its own axis and the angular velocity of the rod, $\boldsymbol{\omega}_R$. The components used to describe the angular velocity of rotor 1 are given by $(\omega_{o1}^{(1)} \, , \, \omega_{o2}^{(1)} \, , \, \omega_{o3}^{(1)})$ in the $(\boldsymbol{j}_{o1} \, , \, -\boldsymbol{i}_{\phi} \, , \, \boldsymbol{k}_{o1})$ coordinate system, and the components used to describe the angular velocity of rotor 2 are given by $(\omega_{o1}^{(2)} \, , \, \omega_{o2}^{(2)} \, , \, \omega_{o3}^{(2)})$ in the $(-\boldsymbol{i}_{\theta} \, , \, \boldsymbol{k}_{o2} \, , \, \boldsymbol{j}_{o2})$ coordinate system. Using equations (2.22) to (2.24) together with equations (2.2) and (2.3) , $\boldsymbol{\omega}_R$ can be written as:

$$\boldsymbol{\omega}_R = \frac{d\theta}{dt} \boldsymbol{i}_{\phi} + \frac{d\phi}{dt} \sin\theta(-\boldsymbol{i}_{\theta}) + \frac{d\phi}{dt} \cos\theta \, \boldsymbol{k} \, . \tag{2.33}$$

The components of $\boldsymbol{\omega}_R$ in the basis $(\boldsymbol{j}_{o1} \, , \, -\boldsymbol{i}_{\phi} \, , \, \boldsymbol{k}_{o1})$ fixed to rotor 1, can be calculated using the innerproduct, for example

$$\begin{aligned} \omega_{o1}^{(1)} &= \boldsymbol{\omega}_R \cdot \boldsymbol{j}_{o1} \\ &= \frac{d\phi}{dt} \sin\theta(-\sin\alpha_1) + \frac{d\phi}{dt} \cos\theta \cos\alpha_1 \\ &= -\frac{d\phi}{dt} \cos(\theta + \alpha_1) \, . \end{aligned} \tag{2.34}$$

The other components can be calculated similarly. Note that the rotation of the rotors around their own axis is given for rotor 1 by $(d\alpha_1/dt)\ \boldsymbol{i}_\phi$, and for rotor 2 by $(d\alpha_2/dt)\ (-\boldsymbol{i}_\theta)$. All the components of the angular velocity vectors of the rotors can be calculated using the above mentioned procedure, this yields

$$\omega_{o1}^{(1)} = -\frac{d\phi}{dt}\cos(\theta + \alpha_1)\ , \tag{2.35}$$

$$\omega_{o2}^{(1)} = -\left(\frac{d\alpha_1}{dt} + \frac{d\theta}{dt}\right)\ , \tag{2.36}$$

$$\omega_{o3}^{(1)} = \frac{d\phi}{dt}\sin(\theta + \alpha_1)\ , \tag{2.37}$$

for rotor 1, and

$$\omega_{o1}^{(2)} = \frac{d\alpha_2}{dt} - \frac{d\phi}{dt}\sin\theta\ , \tag{2.38}$$

$$\omega_{o2}^{(2)} = -\left(\frac{d\theta}{dt}\cos\alpha_2 + \frac{d\phi}{dt}\sin\alpha_2\cos\theta\right)\ , \tag{2.39}$$

$$\omega_{o3}^{(2)} = \frac{d\theta}{dt}\sin\alpha_2 - \frac{d\phi}{dt}\cos\alpha_2\cos\theta\ , \tag{2.40}$$

for rotor 2.

The moments of inertia of the system are obtained by making use of the "thin wheel" and "slender rod" approximations: $I_{D1} = I_{D2} = 0.25 m_D a^2$, $I_{D3} = 0.5 m_D a^2$; $I_{R1} = I_{R3} = (m_{R1}L_{11}^2 + m_{R2}L_{12}^2)/3$, $I_{R2} = 0$; $I_{o1}^{(1)} = I_{o2}^{(1)} = m_{o1}L_{o1}^2/12$, $I_{o3}^{(1)} = 0$; $I_{o1}^{(2)} = I_{o3}^{(2)} = m_{o2}L_{o2}^2/12$, $I_{o2}^{(2)} = 0$.

2.4 The Lagrangian

In the sequel the Lagrangian method [4] , is used in order to obtain the equations of motion of the disk-rod-rotors system. The Lagrangian function can be expressed as

$$\mathfrak{L} = K_D + K_R + K_{o1} + K_{o2} - V \,, \tag{2.41}$$

where

$$\begin{aligned} K_D = \frac{1}{2} I_{D1} \left[\left(\frac{d\theta}{dt} \right)^2 + \left(\frac{d\phi}{dt} \right)^2 \sin^2 \theta \right] + \frac{1}{2} I_{D3} \left[\frac{d\psi_1}{dt} + \frac{d\phi}{dt} \cos\theta \right]^2 \\ + \frac{1}{2} m_D \left[\left(\frac{dx}{dt} \right)^2 + \left(\frac{dy}{dt} \right)^2 + \left(\frac{dz}{dt} \right)^2 \right] , \end{aligned} \tag{2.42}$$

is the kinetic energy of the disk,

$$\begin{aligned} K_R = \frac{1}{2} I_{R1} \left[\left(\frac{d\theta}{dt} \right)^2 + \left(\frac{d\phi}{dt} \right)^2 \cos^2 \theta \right] \\ + \frac{1}{2} m_R \left[\left(\frac{dx}{dt} \right)^2 + \left(\frac{dy}{dt} \right)^2 + \left(\frac{dz}{dt} \right)^2 \right] , \end{aligned} \tag{2.43}$$

is the kinetic energy of the rod,

$$\begin{aligned} K_{o1} = \frac{1}{2} I_{o1}^{(1)} \left[\left(\frac{d\phi}{dt} \right)^2 \cos^2(\theta + \alpha_1) + \left(\frac{d\alpha_1}{dt} + \frac{d\theta}{dt} \right)^2 \right] \\ + \frac{1}{2} m_{o1} \left[\left(L_{12}^2 + 2aL_{12} \right) \left(\left(\frac{d\theta}{dt} \right)^2 + \left(\frac{d\phi}{dt} \right)^2 \cos^2 \theta \right) \right] \\ + m_{o1}\, a\, L_{12} \frac{d\phi}{dt} \frac{d\psi_1}{dt} \cos\theta \\ + \frac{1}{2} m_{o1} \left[\left(\frac{dx}{dt} \right)^2 + \left(\frac{dy}{dt} \right)^2 + \left(\frac{dz}{dt} \right)^2 \right] , \end{aligned} \tag{2.44}$$

is the kinetic energy of rotor 1,

$$\begin{aligned} K_{o2} = \frac{1}{2} I_{o1}^{(2)} \left[\left(\frac{d\alpha_2}{dt} - \frac{d\phi}{dt} \sin\theta \right)^2 + \left(\frac{d\theta}{dt} \sin\alpha_2 - \frac{d\phi}{dt} \cos\alpha_2 \cos\theta \right)^2 \right] \\ + \frac{1}{2} m_{o2} \left[\left(L_{13}^2 + 2aL_{13} \right) \left(\left(\frac{d\theta}{dt} \right)^2 + \left(\frac{d\phi}{dt} \right)^2 \cos^2 \theta \right) \right] \\ + m_{o2}\, a\, L_{13} \frac{d\phi}{dt} \frac{d\psi_1}{dt} \cos\theta \\ + \frac{1}{2} m_{o2} \left[\left(\frac{dx}{dt} \right)^2 + \left(\frac{dy}{dt} \right)^2 + \left(\frac{dz}{dt} \right)^2 \right] , \end{aligned} \tag{2.45}$$

is the kinetic energy of rotor 2, and

$$V = \left[a(m_D + m_R) + m_{o1}(a + L_{12}) + m_{o2}(a + L_{13})\right] g \sin\theta \,, \tag{2.46}$$

is the potential energy of the system.

In this work it is assumed that the motion of the disk on the plane involves rolling without slipping. This implies that the condition

$$\boldsymbol{v}_0 + \boldsymbol{\omega}_D \times \boldsymbol{r}_D = 0 \,, \tag{2.47}$$

must hold at the contact point between the disk and the plane, where $\boldsymbol{v}_0 = \dot{x}\ \boldsymbol{I} + \dot{y}\ \boldsymbol{J} + \dot{z}\ \boldsymbol{K}$ and $\boldsymbol{\omega}_D = \omega_{Dx}\ \boldsymbol{I} + \omega_{Dy}\ \boldsymbol{J} + \omega_{Dz}\ \boldsymbol{K}$. From equations (2.1)-(2.3) it follows that $\psi_1 = 0$ at the contact point between the disk and the plane, this implies that $\boldsymbol{i}_1 = \boldsymbol{i}_\theta$ and $\boldsymbol{j}_1 = \boldsymbol{i}_\phi$ at the contact point, therefore, the point of contact is given by $\boldsymbol{r}_D = a\,\boldsymbol{i}_\theta$. Hence, from equation (2.47) the following nonholonomic constraints are obtained

$$a\left[\frac{d\theta}{dt}\sin\theta\cos\phi + \frac{d\phi}{dt}\cos\theta\sin\phi + \frac{d\psi_1}{dt}\sin\phi\right] - \frac{dx}{dt} = 0 \,, \tag{2.48}$$

$$a\left[\frac{d\theta}{dt}\sin\theta\sin\phi - \frac{d\phi}{dt}\cos\theta\cos\phi - \frac{d\psi_1}{dt}\cos\phi\right] - \frac{dy}{dt} = 0 \,, \tag{2.49}$$

$$a\,\frac{d\theta}{dt}\cos\theta - \frac{dz}{dt} = 0 \,. \tag{2.50}$$

Define

$$\boldsymbol{q} = (\theta\,,\ \phi\,,\ \psi_1\,,\ \alpha_1\,,\ \alpha_2) \quad , \quad \boldsymbol{p} = \left(\frac{d\theta}{dt}\,,\ \frac{d\phi}{dt}\,,\ \frac{d\psi_1}{dt}\,,\ \frac{d\alpha_1}{dt}\,,\ \frac{d\alpha_2}{dt}\right) .$$

Hence, the Lagrange equations, [4] , with the nonholonomic constraints given by equations (2.48)-(2.50) , are given by

$$\frac{d}{dt}\left(\frac{\partial \mathfrak{L}}{\partial p_1}\right) - \frac{\partial \mathfrak{L}}{\partial q_1} = \lambda_1\, a\sin\theta\cos\phi + \lambda_2\, a\sin\theta\sin\phi + \lambda_3\, a\cos\theta \,, \tag{2.51}$$

$$\frac{d}{dt}\left(\frac{\partial \mathfrak{L}}{\partial p_2}\right) - \frac{\partial \mathfrak{L}}{\partial q_2} = \lambda_1\, a\cos\theta\sin\phi - \lambda_2\, a\cos\theta\cos\phi\ , \tag{2.52}$$

$$\frac{d}{dt}\left(\frac{\partial \mathfrak{L}}{\partial p_3}\right) - \frac{\partial \mathfrak{L}}{\partial q_3} = \Gamma_{\psi 1} + \lambda_1\, a\sin\phi - \lambda_2\, a\cos\phi\ , \tag{2.53}$$

$$\frac{d}{dt}\left(\frac{\partial \mathfrak{L}}{\partial p_4}\right) - \frac{\partial \mathfrak{L}}{\partial q_4} = \Gamma_{\alpha 1}\ , \tag{2.54}$$

$$\frac{d}{dt}\left(\frac{\partial \mathfrak{L}}{\partial p_5}\right) - \frac{\partial \mathfrak{L}}{\partial q_5} = \Gamma_{\alpha 2}\ . \tag{2.55}$$

In a similar manner the Lagrange equations for x , y and z are given by

$$m\frac{d^2x}{dt^2} = -\lambda_1\ ,\ m\frac{d^2y}{dt^2} = -\lambda_2\ ,\ m\frac{d^2z}{dt^2} = -\lambda_3\ , \tag{2.56}$$

where $m = m_D + m_R + m_{o1} + m_{o2}$ and λ_i , $i = 1, 2, 3$, are Lagrange multipliers and $\Gamma_{\psi 1}$, $\Gamma_{\alpha 1}$ and $\Gamma_{\alpha 2}$ are the respective applied moments. That is, $\Gamma_{\psi 1}$ is the disk's applied "pedalling" moment, $\Gamma_{\alpha 1}$ is the applied moment of rotor 1 and $\Gamma_{\alpha 2}$ is the applied moment of rotor 2. By differentiating the nonholonomic contraints, equations (2.48)-(2.50), with respect to time and using equations (2.56) , expressions for the Lagrange multipliers are obtained. Hence, the (generalized) constraint forces, denoted by Γ^c_θ , Γ^c_ϕ and $\Gamma^c_{\psi 1}$, reduce to

$$\begin{aligned}\Gamma^c_\theta &= \lambda_1 a\sin\theta\cos\phi + \lambda_2 a\sin\theta\sin\phi + \lambda_3 a\cos\theta \\ &= -ma^2\left[\frac{d^2\theta}{dt^2} + \frac{d\phi}{dt}\sin\theta\left(\frac{d\psi_1}{dt} + \frac{d\phi}{dt}\cos\theta\right)\right]\ ,\end{aligned} \tag{2.57}$$

$$\begin{aligned}\Gamma^c_\phi &= \lambda_1 a\cos\theta\sin\phi - \lambda_2 a\cos\theta\cos\phi \\ &= -ma^2\left[\frac{d^2\phi}{dt^2}\cos^2\theta + \frac{d^2\psi_1}{dt^2}\cos\theta - 2\frac{d\theta}{dt}\frac{d\phi}{dt}\sin\theta\cos\theta\right]\ ,\end{aligned} \tag{2.58}$$

$$\begin{aligned}\Gamma^c_{\psi 1} &= \lambda_1 a\sin\phi - \lambda_2 a\cos\phi \\ &= -ma^2\left[\frac{d^2\phi}{dt^2}\cos\theta + \frac{d^2\psi_1}{dt^2} - 2\frac{d\theta}{dt}\frac{d\phi}{dt}\sin\theta\right]\ .\end{aligned} \tag{2.59}$$

2.5 Equations of motion

Define $\boldsymbol{\Gamma} = (0, 0, \Gamma_{\psi 1}, \Gamma_{\alpha 1}, \Gamma_{\alpha 2})^T$. Hence, by inserting equations (2.57)-(2.59) into equations (2.51)-(2.53) the following equation is obtained

$$\boldsymbol{M}(\boldsymbol{q})\frac{d^2\boldsymbol{q}}{dt^2} + \boldsymbol{h}(\boldsymbol{q}, \boldsymbol{p}) = \boldsymbol{\Gamma}, \tag{2.60}$$

where the components of $\boldsymbol{M}(\boldsymbol{q})$ are denoted by m_{ij} , $i, j = 1, 2, 3, 4, 5$

$$m_{11} = I_1 + I_{D1} + I_{o1}^{(1)} + I_{o1}^{(2)} \sin^2 \alpha_2 + ma^2 \quad ,$$

$$m_{12} = -I_{o1}^{(2)} \cos\theta \sin\alpha_2 \cos\alpha_2, \quad , \quad m_{13} = 0 \quad , \quad m_{14} = I_{o1}^{(1)} \quad , \quad m_{15} = 0,$$

$$m_{22} = (I_{D1} + I_{o1}^{(2)}) \sin^2\theta + (I_1 + I_{D3} + I_{o1}^{(2)} \cos^2\alpha_2 + ma^2) \cos^2\theta + I_{o1}^{(1)} \cos^2(\theta + \alpha_1),$$

$$m_{21} = m_{12} \quad , \quad m_{23} = (I_{D3} + m_{o1} L_{12} a + m_{o2} L_{13} a + ma^2) \cos\theta,$$

$$m_{24} = 0 \quad , \quad m_{25} = -I_{o1}^{(2)} \sin\theta,$$

$$m_{31} = m_{13} \quad , \quad m_{32} = m_{23} \quad , \quad m_{33} = I_{D3} + ma^2,$$

$$m_{34} = 0 \quad , \quad m_{35} = 0,$$

$$m_{41} = m_{14} \quad , \quad m_{42} = m_{24} \quad , \quad m_{43} = m_{34} \quad , \quad m_{44} = I_{o1}^{(1)} \quad , \quad m_{45} = 0,$$

$$m_{51} = m_{15} \quad , \quad m_{52} = m_{25} \quad , \quad m_{53} = m_{35} \quad , \quad m_{54} = m_{45} \quad , \quad m_{55} = I_{o1}^{(2)},$$

where $I_1 = I_{R1} + m_{o1}(L_{12}^2 + 2aL_{12}) + m_{o2}(L_{13}^2 + 2aL_{13})$. The components of the vector $\boldsymbol{h}(\boldsymbol{q}, \boldsymbol{p})$ are given in Appendix A.

In the rest of the work control strategies will be developed to control the motion of the disk, the coordinates which describe only the disk are given by

$$\boldsymbol{\Phi} = (\theta \, , \, \phi \, , \, \psi_1)^T \tag{2.61}$$

Equation (2.60) is given in the subspace spanned by $\boldsymbol{\Phi}$ as

$$\boldsymbol{\Omega}(\boldsymbol{q})\frac{d^2\boldsymbol{\Phi}}{dt^2} + \boldsymbol{F}(\boldsymbol{q},\boldsymbol{p}) = \boldsymbol{\Gamma}' \,, \tag{2.62}$$

where

$$\begin{aligned} \boldsymbol{\Gamma}' &= (\Gamma_{\psi 1}\,,\ \Gamma_{\alpha 1}\,,\ \Gamma_{\alpha 2})^T \,, \\ \boldsymbol{F} &= \left(h_3\,,\ h_4 - h_1\,,\ h_5 + \frac{h_2}{\sin\theta}\right)^T \,, \end{aligned} \tag{2.63}$$

and

$$\boldsymbol{\Omega} = \begin{pmatrix} 0 & m_{23} & m_{33} \\ -m'_{11} & -m_{12} & 0 \\ \frac{m_{12}}{\sin\theta} & \frac{m'_{22}}{\sin\theta} & \frac{m_{23}}{\sin\theta} \end{pmatrix} \,, \tag{2.64}$$

where

$$m'_{11} = m_{11} - I^{(1)}_{o1} \,, \tag{2.65}$$

and

$$m'_{22} = m_{22} - I^{(2)}_{o1}\sin^2\theta \,. \tag{2.66}$$

From equation (2.64) it follows that

$$\det\boldsymbol{\Omega}(\boldsymbol{\Phi}) = \frac{m'_{11}D_1 + D_2}{\sin\theta} \,, \tag{2.67}$$

where

$$D_1 = m^2_{23} - m'_{22}m_{33} \,, \tag{2.68}$$

$$D_2 = m^2_{12}m_{33} \,. \tag{2.69}$$

furthermore it can be shown that $m'_{11}D_1 + D_2 < 0$ and it follows that $\boldsymbol{\Omega}$ is invertible if $\sin\theta \neq 0$, that is if $\theta \neq n\pi$, $n = 0, 1, 2, \ldots$.

From equation (2.60) the equations of motion for the rotors are obtained as

$$\frac{d^2\alpha_1}{dt^2} = \frac{1}{I_{o1}^{(1)}}\left(\Gamma_{\alpha 1} - h_4\right) - \frac{d^2\theta}{dt^2}\,, \tag{2.70}$$

$$\frac{d^2\alpha_2}{dt^2} = \frac{1}{I_{o1}^{(2)}}\left(\Gamma_{\alpha 2} - h_5\right) + \frac{d^2\phi}{dt^2}\sin\theta\,. \tag{2.71}$$

Let $\boldsymbol{r}_c = x_c\,\boldsymbol{I} + y_c\,\boldsymbol{J}$ be the point of contact between the disk and the plane and let $\boldsymbol{r}$ denote the center of mass of the disk, then

$$\boldsymbol{r}_c = \boldsymbol{r} + a\boldsymbol{i}_\theta \tag{2.72}$$

Hence, the nonholonomic constrainsts in terms of the point of contact between the disk and the plane are given by

$$\frac{dx_c}{dt} = a\frac{d\psi_1}{dt}\sin\phi \quad , \quad \frac{dy_c}{dt} = -\,a\frac{d\psi_1}{dt}\cos\phi \tag{2.73}$$

2.6 Conclusion and remarks

A system configuration concerning a disk, a controlled rod and two overhead rotors was given. Coordinate systems were defined in which the motion of the system was derived and transformations between the different coordinate systems were considered. It was shown that the disk is subject to nonholonomic contraints which result from the condition that the disk is rolling without slipping. The Lagrangian method was then used together with the nonholonomic constraints to derive the equations of motion of the system.

Finally, the dynamical model of the system dealt with here was given in terms of the motion of the disk, equation (2.62) , together with the dynamics of the rotors given by equations (2.70) and (2.71). From the nonholonomic constraints the motion of the point of contact between the disk and the horizontal $(X\ ,\ Y)$ - plane was derived in terms of the coordinates describing the disk, equation (2.73). Together, these equations completely describe the system dealt with here.

It should be noted that it also follows from equation (2.62) that the torque applied to the upper rotor (rotor 1) induces a "tilting moment" on the motion of the disk, whereas the torque applied to the lower rotor (rotor 2) induces a "directional moment" on the motion of the disk.

Chapter 3

Feedback Control

3.1 Introduction

In this chapter a kind of inverse dynamics control is used to design feedback control laws for the applied torques on the disk and for both of the rotors such that the motion of the disk will be stabilised and the disk will be able to asymptotically track any given smooth ground trajectory. This problem is also dealt with in [32].

In this work "stabilising the motion of the disk" implies that the inclination of disk will be stabilised about its vertical position, i.e. the leaning angle, θ , will be controlled in such a manner that $\theta \to \pi/2$ as $t \to \infty$.

The notion of asymptotic tracking as used here is as follows. Let the point of contact between the disk and the $(X\ ,\ Y)$ - plane be denoted by $(x_c\ ,\ y_c)$. Furthermore, let $(x_{dr}(t)\ ,\ y_{dr}(t))\ ,\ t \geq 0$, denote the coordinates, in the $(X\ ,\ Y)$ - plane, of a given smooth ground trajectory. Denote

$$\boldsymbol{\eta}(t) = \left(x_c(t)\ ,\ \frac{dx_c(t)}{dt}\ ,\ \frac{d^2x_c(t)}{dt^2}\ ,\ \frac{d^3x_c(t)}{dt^3}\ ,\ y_c(t)\ ,\ \frac{dy_c(t)}{dt}\ ,\ \frac{d^2y_c(t)}{dt^2}\ ,\ \frac{d^3y_c(t)}{dt^3} \right)^T ,$$

and

$$\boldsymbol{\eta}_{dr}(t) = \left(x_{dr}(t)\,,\ \frac{dx_{dr}(t)}{dt}\,,\ \frac{d^2x_{dr}(t)}{dt^2}\,,\ \frac{d^3x_{dr}(t)}{dt^3}\,,\ y_{dr}(t)\,,\ \frac{dy_{dr}(t)}{dt}\,,\ \frac{d^2y_{dr}(t)}{dt^2}\,,\ \frac{d^3y_{dr}(t)}{dt^3} \right)^T .$$

If the disk is said to asymptotically track a given smooth ground trajectory, $(x_{dr}(t)\,,\ y_{dr}(t))\,,\ t \geq 0$, it implies that

$$\lim_{t\to\infty} \left(\boldsymbol{\eta}(t) - \boldsymbol{\eta}_{dr}(t) \right) = \mathbf{0}\,.$$

3.2 Inverse dynamics control

In this section a procedure is developed to design a feedback control law

$$\boldsymbol{\Gamma}(\boldsymbol{\mu})^C = (0\,,\ 0\,,\ \Gamma^C_{\psi 1}(\boldsymbol{\mu})\,,\ \Gamma^C_{\alpha 1}(\boldsymbol{\mu})\,,\ \Gamma^C_{\alpha 2}(\boldsymbol{\mu}))\,,$$

where the vector $\boldsymbol{\mu}$ will be defined later, such that the motion of the disk will be stabilised by forcing the disk to move asymptotically at $\theta = \pi/2$ while also asymptotically tracking a given smooth reference path on the plane.

First introduce the control law

$$\boldsymbol{\Gamma}' = \boldsymbol{\Omega}(\boldsymbol{q})\boldsymbol{u} + \boldsymbol{F}(\boldsymbol{q},\boldsymbol{p})\,, \tag{3.1}$$

which is defined in any region $(\boldsymbol{q},\boldsymbol{p})$ which excludes $\sin\theta = 0$, and where $\boldsymbol{u} = (u_1\,,\ u_2\,,\ u_3)^T$. It then follows from equation (2.62) that

$$\begin{pmatrix} \frac{d^2\theta}{dt^2} \\ \frac{d^2\phi}{dt^2} \\ \frac{d^2\psi_1}{dt^2} \end{pmatrix} = \begin{pmatrix} u_1 \\ u_2 \\ u_3 \end{pmatrix} . \tag{3.2}$$

For stabilisation the applied control law for u_1 is chosen as

$$u_1 = -k_1 \frac{d\theta}{dt} - k_2\left(\theta - \frac{\pi}{2}\right) , \tag{3.3}$$

where k_i , $i = 1, 2$, are chosen such that the polynomial

$$f_2(s) = s^2 + k_1 s + k_2 ,$$

is Hurwitz (all the roots of $f_2(s)$ are in the left hand side of the s - domain). For this case it then follows, [33], that

$$\theta(t) \to \frac{\pi}{2} \quad \text{and} \quad \frac{d^k\theta}{dt^k} \to 0 \quad \text{as} \quad t \to \infty \quad , \quad k = 1, 2$$

In order to obtain the functions u_2 and u_3 define the following auxiliary functions

$$g_{c1} = 2u_3 \frac{d\phi}{dt} \cos\phi - \frac{d\psi_1}{dt}\left(\frac{d\phi}{dt}\right)^2 \sin\phi , \tag{3.4}$$

$$g_{c2} = 2u_3 \frac{d\phi}{dt} \sin\phi + \frac{d\psi_1}{dt}\left(\frac{d\phi}{dt}\right)^2 \cos\phi , \tag{3.5}$$

where from equation (3.2) it follows that, $u_3 = d^2\psi_1/dt^2$. By calculating d^3x_c/dt^3 and d^3y_c/dt^3 from equation (2.73) and using the auxiliary functions g_{c1} and g_{c2} defined by equations (3.4) and (3.5) it follows that

$$\begin{pmatrix} \frac{d^3x_c}{dt^3} \\ \frac{d^3y_c}{dt^3} \end{pmatrix} = a \begin{pmatrix} \sin\phi & \frac{d\psi_1}{dt}\cos\phi \\ -\cos\phi & \frac{d\psi_1}{dt}\sin\phi \end{pmatrix} \begin{pmatrix} \frac{du_3}{dt} \\ u_2 \end{pmatrix} + \begin{pmatrix} ag_{c1} \\ ag_{c2} \end{pmatrix} , \tag{3.6}$$

where from equation (3.2) it follows that, $u_2 = d^2\phi/dt^2$, and $du_3/dt = d^3\psi_1/dt^3$. Denote

$$\mathbf{\Lambda} = \begin{pmatrix} \sin\phi & \frac{d\psi_1}{dt}\cos\phi \\ -\cos\phi & \frac{d\psi_1}{dt}\sin\phi \end{pmatrix} , \tag{3.7}$$

and note that $\det \mathbf{\Lambda} = d\psi_1/dt$. That is, $\mathbf{\Lambda}$ is inverteble if the disk is rolling, $d\psi_1/dt \neq 0$.

An auxiliary control law is introduced of the form

$$\begin{pmatrix} \frac{du_3}{dt} \\ u_2 \end{pmatrix} = a^{-1}\mathbf{\Lambda}^{-1} \begin{pmatrix} \nu_1 - ag_{c1} \\ \nu_2 - ag_{c2} \end{pmatrix} , \tag{3.8}$$

which is valid in all regions of $(\boldsymbol{q}, \boldsymbol{p})$ which excludes $d\psi_1/dt = 0$. Using equation (3.6) yields

$$\begin{pmatrix} \frac{d^3x_c}{dt^3} \\ \frac{d^3y_c}{dt^3} \end{pmatrix} = \begin{pmatrix} \nu_1 \\ \nu_2 \end{pmatrix} . \tag{3.9}$$

Let $\{(x_{dr}(t), y_{dr}(t)), t \geq 0\}$ be a representation of a given smooth ground reference trajectory in the $(X\ ,\ Y)$ - plane. The functions ν_1 and ν_2 are chosen in the following form

$$\begin{aligned} \nu_1 = \frac{d^3x_{dr}}{dt^3} - \gamma_1\left(\frac{d^2x_c}{dt^2} - \frac{d^2x_{dr}}{dt^2}\right) - \gamma_2\left(\frac{dx_c}{dt} - \frac{dx_{dr}}{dt}\right) \\ - \gamma_3(x_c - x_{dr}) \end{aligned} , \tag{3.10}$$

$$\begin{aligned} \nu_2 = \frac{d^3y_{dr}}{dt^3} - \gamma_1\left(\frac{d^2y_c}{dt^2} - \frac{d^2y_{dr}}{dt^2}\right) - \gamma_2\left(\frac{dy_c}{dt} - \frac{dy_{dr}}{dt}\right) \\ - \gamma_3(y_c - y_{dr}) \end{aligned} , \tag{3.11}$$

where $\gamma_i\ ,\ i = 1, 2, 3$ are chosen in such a manner that the polynomial

$$f_3(s) = s^3 + \gamma_1\, s^2 + \gamma_2\, s + \gamma_3\ ,$$

is Hurwitz. In this case it follows from (3.9) that

$$\frac{d^k x_c(t)}{dt^k} - \frac{d^k x_{dr}(t)}{dt^k} \to 0 \ \text{ as } \ t \to \infty \quad , \quad k = 0, 1, 2, 3$$

and

$$\frac{d^k y_c(t)}{dt^k} - \frac{d^k y_{dr}(t)}{dt^k} \to 0 \ \text{ as } \ t \to \infty \quad , \quad k = 0, 1, 2, 3$$

It can thus be seen that ν_1 and ν_2 are determined from equations (3.10) and (3.11) respectively. u_2 and du_3/dt can then be determined from equation (3.8), and by taking $u_3(0) = 0$, u_3 is obtained. u_1 can be directly calculated from equation (3.3), and

finally, once the vector $\boldsymbol{u}$ is known, the required applied torques $\Gamma_{\psi 1}$, $\Gamma_{\alpha 1}$ and $\Gamma_{\alpha 2}$ are determined using equation (3.1).

Denote the required control law by

$$\boldsymbol{\Gamma^C(\mu)} = (0\ ,\ 0\ ,\ \Gamma^C_{\psi 1}(\boldsymbol{\mu})\ ,\ \Gamma^C_{\alpha 1}(\boldsymbol{\mu})\ ,\ \Gamma^C_{\alpha 2}(\boldsymbol{\mu}))^T\ ,$$

where

$$\boldsymbol{\mu} = \left(\boldsymbol{q}\ ,\ \boldsymbol{p}\ ,\ e_{1c}\ ,\ e_{2c}\ ,\ \frac{de_{1c}}{dt}\ ,\ \frac{de_{2c}}{dt}\ ,\ \frac{d^2e_{1c}}{dt^2}\ ,\ \frac{d^2e_{2c}}{dt^2}\ ,\ \frac{d^3x_{dr}}{dt^3}\ ,\ \frac{d^3y_{dr}}{dt^3}\right)\ ,$$

and

$$e_{1c} = x_c - x_{dr} \quad , \quad e_{2c} = y_c - y_{dr}\ .$$

Finally it should be noted that the control law defined by equations (3.3), (3.10) and (3.11) is an exponentially convergent control law, i.e. the error decreases exponentially to zero, and if the system initially has a zero error it will remain zero for all time. The rate of convergenge is determinded by the values of k_1 , k_2 , γ_1 , γ_2 , γ_3 . In the next chapter a method is decribed which obtains an exact position in a finte time.

3.3 Numerical study

The control strategy developed above was used in a simulation of the disk-rod-rotors system. The parameters used were as follows

$$m_D = 10 \text{ kg} \qquad m_{R1} = 0.75 \text{ kg} \qquad m_{R2} = 0.25 \text{ kg}$$
$$m_{o1} = m_{o2} = 0.5 \text{ kg} \qquad a = 0.4 \text{ m} \qquad L_{12} = 0.75 \text{ m}$$
$$L_{13} = 0.5 \text{ m} \qquad L_{11} = 0.25 \text{ m} \qquad L_{o1} = L_{o2} = 0.3 \text{ m}$$
$$k_1 = 10 \qquad k_2 = 24 \qquad \gamma_1 = 15$$
$$\gamma_2 = 75 \qquad \gamma_3 = 125$$

The initial conditions used are given by

$$\theta(0) = \frac{60\,\pi}{180} \text{ rad} \qquad \frac{d\theta(0)}{dt} = 0 \text{ rad/sec} \qquad \phi(0) = \frac{\pi}{2} \text{ rad}$$
$$\frac{d\phi(0)}{dt} = 0 \text{ rad/sec} \qquad \psi_1(0) = 0 \text{ rad} \qquad \frac{d\psi_1(0)}{dt} = 4 \text{ rad/sec}$$
$$\alpha_i(0) = 0 \text{ rad} \qquad \frac{d\alpha_i(0)}{dt} = 0 \text{ rad/sec} \qquad i = 1, 2$$
$$u_3(0) = 0 \text{ rad/sec}^2 \qquad x_c(0) = 0 \text{ m} \qquad y_c = 0 \text{ m}$$

Using equation (2.73) the parameters and initial conditions yield the following conditions

$$\frac{dx_c(0)}{dt} = 1.6 \text{ m/sec} \quad , \quad \frac{dy_c(0)}{dt} = 0 \text{ m/sec}$$

The reference path which was used is given by

$$x_{dr}(t) = 8\cos(\pi t/5) \quad , \quad y_{dr}(t) = 8\sin(\pi t/5) \tag{3.12}$$

The simulation was performed using a Runge-Kutta order 4 algoritm with a timestep of 10^{-5} sec and the data was stored at intervals of 0.002 sec. Some of the results are displayed in figures (3.1) - (3.15).

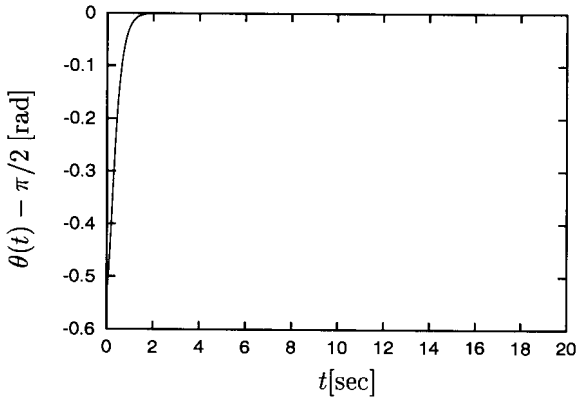

Figure 3.1: The values of $\theta(t) - \pi/2$, $t \in [0, t_f]$ in radians

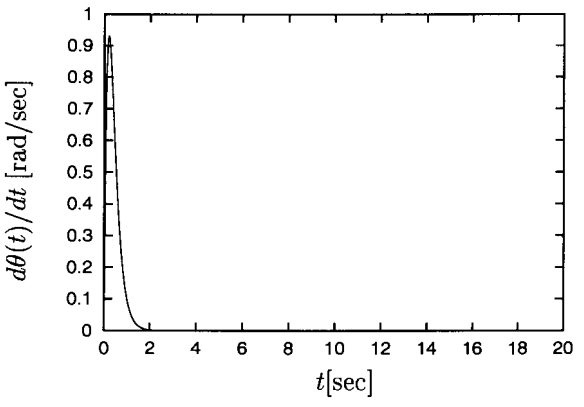

Figure 3.2: The values of $d\theta(t)/dt$, $t \in [0, t_f]$ in rad/ sec

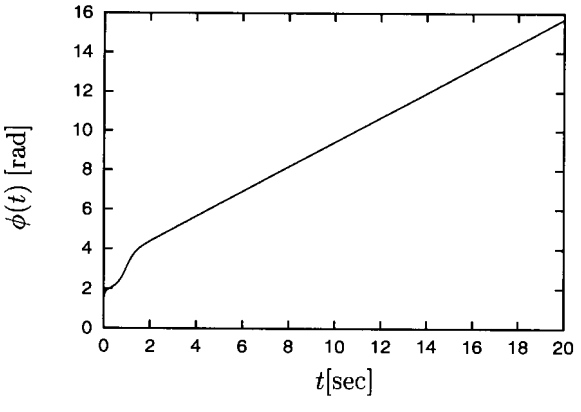

Figure 3.3: The values of $\phi(t)$, $t \in [0, t_f]$ in radians

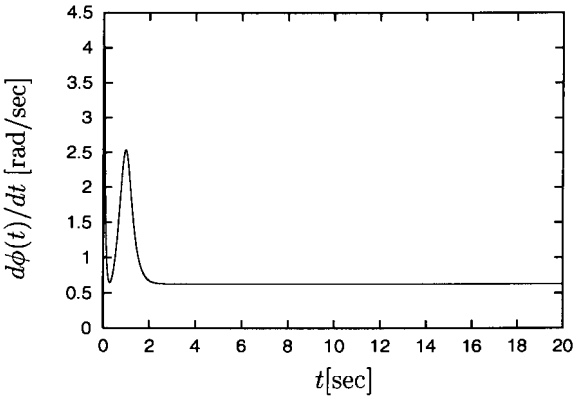

Figure 3.4: The values of $d\phi(t)/dt$, $t \in [0, t_f]$ in rad/ sec

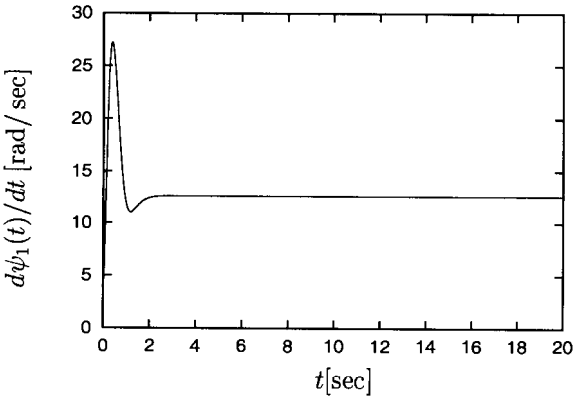

Figure 3.5: The values of $d\psi_1(t)/dt$, $t \in [0, t_f]$ in rad/ sec

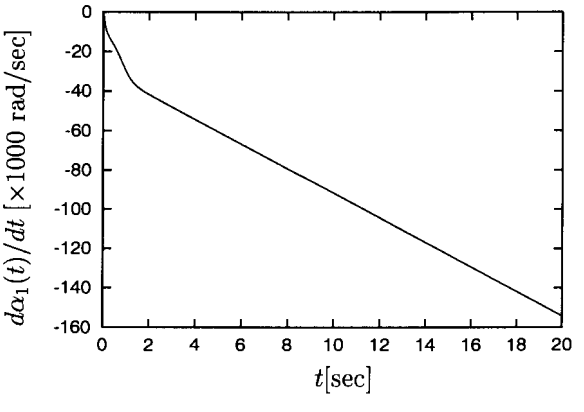

Figure 3.6: The values of $d\alpha_1(t)/dt$, $t \in [0, t_f]$ in ×1000 rad/ sec

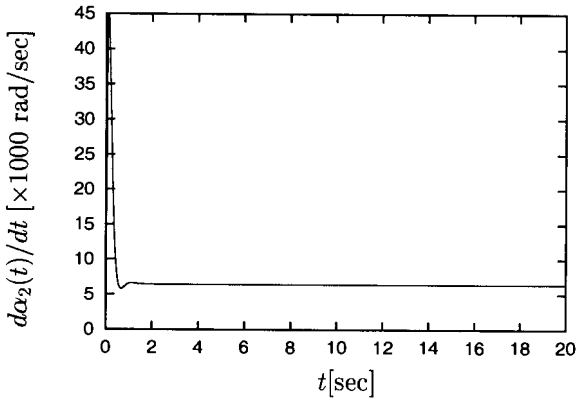

Figure 3.7: The values of $d\alpha_2(t)/dt$, $t \in [0, t_f]$ in $\times 1000$ rad/sec

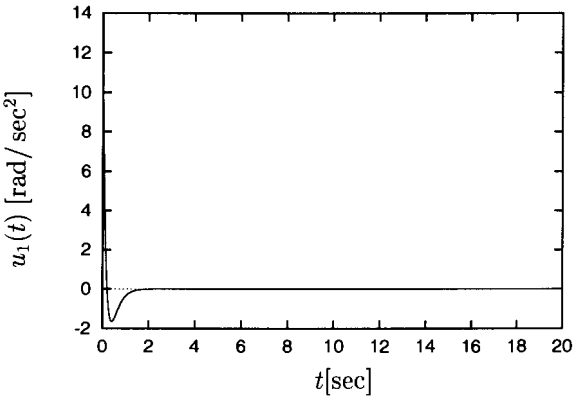

Figure 3.8: The values of $u_1(t)$, $t \in [0, t_f]$ in rad/sec^2

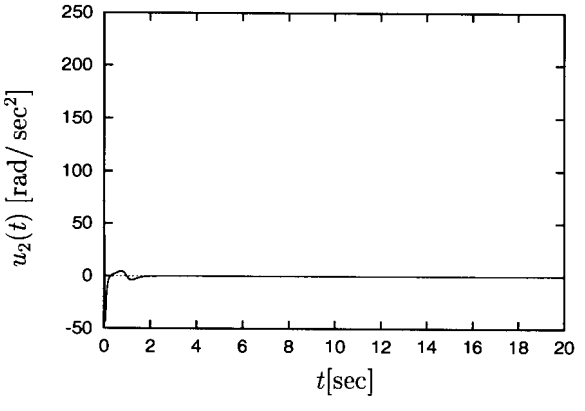

Figure 3.9: The values of $u_2(t)$, $t \in [0, t_f]$ in rad/sec^2

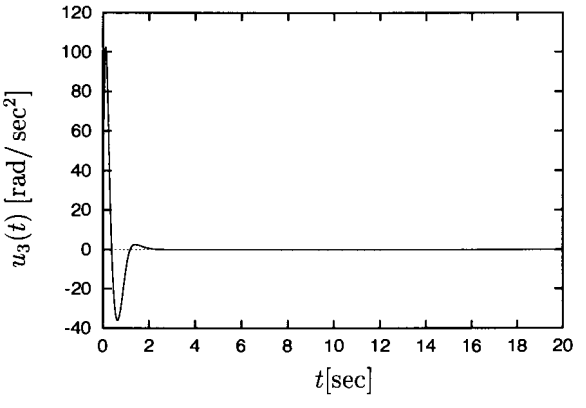

Figure 3.10: The values of $u_3(t)$, $t \in [0, t_f]$ in rad/sec^2

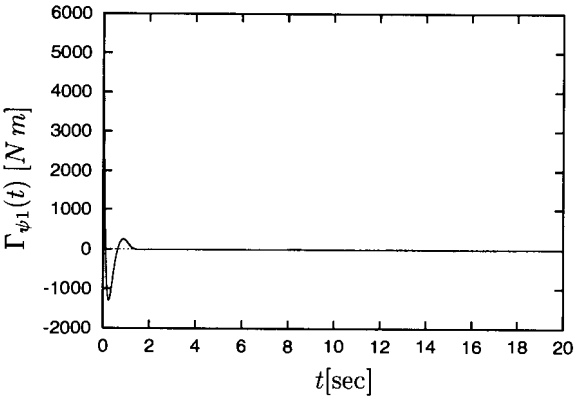

Figure 3.11: The values of $\Gamma_{\psi 1}(t)$, $t \in [0, t_f]$ in N·m

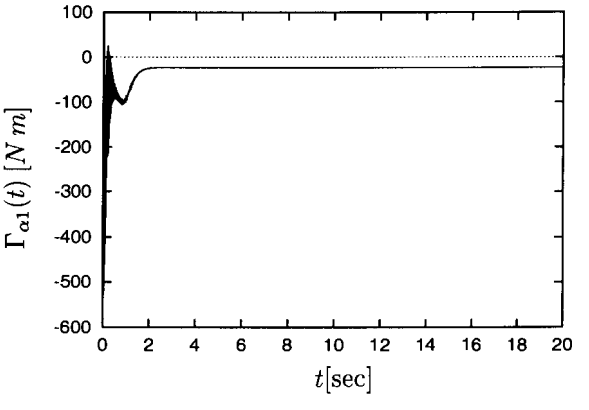

Figure 3.12: The values of $\Gamma_{\alpha 1}(t)$, $t \in [0, t_f]$ in N·m

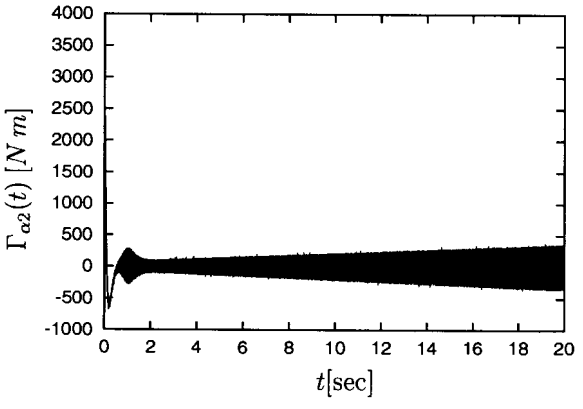

Figure 3.13: The values of $\Gamma_{\alpha 2}(t)$, $t \in [0, t_f]$ in N·m

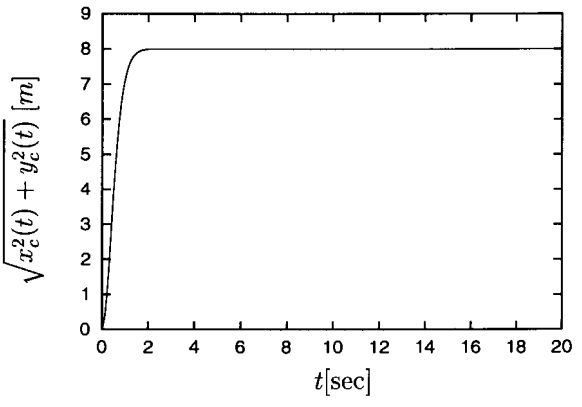

Figure 3.14: The values of $\sqrt{x_c^2(t) + y_c^2(t)}$, $t \in [0, t_f]$ in m

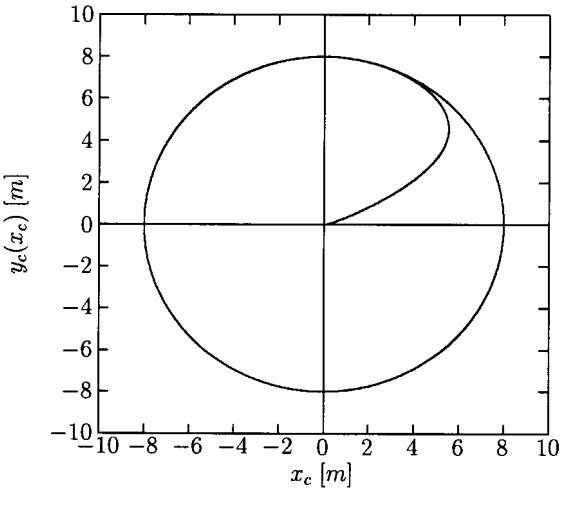

Figure 3.15: The values of y_c as a function of x_c

3.4 Conclusion and remarks

In this chapter a stabilisation and control problem is dealt with concerning the motion of the disk - rod - rotors system which was described in the previous chapter. A kind of inverse dynamics control was used to obtain a feedback control law for the torques applied to the pedalling mechanism of the disk and to each of the rotors. The proposed feedback control law was designed such that the motion of the disk will be stabilised (the disk's plane will be vertical to the horizontal plane), while simultaneously controlling the speed and direction of the disk in such a manner that the disk will be able to asymptotically track any given smooth ground trajectory.

In section 3.2 the auxilary control functions u_1 , u_2 , u_3 are introduced via an inverse dynamics control law. These controls, as can be seen from equation (3.2), are directly related to the kinematics of the system. The control law given by equation (3.1) seperates the kinematics from the dynamics of the system. It is therefore possible to control the kinematics of the system directly, for example the control of θ and $d^k\theta/dt$, $k = 1, 2$, using the auxilary control variable u_1 , equation (3.3) .

In section 3.2 a procedure is developed to obtain tracking control of the disk. This is done by relating x_c and y_c and three of their time derivatives to u_2 and du_3/dt. Aditional auxilary control functions ν_1 and ν_2 are introduced by using an inverse control law, equation (3.8) . This enables the direct control of the kinematics of $d^k x_c/dt$ and $d^k y_c/dt$, $k = 0, 1, 2, 3$ through the auxilary controls ν_1 and ν_2 . The control law (3.1) therefore seperates the dynamics from the kinematics of the system. Similarly the control law (3.8) seperates the kinematics from the kinematical constraints placed on the system which results from the condition that the disk is rolling without slipping which was placed on the system. The design of the controller was therefore done directly on the kinematics of the system. It should be noted that, though the feedback controller uses x_c and y_c and their derivatives, these states are not observed directly but rather calculted using equation (2.73) together with the states observed,

namely $\boldsymbol{q}$ and $\boldsymbol{p}$.

Finally, an example was solved involving the tracking of a given smooth trajectory. The same reference trajectory and initial condition of the disk was used in [34] , the system considered there involved only a disk, without the rod and rotors. The kinematics obtained in both examples was however the same. This is due to the method used in section 3.2 , as discused previously here.

Chapter 4

Path Controllability

4.1 Introduction

In this chapter the concept of path-controllability is introduced, and, together with the use of inverse dynamics control, the stabilisation and guidance of the disk-rod-rotors system is considered. In particular, control laws will be derived under which the motion of the disk is stabilised and the disk is steered from a point $\boldsymbol{P}_1$ to a point $\boldsymbol{P}_2$, both in the (X, Y) - plane, during a given finite time interval $[0, t_f]$.

The control problem dealt with in this chapter can be stated as follows: Given two points $\boldsymbol{P}_1$ and $\boldsymbol{P}_2$ in the (X, Y) - plane and let $[0, t_f]$ be a time interval where $t_f > 0$ is a given number. As before denote by $\boldsymbol{r}_c$ the point of contact between the disk and the (X, Y) - plane. The problem considered here is to find torques applied to the pedalling mechanism of the disk, and to each of the rotors, such that the disk will be stabilised (the disk's plane will be vertical to the horizontal plane), while simultaneously the speed and direction of the disk will be controlled such that $\boldsymbol{r}_c$ will move from $\boldsymbol{P}_1$ to $\boldsymbol{P}_2$ during the interval $[0, t_f]$.

The coordinates of $\boldsymbol{r}_c$ in the inertial (X,Y) - coordinate system is denoted by $(x_c\,,\, y_c)$.

Denote

$$\boldsymbol{\eta}(t) = \left(x_c(t)\,,\ \frac{dx_c(t)}{dt}\,,\ \frac{d^2x_c(t)}{dt^2}\,,\ y_c(t)\,,\ \frac{dy_c(t)}{dt}\,,\ \frac{d^2y_c(t)}{dt^2} \right)^T . \tag{4.1}$$

Furthermore, let $\boldsymbol{Q}_1$ and $\boldsymbol{Q}_2$ be any two points in $\mathbb{R}^6$, and let $[0, t_f)$ be any given finite time interval. If torques to the pedalling mechanism and to each of the rotors can be found on $[0, t_f)$ such that $\boldsymbol{\eta}(\cdot)$ will move from $\boldsymbol{\eta}(0) = \boldsymbol{Q}_1$ to $\boldsymbol{\eta}(t_f) = \boldsymbol{Q}_2$, then the disk-rod-rotors system is said to be path controllable. More specifically, $\boldsymbol{Q}_i = (x_{pi}\,,\ c_{1i}\,,\ c_{2i}\,,\ y_{pi}\,,\ c_{3i}\,,\ c_{4i})^T$, where the points $\boldsymbol{P}_1$ and $\boldsymbol{P}_2$ in the $(X\,,\ Y)$ - plane are denoted by $\boldsymbol{P}_i = (x_{pi}\,,\ y_{pi})$, $i = 1, 2$ and c_{ki} , $k = 1, 2, 3, 4$, and $i = 1, 2$ are real numbers to be specified later.

4.2 Inverse dynamics control

In this section the same inverse dynamics control law used in the previous chapter is applied to the dynamical model, equation (2.62), of the system derived in chapter 2. This leads to a decoupled double integrater system relating the kinematics of the system with the control inputs. This is used in the next section to derive control laws under which the path controllability of the system is proved.

The control law defined by equation (3.1) is used to obtain the decoupled double integrater system (3.2) which is again stated here

$$\begin{pmatrix} \frac{d^2\theta}{dt^2} \\ \frac{d^2\phi}{dt^2} \\ \frac{d^2\psi_1}{dt^2} \end{pmatrix} = \begin{pmatrix} u_1 \\ u_2 \\ u_3 \end{pmatrix} . \tag{4.2}$$

The same stabilisation criteria as in the previous chapter is placed on the disk, as a result the control law for u_1 is again chosen as equation (3.3) given by

$$u_1 = -k_1 \frac{d\theta}{dt} - k_2\left(\theta - \frac{\pi}{2}\right) , \tag{4.3}$$

where k_i , $i = 1, 2$ are chosen such that the polynomial

$$f_2(s) = s^2 + k_1 s + k_2 \ ,$$

is Hurwitz. It then follows that

$$\theta(t) \to \frac{\pi}{2} \ \text{ and } \ \frac{d^k\theta}{dt^k} \to 0 \ \text{ as } \ t \to \infty \quad , \ k = 1, 2 \ .$$

A finite time solution for the stabilisation problem is also possible, see for example [35].

4.3 Point to point control

In this section the functions u_2 and u_3 are determined such that $\boldsymbol{\eta}(\cdot)$ will move in such a manner that $\boldsymbol{\eta}(0) = \boldsymbol{Q}_1$ and $\boldsymbol{\eta}(t_f) = \boldsymbol{Q}_2$, where $\boldsymbol{Q}_1$ and $\boldsymbol{Q}_2$ are given points in $\mathbb{R}^6$.

The procedure used in the previous chapter of equations (3.4) to (3.7) can be followed, together with the control law (3.8) given by

$$\begin{pmatrix} \frac{du_3}{dt} \\ u_2 \end{pmatrix} = a^{-1}\boldsymbol{\Lambda}^{-1} \begin{pmatrix} \nu_1 - ag_{c1} \\ \nu_2 - ag_{c2} \end{pmatrix} \ , \tag{4.4}$$

which is valid in all regions of $(\boldsymbol{q}, \boldsymbol{p})$ which excludes $d\psi_1/dt = 0$. Finally equation (3.9) is obtained as

$$\begin{pmatrix} \frac{d^3x_c}{dt^3} \\ \frac{d^3y_c}{dt^3} \end{pmatrix} = \begin{pmatrix} \nu_1 \\ \nu_2 \end{pmatrix} \ , \tag{4.5}$$

which, together with the notation

$$\eta_1 = x_c \ , \ \eta_2 = \frac{dx_c}{dt} \ , \ \eta_3 = \frac{d^2x_c}{dt^2} \ , \ \eta_4 = y_c \ , \ \eta_5 = \frac{dy_c}{dt} \ , \ \eta_6 = \frac{d^2y_c}{dt^2} \ ,$$

leads to

$$\frac{d\boldsymbol{\eta}(t)}{dt} = \boldsymbol{A}\boldsymbol{\eta}(t) + \boldsymbol{B}\boldsymbol{\nu}(t)\ , \tag{4.6}$$

where

$$\boldsymbol{\eta} = \left\{\boldsymbol{\eta}(t) = \left(\eta_1(t)\ ,\ \eta_2(t)\ ,\ \eta_3(t)\ ,\ \eta_4(t)\ ,\ \eta_5(t)\ ,\ \eta_6(t)\right)^T\ ,\ t \in [0, t_f]\right\}\ ,$$

$$\boldsymbol{\nu} = \left\{\boldsymbol{\nu}(t) = \left(\nu_1(t)\ ,\ \nu_2(t)\right)^T\ ,\ t \in [0, t_f]\right\}\ ,$$

$$\boldsymbol{A} = \begin{pmatrix} 0 & 1 & 0 & 0 & 0 & 0 \\ 0 & 0 & 1 & 0 & 0 & 0 \\ 0 & 0 & 0 & 0 & 0 & 0 \\ 0 & 0 & 0 & 0 & 1 & 0 \\ 0 & 0 & 0 & 0 & 0 & 1 \\ 0 & 0 & 0 & 0 & 0 & 0 \end{pmatrix}\ ,\quad \boldsymbol{B} = \begin{pmatrix} 0 & 0 \\ 0 & 0 \\ 1 & 0 \\ 0 & 0 \\ 0 & 0 \\ 0 & 1 \end{pmatrix}\ . \tag{4.7}$$

The system given by equations (4.6) and (4.7) is controllable, [1]. That is, given any two points $\boldsymbol{Q}_1$ and $\boldsymbol{Q}_2$ in $\mathbb{R}^6$, and any finite time interval $[0, t_f)$, a control function $\boldsymbol{\nu}(t)$, $t \in [0, t_f)$, exists such that $\boldsymbol{\eta}$ will move from $\boldsymbol{\eta}(0) = \boldsymbol{Q}_1$ to $\boldsymbol{\eta}(t_f) = \boldsymbol{Q}_2$.

Let $\boldsymbol{Q}_i$, $i = 1, 2$ be given points in $\mathbb{R}^6$. These points can now be chosen such that

$$\boldsymbol{Q}_1 = \left(x_{p1}\ ,\ \frac{dx_c(0)}{dt}\ ,\ \frac{d^2x_c(0)}{dt^2}\ ,\ y_{p1}\ ,\ \frac{dy_c(0)}{dt}\ ,\ \frac{d^2y_c(0)}{dt^2}\right)^T\ , \tag{4.8}$$

and

$$\boldsymbol{Q}_2 = \left(x_{p2}\ ,\ \frac{dx_c(t_f)}{dt}\ ,\ \frac{d^2x_c(t_f)}{dt^2}\ ,\ y_{p2}\ ,\ \frac{dy_c(t_f)}{dt}\ ,\ \frac{d^2y_c(t_f)}{dt^2}\right)^T\ . \tag{4.9}$$

The coefficients $\{c_{ki}\}$ introduced in Section 1 are therefore given by

$$c_{11} = \frac{dx_c(0)}{dt}\ ,\ c_{21} = \frac{d^2x_c(0)}{dt^2}\ ,\ c_{31} = \frac{dy_c(0)}{dt}\ ,\ c_{41} = \frac{d^2y_c(0)}{dt^2}\ ,$$

$$c_{12} = \frac{dx_c(t_f)}{dt}\ ,\ c_{22} = \frac{d^2x_c(t_f)}{dt^2}\ ,\ c_{32} = \frac{dy_c(t_f)}{dt}\ ,\ c_{42} = \frac{d^2y_c(t_f)}{dt^2}\ .$$

Hence, the point $\boldsymbol{P}_1$ together with the coefficients c_{11} , c_{21} , c_{31} , c_{41} specify the initial conditions of the system. Note that equation (2.73) can also be used to relate the initial conditions of ϕ , $d\phi/dt$, $d\psi/dt$ and $d^2\psi/dt$ to the coefficients c_{11} , c_{21} , c_{31} , c_{41} . The point $\boldsymbol{P}_2$ will depend on the problem under consideration and the coefficients c_{12} , c_{22} , c_{32} , c_{42} are design parameters and can be chosen by the designer.

Finally, the control law $\boldsymbol{\nu} = (\nu_1 \, , \, \nu_2)^T$ is defined as

$$\boldsymbol{\nu}^c(t) = \Big(\exp\big((t_f - t)\boldsymbol{A}\big)\boldsymbol{B}\Big)^T \boldsymbol{C}^{-1}\big(\boldsymbol{\eta}(t_f) - \exp(t_f\boldsymbol{A})\,\boldsymbol{\eta}(0)\big) \, , \qquad t \in [0, t_f) \, , \tag{4.10}$$

where

$$\boldsymbol{C} = \int_0^{t_f} \exp\big((t_f - t)\boldsymbol{A}\big)\boldsymbol{B}\Big(\exp\big((t_f - t)\boldsymbol{A}\big)\boldsymbol{B}\Big)^T dt \, , \tag{4.11}$$

and $\boldsymbol{\eta}(0) = \boldsymbol{Q}_1$ and $\boldsymbol{\eta}(t_f) = \boldsymbol{Q}_2$.

The control law $\boldsymbol{\nu} = \boldsymbol{\nu}^c$ steers $\boldsymbol{\eta}$ in such a manner that $\boldsymbol{\eta}(0) = \boldsymbol{Q}_1$ and $\boldsymbol{\eta}(t_f) = \boldsymbol{Q}_2$, [1].

4.4 Calculation of the control law

If the points $\boldsymbol{Q}_1$ and $\boldsymbol{Q}_2$ are specified in $\mathbb{R}^6$ then the control law $\boldsymbol{\nu} = \boldsymbol{\nu}^c(t)$ given by (4.10) and (4.11) can be calculated analytically as a function of time. In this section an analytic expression is obtained for the control law $\boldsymbol{\nu}^c(t)$, $t \in [0, t_f)$ in terms of the parameters x_{pi} , y_{pi} and c_{ki} where $i = 1, 2$ and $k = 1, 2, 3, 4$, together with the final time, $t_f > 0$.

It should be noted that equation (4.5) constitutes a decoupled system, as a result $\nu_1^c(t)$ and $\nu_2^c(t)$ can be treated seperately with respect to control laws of the form (4.10) and (4.11). In this section, however, $\boldsymbol{\nu}^c(t)$ is treated as a vector, and equation (4.10) as a

matrix equation. In the following derivation the decoupled nature of the equation is clearly visible in the diagonal nature of the matrices.

From equation (4.7) it follows directly that $\boldsymbol{A}^3 = \boldsymbol{0}$, the exponent terms then reduce to

$$\Big(\exp\big((t_f - t)\boldsymbol{A}\big)\boldsymbol{B}\Big)^T = \begin{pmatrix} \boldsymbol{\gamma} & 0 \\ 0 & \boldsymbol{\gamma} \end{pmatrix} , \tag{4.12}$$

where

$$\boldsymbol{\gamma} = \left(\frac{(t_f - t)^2}{2} \, , \; t_f - t \, , \; 1 \right) ,$$

and

$$\exp(t_f \boldsymbol{A}) = \begin{pmatrix} \boldsymbol{\alpha} & 0 \\ 0 & \boldsymbol{\alpha} \end{pmatrix} , \tag{4.13}$$

where

$$\boldsymbol{\alpha} = \begin{pmatrix} 1 & t_f & \frac{t_f^2}{2} \\ 0 & 1 & t_f \\ 0 & 0 & 1 \end{pmatrix} .$$

The matrix $\boldsymbol{C}$ then reduces to

$$\boldsymbol{C} = \begin{pmatrix} \boldsymbol{C'} & 0 \\ 0 & \boldsymbol{C'} \end{pmatrix} , \tag{4.14}$$

and its inverse is given by

$$\boldsymbol{C}^{-1} = \begin{pmatrix} (\boldsymbol{C'})^{-1} & 0 \\ 0 & (\boldsymbol{C'})^{-1} \end{pmatrix} , \tag{4.15}$$

with

$$(\boldsymbol{C'})^{-1} = \frac{3}{t_f^5}\begin{pmatrix} 240 & -120t_f & 20t_f^2 \\ -120t_f & 64t_f^2 & -12t_f^3 \\ 20t_f^2 & -12t_f^3 & 3t_f^4 \end{pmatrix} .$$

Finally, the control law for $\boldsymbol{\nu} = (\nu_1, \nu_2)^T$, using the notation of the previous section, can be written as

$$\nu_1^c(t) = \boldsymbol{\gamma}(\boldsymbol{C'})^{-1}\left(\begin{pmatrix} x_{p2} \\ c_{12} \\ c_{22} \end{pmatrix} - \boldsymbol{\alpha}\begin{pmatrix} x_{p1} \\ c_{11} \\ c_{21} \end{pmatrix}\right) , \tag{4.16}$$

and

$$\nu_2^c(t) = \boldsymbol{\gamma}(\boldsymbol{C'})^{-1}\left(\begin{pmatrix} y_{p2} \\ c_{32} \\ c_{42} \end{pmatrix} - \boldsymbol{\alpha}\begin{pmatrix} y_{p1} \\ c_{31} \\ c_{41} \end{pmatrix}\right) . \tag{4.17}$$

ν_1 and ν_2 are given by equations (4.16) and (4.17) respectively, as functions of time, dependant on the initial condition $\boldsymbol{Q}_1$, the end point constraint $\boldsymbol{Q}_2$ and the final time t_f. u_2 and du_3/dt can then be determined from equation (4.4), and taking $u_3(0) = 0$, u_3 is obtained. u_1 can be directly calculated from equation (4.3). Finally the required applied torques Γ_ψ , $\Gamma_{\alpha 1}$ and $\Gamma_{\alpha 2}$ are determined using equation (3.1).

It should be noted that the control law for $\boldsymbol{\nu}^c(t)$ defined by equations (4.10) and (4.11) is an open loop control strategy. As a consequence, the control variables u_2 and u_3 will be functions of time only, and, dependant only on the initial and final points $\boldsymbol{Q}_1$ and $\boldsymbol{Q}_2$ respectively, and the final time t_f . The control law for u_1 is given by (4.3) , which is a closed loop feedback control law which is dependant on the value of $\theta(t)$ and $d\theta(t)/dt$, $t \in [0, t_f]$. As a result the required control law is denoted by

$$\boldsymbol{\Gamma^C}(\boldsymbol{\mu}\ ,\ t) = (0\ ,\ 0\ ,\ \Gamma_{\psi 1}^C(\boldsymbol{\mu}\ ,\ t)\ ,\ \Gamma_{\alpha 1}^C(\boldsymbol{\mu}\ ,\ t)\ ,\ \Gamma_{\alpha 2}^C(\boldsymbol{\mu}\ ,\ t))^T\ ,\ t \in [0, t_f)\ ,$$

where

$$\boldsymbol{\mu} = \left(\boldsymbol{q}\,,\, \boldsymbol{p}\,,\, \boldsymbol{Q}_1\,,\, \boldsymbol{Q}_2\,,\, t_f \right) .$$

Thus, the control law $\boldsymbol{\Gamma^C}(\boldsymbol{\mu}, t)$ constitutes the solution to the stabilisation and guidance problem posed in section 1. Furthermore, the calculation of the applied torques require the use of both the control law given by equation (4.4) , which is valid in any region excluding $d\psi_1/dt = 0$, and also the control law given by equation (3.1) which is valid for all regions excluding $\sin\theta = 0$. The control law $\boldsymbol{\Gamma^C}(\boldsymbol{\mu}\,,\, t)$ is therefore valid in all regions excluding $d\psi_1(t)/dt = 0$ or $\sin\theta(t) = 0$, $\forall\, t \in [0, t_f]$.

4.5 Numerical study

The control strategy developed above was used in a simulation of the disk-rod-rotors system. The parameters used were as follows

$$\begin{array}{lll} m_D = 10 \text{ kg} & m_{R1} = 0.75 \text{ kg} & m_{R2} = 0.25 \text{ kg} \\ m_{o1} = m_{o2} = 0.5 \text{ kg} & a = 0.4 \text{ m} & L_{12} = 0.75 \text{ m} \\ L_{13} = 0.5 \text{ m} & L_{11} = 0.25 \text{ m} & L_{o1} = L_{o2} = 0.3 \text{ m} \\ k_1 = 10 & k_2 = 24 & \end{array}$$

The initial conditions used are given by

$$\begin{array}{lll} \theta(0) = \dfrac{60\,\pi}{180} \text{ rad} & \dfrac{d\theta(0)}{dt} = 0 \text{ rad/sec} & \phi(0) = \dfrac{\pi}{2} \text{ rad} \\ \dfrac{d\phi(0)}{dt} = 0 \text{ rad/sec} & \psi_1(0) = 0 \text{ rad} & \dfrac{d\psi_1(0)}{dt} = 4 \text{ rad/sec} \\ \alpha_i(0) = 0 \text{ rad} & \dfrac{d\alpha_i(0)}{dt} = 0 \text{ rad/sec} & i = 1, 2 \\ u_3(0) = 0 \text{ rad/sec}^2 & x_c(0) = 0 \text{ m} & y_c(0) = 0 \text{ m} \end{array}$$

Using equation (2.73) the parameters and initial conditions yield the following conditions

$$\frac{dx_c(0)}{dt} = 1.6 \text{ m/ sec} \quad , \quad \frac{dy_c(0)}{dt} = 0 \text{ m/ sec} \ .$$

The simulation was performed using a Runge-Kutta order 4 algoritm with a timestep of 10^{-5} sec and the data was stored at intervals of 0.002 sec. Some of the results are displayed in figures (4.1) - (4.18).

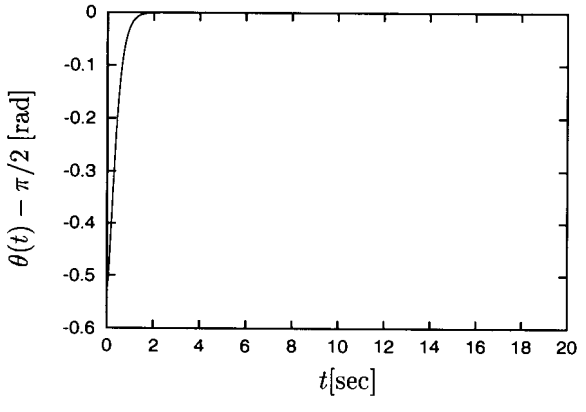

Figure 4.1: The values of $\theta(t) - \pi/2$, $t \in [0, t_f]$ in radians

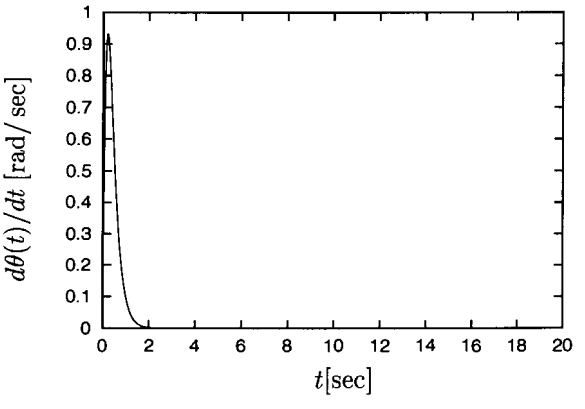

Figure 4.2: The values of $d\theta(t)/dt$, $t \in [0, t_f]$ in rad/ sec

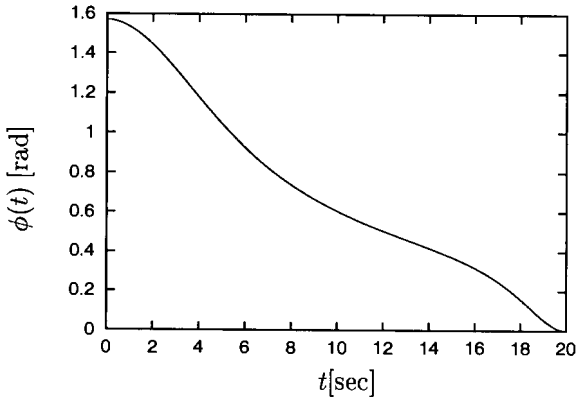

Figure 4.3: The values of $\phi(t)$, $t \in [0, t_f]$ in radians

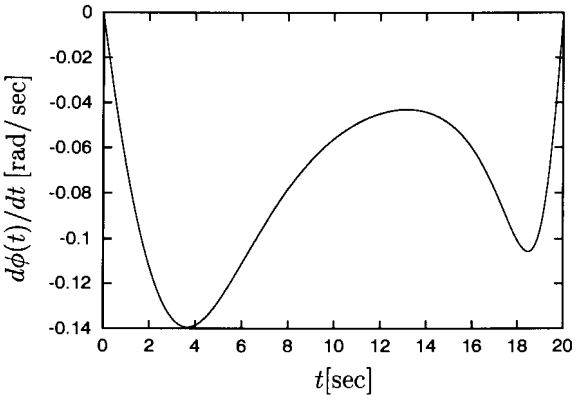

Figure 4.4: The values of $d\phi(t)/dt$, $t \in [0, t_f]$ in rad/ sec

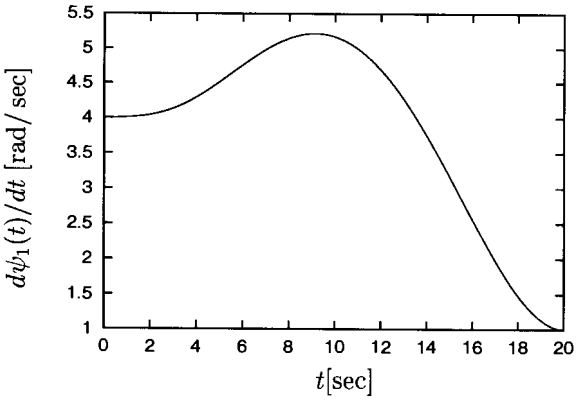

Figure 4.5: The values of $d\psi_1(t)/dt$, $t \in [0, t_f]$ in rad/ sec

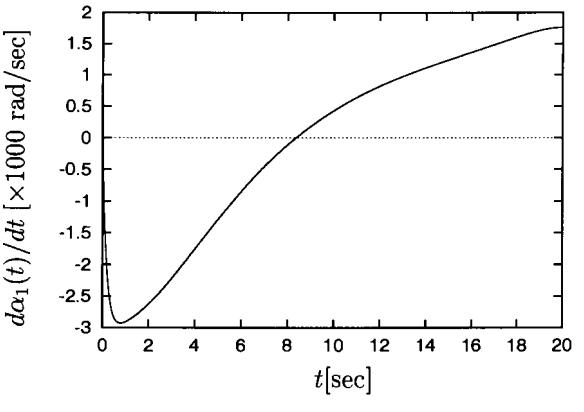

Figure 4.6: The values of $d\alpha_1(t)/dt$, $t \in [0, t_f]$ in $\times 1000$ rad/ sec

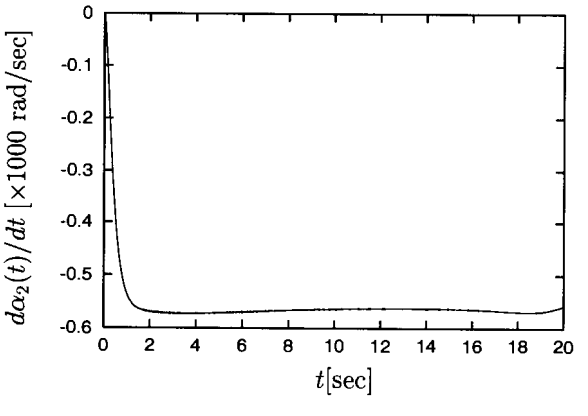

Figure 4.7: The values of $d\alpha_2(t)/dt$, $t \in [0, t_f]$ in $\times 1000$ rad/ sec

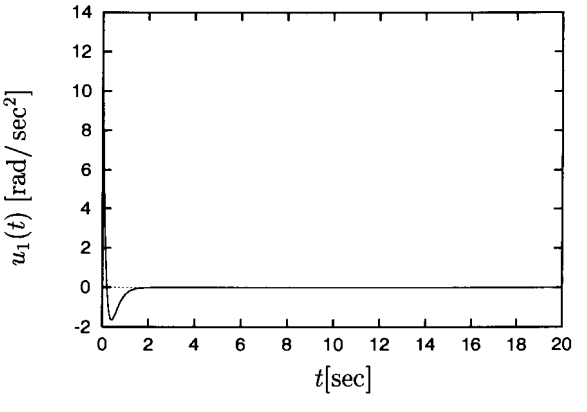

Figure 4.8: The values of $u_1(t)$, $t \in [0, t_f]$ in rad/ sec^2

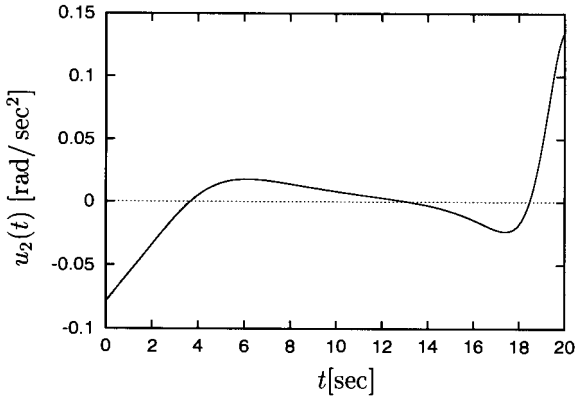

Figure 4.9: The values of $u_2(t)$, $t \in [0, t_f]$ in rad/ sec^2

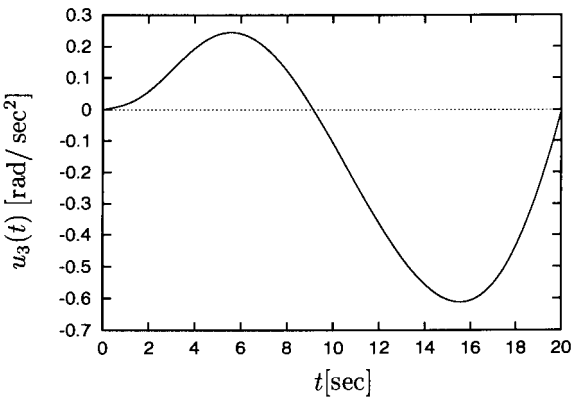

Figure 4.10: The values of $u_3(t)$, $t \in [0, t_f]$ in rad/ sec^2

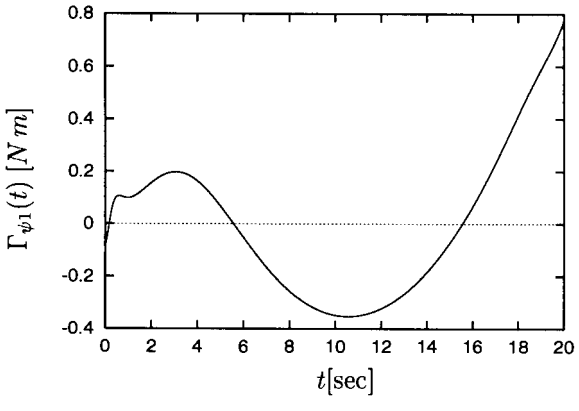

Figure 4.11: The values of $\Gamma_{\psi 1}(t)$, $t \in [0, t_f]$ in N·m

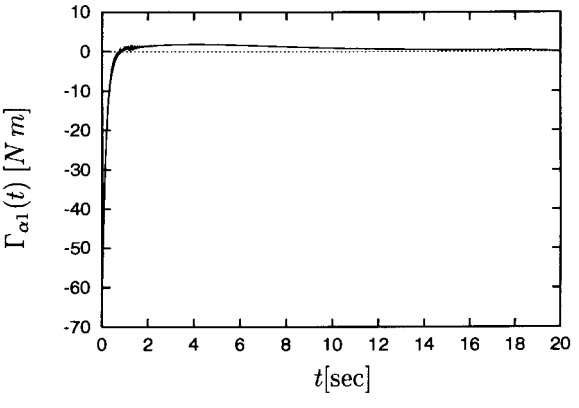

Figure 4.12: The values of $\Gamma_{\alpha 1}(t)$, $t \in [0, t_f]$ in N·m

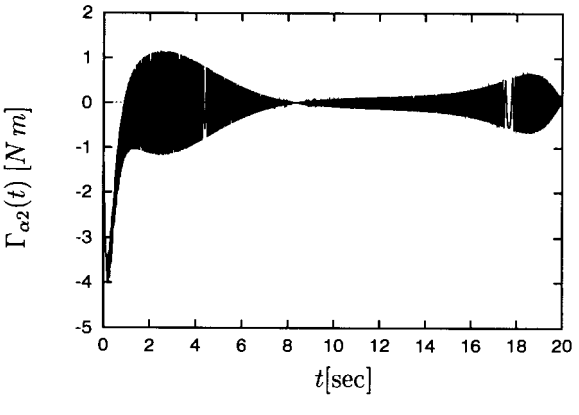

Figure 4.13: The values of $\Gamma_{\alpha 2}(t)$, $t \in [0, t_f]$ in N·m

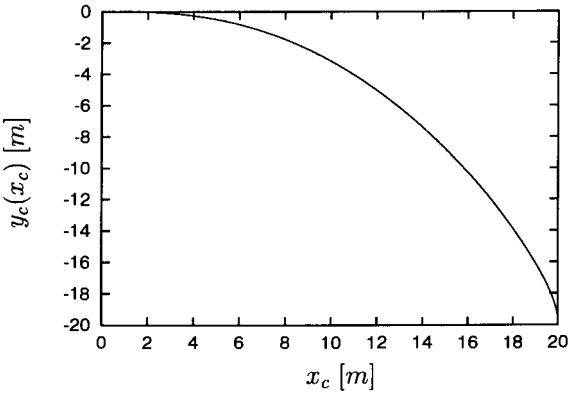

Figure 4.14: The values of y_c as a function of x_c

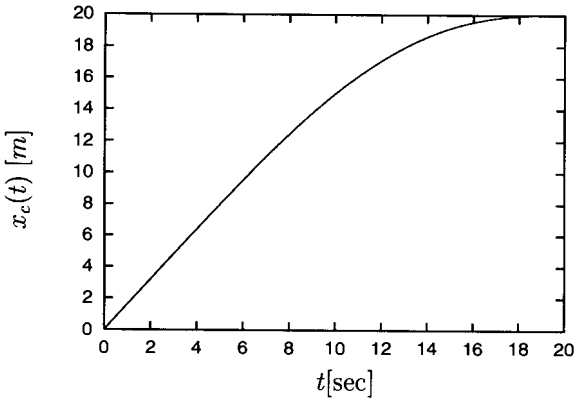

Figure 4.15: The values of $x_c(t)$, $t \in [0, t_f]$ in m

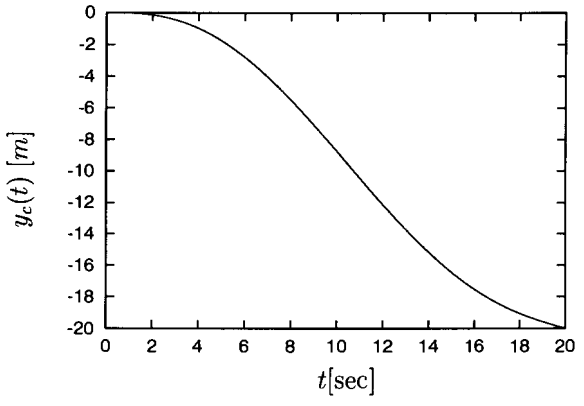

Figure 4.16: The values of $y_c(t)$, $t \in [0, t_f]$ in m

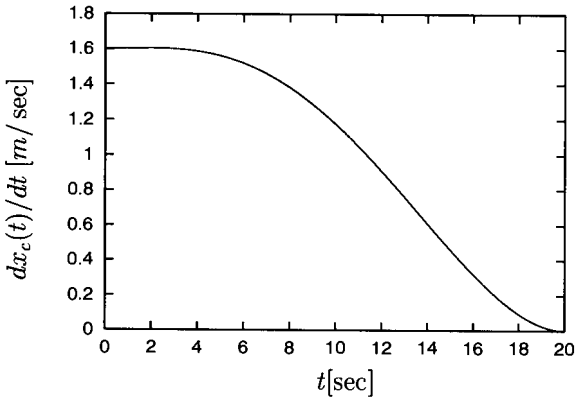

Figure 4.17: The values of $dx_c(t)/dt, t \in [0, t_f]$ in m/ sec

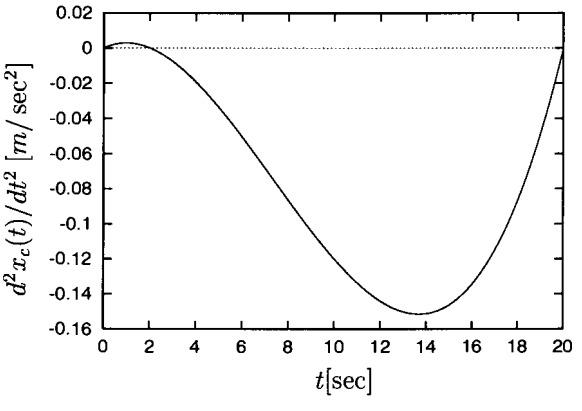

Figure 4.18: The values of $d^2x_c(t)/dt^2$, $t \in [0, t_f]$ in m/ sec^2

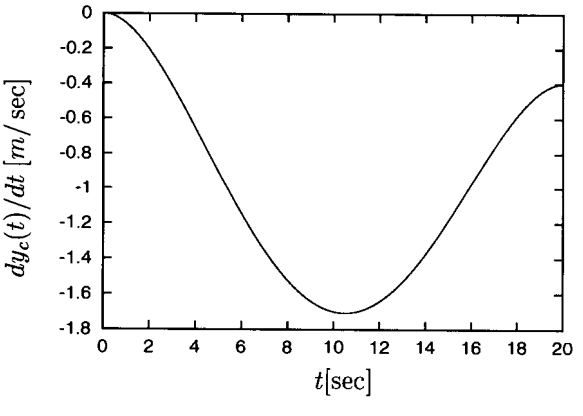

Figure 4.19: The values of dy_c/dt , $t \in [0, t_f]$ in m/ sec

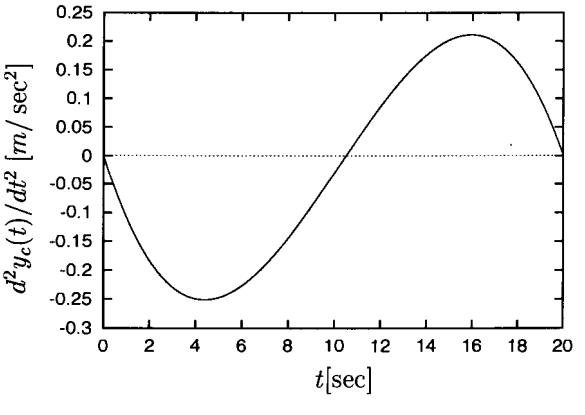

Figure 4.20: The values of $d^2y_c(t)/dt^2$, $t \in [0, t_f]$ in m/ sec^2

4.6 Conclusion and remarks

In this chapter a stabilisation and guidance problem is dealt with concerning the disk - rod - rotors system as described above. It was shown that the inverse dynamics control law, as discused in chapter 3 , yields a double integrator system. This system was used directly to obtain a control law such that the motion of the disk will be stabilised (the disk's plane will be vertical with respect to the horizontal plane).

In order to discuss the path controllability of the system the nonholonomic contraints involved with the motion of the disk were used to obtain a linear relationship between the point of contact between the disk and the $(X\ ,\ Y)$ - plane. Subsequently, this relationship was used to obtain a linear control problem in $\mathbb{R}^6$. It was shown that the linear control problem is controllable and as a result that the disk - rod - rotors system is path controllable.

A controller was developed for the linear system and finally a control law was proposed for the applied torques on the pedalling mechanism and to each of the rotors such that the motion of the disk will be stabilised and such that the speed and direction of the motion of the disk will be controlled in such a manner that the point of contact between the disk and the horizontal plane will move from one given point to another during a given time interval. Furthermore it was shown that the above mentioned control law is valid in all regions provided that the trajectory of the system never enters a region where $d\psi_1(t)/dt = 0$ or $\sin\theta(t) = 0\ ,\ \forall\ t \in [0, t_f]$. This condition does not pose any difficulty for well posed initial conditions since the stabilisation of the disk ensures that $\sin\theta \neq 0$ as $t \to \infty$.

Finally it should be noted that the control law governing the point to point control of the disk is an open loop control strategy and the controller does not compensate for any model uncertainties, variations in the initial conditions or any external disturbances. The control strategy could however be used to generate a path in $\mathbb{R}^6$ describing $x_c(t)$ and $y_c(t)$ and three of their derivatives on the time interval $[0, t_f]$. A feedback

tracking controller could then be used to track the path in a similar fashion as described in the previous chapter. Other methods for tracking the desired path could also be used, see for example [36] . A different approach using a piecewise smooth feedback control law in which the path to be tracked is given by a series of points can be found in [23] .

Chapter 5

Robustness

5.1 Introduction

This chapter deals with the robustness of the the tracking controller developed in chapter 3. The term robustness is used here to describe the compensation and/or invariance of the controller in the face of uncertainties in the system parameters. Feedback linearization strategies and inverse dynamics control laws such as given by equations (3.1) and (3.8) do not guarantee robustness, nor does the theory of these methods attempt to directly compensate for any parametric uncertainty.

Various robust control strategies have been developed in which the controller design compensates directly for possible uncertainties in dynamic systems. See for example [37] for the use of switching surfaces with min-max controllers and [38] for the use of continuous state feedback. Sliding control methods can also be used for uncertain nonlinear systems, see [39] for a development of control strategies for multivariable systems in the presence of disturbances and time-dependent parameter variations.

Another method to obtain robustness is to use adaptive control strategies. Adaptive control systems make use of on-line parameter estimation, see for example [40] and

[41]. Adaptive controllers have the advantage of improved performance over time and are highly useful in practical problems.

Implementing the above mentioned methods of robust control are beyond the scope of this work. The existing controller developed previously will instead be studied under the influence of parametric variations.

5.2 Tracking controller

The nature of the tracking controller developed in chapter 3 will be examined more closely in this section under the assumption that parametric uncertainties are present. The controller designed in chapter 3 was obtained by applying two successive inverse dynamics control laws which will be restated here but under the assumption that the system parameters differ from the controller parameters.

The parameters which are considered as uncertain are the size of the system (i.e. the lenght of the rod, the rotors and the radius of the disk) and the mass of the various components. In the rest of the chapter functions and constants concerning the system will be denoted in the same way as in chapters 2 and 3 , while in the case of the controller the functions and constants will be denoted by adding ($'$) to the symbols concerned.

The dynamics of the system were developed in chapter 2 and are given by equation (2.62) ,

$$\boldsymbol{\Omega}(\boldsymbol{q})\frac{d^2\boldsymbol{\Phi}}{dt^2} + \boldsymbol{F}(\boldsymbol{q},\boldsymbol{p}) = \boldsymbol{\Gamma}' \,, \tag{5.1}$$

where the matrix $\boldsymbol{\Omega}(\boldsymbol{q})$ and the vector $\boldsymbol{F}(\boldsymbol{q},\boldsymbol{p})$ both depend on the system parameters used. The control law given by equation (3.1) is assumed here to use a different set of parameters and can thus be stated as

$$\boldsymbol{\Gamma'} = \boldsymbol{\Omega'(q)u} + \boldsymbol{F'(q,p)} \,, \tag{5.2}$$

where the matrix $\boldsymbol{\Omega'(q)}$ and the vector $\boldsymbol{F'(q,p)}$ differ from $\boldsymbol{\Omega(q)}$ and $\boldsymbol{F(q,p)}$ only due to the difference in the parameters used. Using equations (5.1) and (5.2) gives the relation

$$\frac{d^2\boldsymbol{\Phi}}{dt^2} = \boldsymbol{\Omega^{-1}\,\Omega'\,u} + \boldsymbol{\Omega^{-1}\,(F' - F)} \,. \tag{5.3}$$

The decoupled linear relation given by equation (3.2) are therefore not valid if the controller has parameters which differ from the actual system parameters.

The dynamics for the point of contact between the disk and the horizontal plane is given by equation (3.6) ,

$$\begin{pmatrix} \frac{d^3x_c}{dt^3} \\ \frac{d^3y_c}{dt^3} \end{pmatrix} = a\,\boldsymbol{\Lambda} \begin{pmatrix} \frac{d^3\psi_1}{dt^3} \\ \frac{d^2\phi}{dt^2} \end{pmatrix} + \begin{pmatrix} a\,g_{c1}^{(\psi)} \\ a\,g_{c2}^{(\psi)} \end{pmatrix} \,, \tag{5.4}$$

where

$$g_{c1}^{(\psi)} = 2\frac{d^2\psi_1}{dt^2}\frac{d\phi}{dt}\cos\phi - \frac{d\psi_1}{dt}\left(\frac{d\phi}{dt}\right)^2 \sin\phi \,, \tag{5.5}$$

$$g_{c2}^{(\psi)} = 2\frac{d^2\psi_1}{dt^2}\frac{d\phi}{dt}\sin\phi + \frac{d\psi_1}{dt}\left(\frac{d\phi}{dt}\right)^2 \cos\phi \,. \tag{5.6}$$

This is similar to the functions (3.4) and (3.5) but $d^2\psi_1/dt^2$ was not substituted by u_3. The inverse dynamics control law given by equation (3.8) can now be written as

$$\begin{pmatrix} \frac{du_3}{dt} \\ u_2 \end{pmatrix} = (a')^{-1}\boldsymbol{\Lambda}^{-1} \begin{pmatrix} \nu_1 - a'\,g_{c1} \\ \nu_2 - a'\,g_{c2} \end{pmatrix} \,. \tag{5.7}$$

Equations (5.4) and (5.7) can be used in order to obtain the dynamics of the point of contact between the disk and the plane,

$$\begin{pmatrix} \frac{d^3x_c}{dt^3} \\ \frac{d^3y_c}{dt^3} \end{pmatrix} = \frac{a}{a'}\begin{pmatrix} \nu_1 \\ \nu_2 \end{pmatrix} + a\,\boldsymbol{\Lambda}\begin{pmatrix} \frac{d^3\psi_1}{dt^3} - \frac{du_3}{dt} \\ \frac{d^2\phi}{dt^2} - u_2 \end{pmatrix} + \begin{pmatrix} 2a\frac{d\phi}{dt}\cos\phi \\ 2a\frac{d\phi}{dt}\sin\phi \end{pmatrix}\left(\frac{d^2\psi_1}{dt^2} - u_3\right) \,. \tag{5.8}$$

Finally, the control laws for u_1 , ν_1 and ν_2 are given by

$$u_1 = -k_1 \frac{d\theta}{dt} - k_2\left(\theta - \frac{\pi}{2}\right) \quad , \tag{5.9}$$

$$\begin{aligned}\nu_1 = \frac{d^3x_{dr}}{dt^3} - \gamma_1\left(\frac{d^2x_c}{dt^2} - \frac{d^2x_{dr}}{dt^2}\right) - \gamma_2\left(\frac{dx_c}{dt} - \frac{dx_{dr}}{dt}\right) \\ - \gamma_3(x_c - x_{dr})\end{aligned} \quad , \tag{5.10}$$

$$\begin{aligned}\nu_2 = \frac{d^3y_{dr}}{dt^3} - \gamma_1\left(\frac{d^2y_c}{dt^2} - \frac{d^2y_{dr}}{dt^2}\right) - \gamma_2\left(\frac{dy_c}{dt} - \frac{dy_{dr}}{dt}\right) \\ - \gamma_3(y_c - y_{dr})\end{aligned} \quad , \tag{5.11}$$

which are the same control laws which were used in chapter 3 .

The feedback control laws given by equations (5.9) , (5.10) and (5.11) are designed to achieve asymptotic tracking for the case when there is no parameter uncertainty present. In the presence of parametric uncertainty these feedback control laws will still attempt to obtain the desired values for u_1 , ν_1 and ν_2. However, the effect that these control laws will subsequently have on the dynamics of the system given by equations (5.7) and (5.2) is uncertain. The next section deals with the study of the robustness of the system through a numerical study.

5.3 Numerical study

It was shown in the previous section that robustness of the control strategy developed in chapter 3 is not guaranteed. The linear decoupled nature of the control law is not valid in the presence of parametric uncertainty. In this section the robustness of the control strategy is examined via simulation.

The parameters used in the simulations are presented in table 5.1 . In each simulation the same set of parameters was used for the controller and a different set was used for the simulation of the motion of the system. At each timestep of a simu-

	Controller values	System values					
		Case 1	Case 2	Case 3	Case 4	Case 5	Case 6
m_D	10 kg	8 kg	12 kg	10 kg	10 kg	10 kg	10 kg
m_{R1}	0.75 kg	0.6 kg	0.9 kg	0.75 kg	0.75 kg	0.75 kg	0.75 kg
m_{R2}	0.25 kg	0.25 kg	0.25 kg	0.25 kg	0.25 kg	0.25 kg	0.25 kg
m_{o1}	0.5 kg	0.4 kg	0.6 kg	0.5 kg	0.5 kg	0.5 kg	0.5 kg
m_{o2}	0.5 kg	0.4 kg	0.6 kg	0.5 kg	0.5 kg	0.5 kg	0.5 kg
a	0.4 m	0.4 m	0.4 m	0.4 m	0.4 m	0.36 m	0.44 m
L_{11}	0.25 m	0.25 m	0.25 m	0.2 m	0.3 m	0.25 m	0.25 m
L_{12}	0.75 m	0.75 m	0.75 m	0.6 m	0.9 m	0.75 m	0.75 m
L_{13}	0.5 m	0.5 m	0.5 m	0.41 m	0.6 m	0.5 m	0.5 m
L_{o1}	0.3 m	0.3 m	0.3 m	0.24 m	0.36 m	0.3 m	0.3 m
L_{o2}	0.3 m	0.3 m	0.3 m	0.24 m	0.36 m	0.3 m	0.3 m

Table 5.1: Parameter values

lation the controller calculates the applied torque based upon the current position $\boldsymbol{q} = (\theta\,,\,\phi\,,\,\psi_1\,,\,\alpha_1\,,\,\alpha_2)$ and velocity $\boldsymbol{p} = d\boldsymbol{q}/dt$ together with the controller parameters, the motion of the system for that timestep is then simulated by using the torque calculated by the controller together with the parameter values of the system.

The reference path used is given by

$$x_{dr}(t) = 8\cos(\pi t/5) \quad , \quad y_{dr}(t) = 8\sin(\pi t/5)\,, \tag{5.12}$$

and the initial conditions used are given by

$$\theta(0) = \frac{60\,\pi}{180}\ \text{rad} \qquad \frac{d\theta(0)}{dt} = 0\ \text{rad/sec} \qquad \phi(0) = \frac{\pi}{2}\ \text{rad}$$

$$\frac{d\phi(0)}{dt} = 0\ \text{rad/sec} \qquad \psi_1(0) = 0\ \text{rad} \qquad \frac{d\psi_1(0)}{dt} = 4\ \text{rad/sec}$$

$$\alpha_i(0) = 0\ \text{rad} \qquad \frac{d\alpha_i(0)}{dt} = 0\ \text{rad/sec} \qquad i = 1, 2$$

$$u_3(0) = 0\ \text{rad/sec}^2 \qquad x_c(0) = 0\ \text{m} \qquad y_c = 0\ \text{m}$$

$$\frac{dx_c(0)}{dt} = 1.6\ \text{m/sec} \qquad \frac{dy_c(0)}{dt} = 0$$

The following parameters

$$k_1 = 10 \qquad k_2 = 24 \qquad \gamma_1 = 15$$

$$\gamma_2 = 75 \qquad \gamma_3 = 125$$

were used in all the simulations. The simulations were performed using a Runge-Kutta order 4 algoritm with a timestep of 10^{-5} sec and the data was stored at intervals of 0.002 sec.

Some of the results of the system parameters given by case 1 and case 2 are displayed in figures (5.1) - (5.7) . In each of the graphs the plot denoted by 'Controller' displays the result obtained if the system had the same parameters as the controller. Results which are not displayed are due to the fact that there was no noticeble difference between the results. Case 1 and case 2 represent changes only in the mass of the system components. Case 1 has a 20 % decrease and case 2 a 20 % increase in each parameter concerned. It should also be noted that m_{R2} was left unchanged - this causes the center mass of the rod not to coinside with the center mass of the disk, an assumption used in the derivation of the dynamical model. The results shows that the feedback nature of the control strategy ensures that the motion of the system converges to a specific path in state space. For example $\theta(t) - \pi/2$ stabilize at around $3°$ and $-4°$ for case 1 and 2 respectively, instead of the intended $0°$. The point of contact also tracks a path which is virtually the same as the intended path. Although a large change was made to the parameters the results show only small deviations from the intended performance.

Similar results are displayed in figures (5.8) - (5.12) for case 3 and case 4. Here the size of the components of the system, excluding the radius of the disk, was varied with $\pm 20\,\%$. The results resembles the case with no parametric difference better than case 1 and 2, for example, $\theta(t)$ differs with less than 1° from the intended value of $\pi/2$.

Finally, the radius of the disk was varied with $\pm 10\,\%$ in case 5 and 6. Some of the results are displayed in figures (5.13) - (5.19) . The change in the value of $\theta(t)$ is similar to that obtained in case 1 and 2. However, a large change in the values of $x_c(t)$ and $y_c(t)$ was observed. The reason for this is due to fact that the observed quantities used in the feedback control law does not include $x_c(t)$ and $y_c(t)$ or their derivatives, instead the controller calculates the coordinates for the point of contact between the disk and the plane indirectly. Any changes in the dinamics of $x_c(t)$ and $y_c(t)$ due to a change in the radius of the disk will therefore go unnoticed by the controller.

An estimate for the path tracked by $x_c(t)$ and $y_c(t)$ can be obtained as follows: From the results obtained we conclude the following relations

$$u_3(t) \approx \frac{d^2\psi_1(t)}{dt^2} \quad , \quad \frac{du_3(t)}{dt} \approx \frac{d^3\psi_1(t)}{dt^3} \quad , \quad u_2(t) \approx \frac{d^2\phi(t)}{dt^2} \; . \tag{5.13}$$

Equation (5.8) can then be approximated by

$$\frac{a'}{a}\begin{pmatrix} \frac{d^3x_c}{dt^3} \\ \frac{d^3y_c}{dt^3} \end{pmatrix} = \begin{pmatrix} \nu_1 \\ \nu_2 \end{pmatrix} \; , \tag{5.14}$$

which is a linear decoupled system with the values of $x_c(t)$ and $y_c(t)$ being scaled by a factor (a'/a) from the desired value.

The goal of the controller is to obtain

$$\sqrt{x_c^2(t) + y_c^2(t)} = 8 \text{ meters} \; , \tag{5.15}$$

this would result in

$$\sqrt{x_c^2(t) + y_c^2(t)} = \frac{a'}{a} 8 \text{ meters} , \tag{5.16}$$

which yields 7.2 m for case 5 and 8.8 m for case 6 , this is in fact very close to values obtained - see figures (5.18) and (5.19) . Similarly, for case 1 to case 4, there is no uncertainty in the radius of the disk and the results shows very little deviation from the desired values.

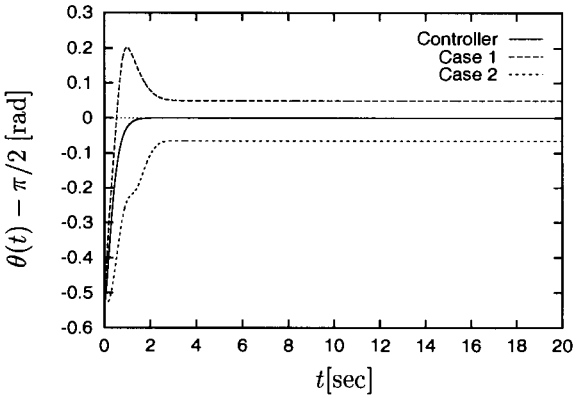

Figure 5.1: The values of $\theta(t) - \pi/2$, $t \in [0, t_f]$ in radians. Variation of system mass considered - comparison of Case 1 and Case 2.

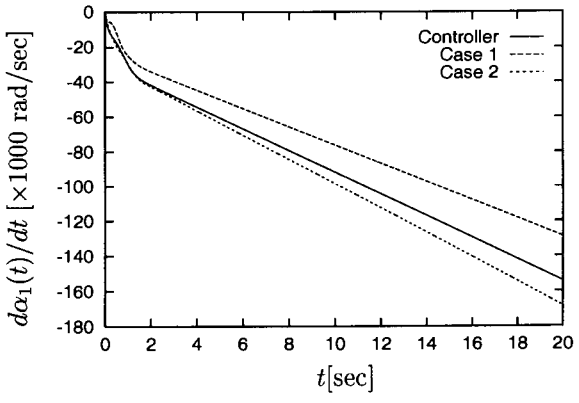

Figure 5.2: The values of $d\alpha_1(t)/dt$, $t \in [0, t_f]$ in $\times 1000$ rad/ sec. Variation of system mass considered - comparison of Case 1 and Case 2.

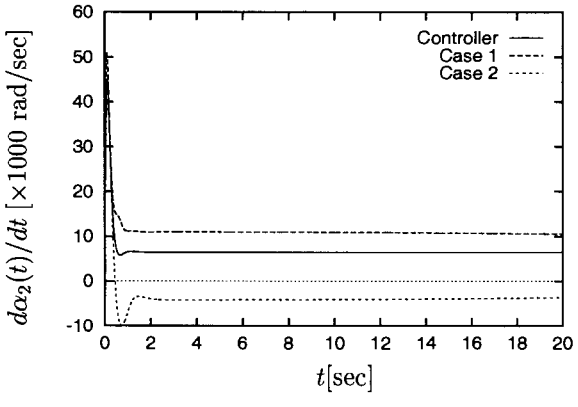

Figure 5.3: The values of $d\alpha_2(t)/dt$, $t \in [0, t_f]$ in $\times 1000$ rad/ sec. Variation of system mass considered - comparison of Case 1 and Case 2.

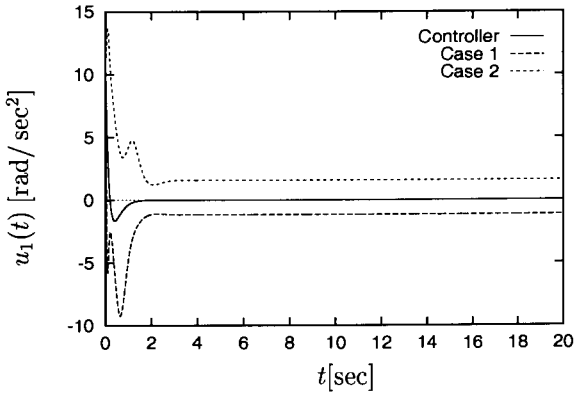

Figure 5.4: The values of $u_1(t)$, $t \in [0, t_f]$ in rad/ sec^2. Variation of system mass considered - comparison of Case 1 and Case 2.

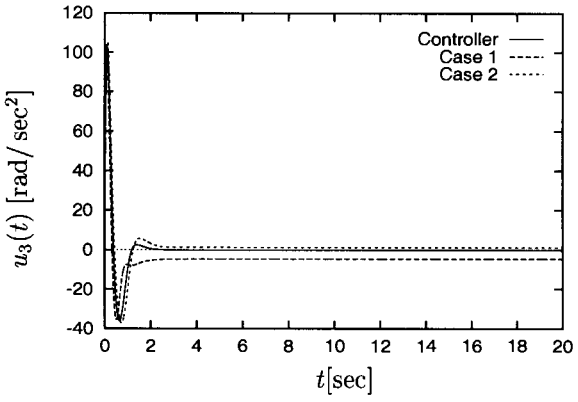

Figure 5.5: The values of $u_3(t)$, $t \in [0, t_f]$ in rad/sec^2. Variation of system mass considered - comparison of Case 1 and Case 2.

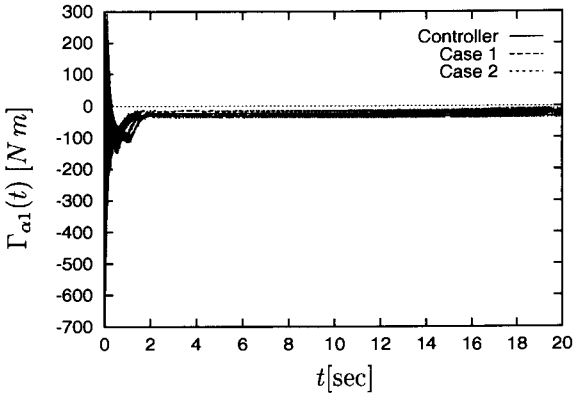

Figure 5.6: The values of $\Gamma_{\alpha 1}(t)$, $t \in [0, t_f]$ in N·m. Variation of system mass considered - comparison of Case 1 and Case 2.

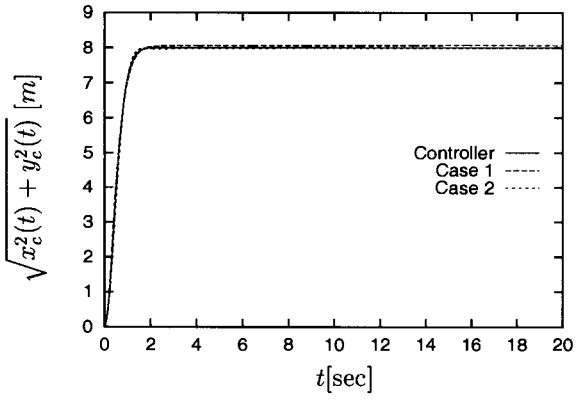

Figure 5.7: The values of $\sqrt{x_c^2(t) + y_c^2(t)}$, $t \in [0, t_f]$ in m. Variation of system mass considered - comparison of Case 1 and Case 2.

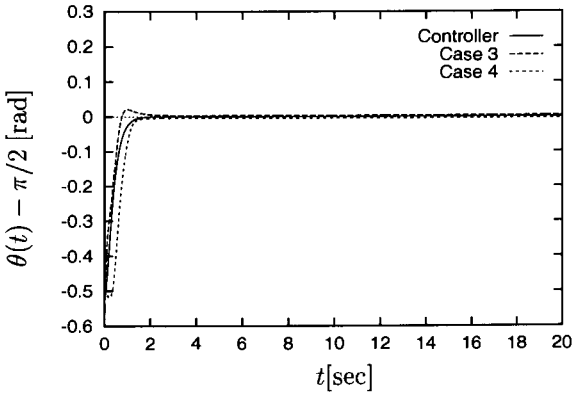

Figure 5.8: The values of $\theta(t) - \pi/2$, $t \in [0, t_f]$ in radians. Variation of system size considered - comparison of Case 3 and Case 4.

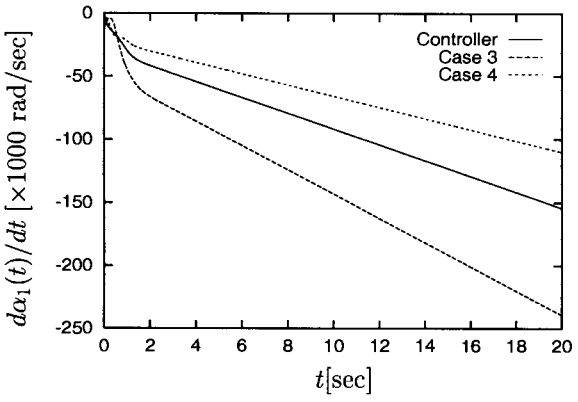

Figure 5.9: The values of $d\alpha_1(t)/dt$, $t \in [0, t_f]$ in $\times 1000$ rad/sec. Variation of system size considered - comparison of Case 3 and Case 4.

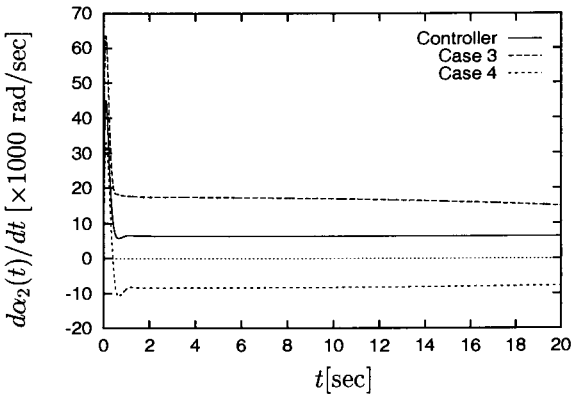

Figure 5.10: The values of $d\alpha_2(t)/dt, t \in [0, t_f]$ in $\times 1000$ rad/sec. Variation of system size considered - comparison of Case 3 and Case 4.

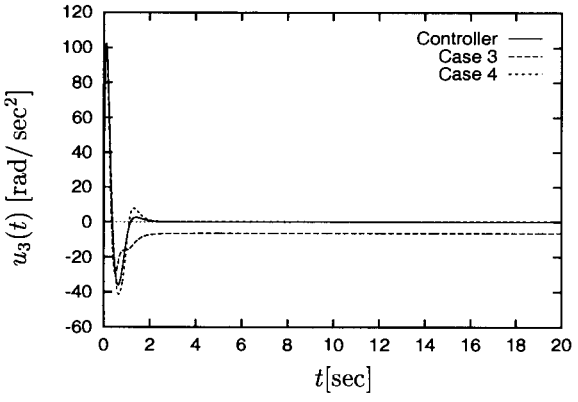

Figure 5.11: The values of $u_3(t)$, $t \in [0, t_f]$ in rad/sec^2. Variation of system size considered - comparison of Case 3 and Case 4.

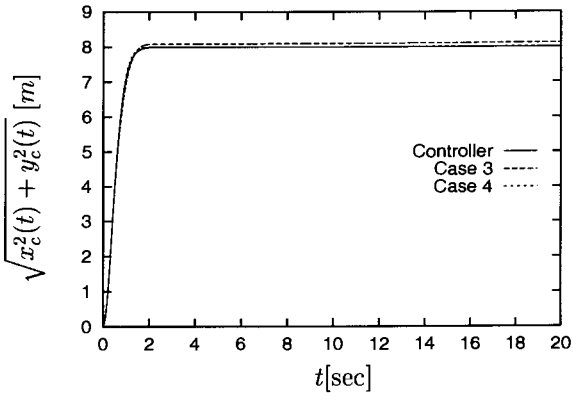

Figure 5.12: The values of $\sqrt{x_c^2(t) + y_c^2(t)}$, $t \in [0, t_f]$ in m. Variation of system size considered - comparison of Case 3 and Case 4.

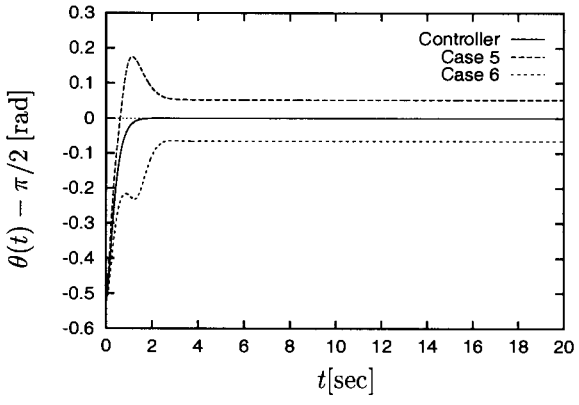

Figure 5.13: The values of $\theta(t) - \pi/2, t \in [0, t_f]$ in radians. Variation of radius of disk considered - comparison of Case 5 and Case 6.

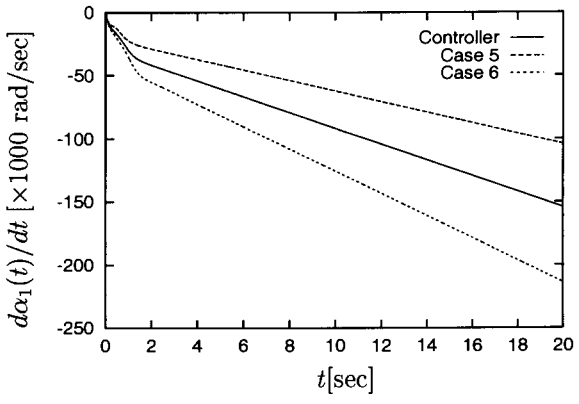

Figure 5.14: The values of $d\alpha_1(t)/dt, t \in [0, t_f]$ in $\times 1000$ rad/sec. Variation of radius of disk considered - comparison of Case 5 and Case 6.

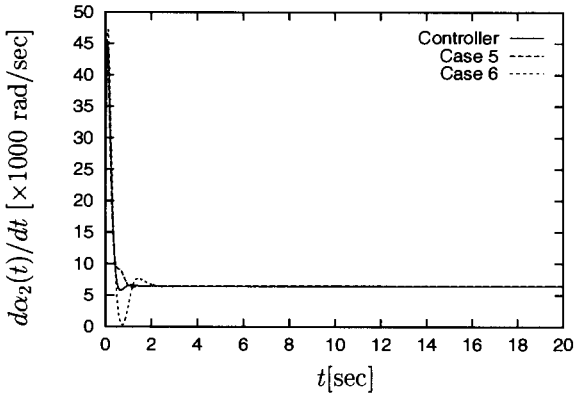

Figure 5.15: The values of $d\alpha_2(t)/dt, t \in [0, t_f]$ in $\times 1000$ rad/sec. Variation of radius of disk considered - comparison of Case 5 and Case 6.

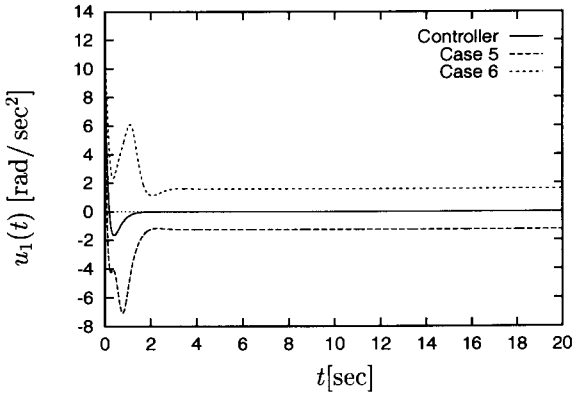

Figure 5.16: The values of $u_1(t)$, $t \in [0, t_f]$ in rad/sec^2. Variation of radius of disk considered - comparison of Case 5 and Case 6.

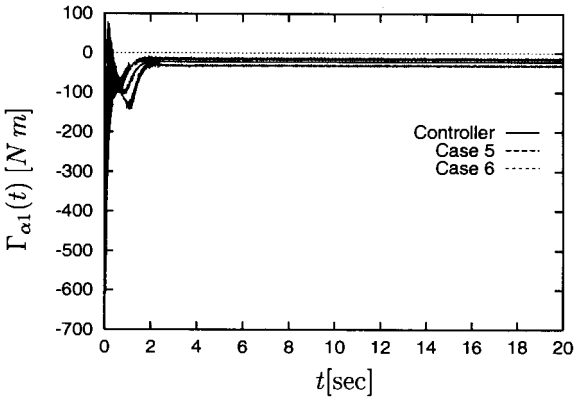

Figure 5.17: The values of $\Gamma_{\alpha 1}(t)$, $t \in [0, t_f]$ in N·m. Variation of radius of disk considered - comparison of Case 5 and Case 6.

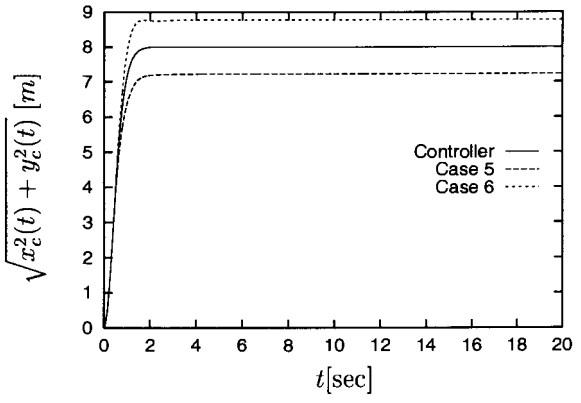

Figure 5.18: The values of $\sqrt{x_c^2(t) + y_c^2(t)}$, $t \in [0, t_f]$ in m. Variation of radius of disk considered - comparison of Case 5 and Case 6.

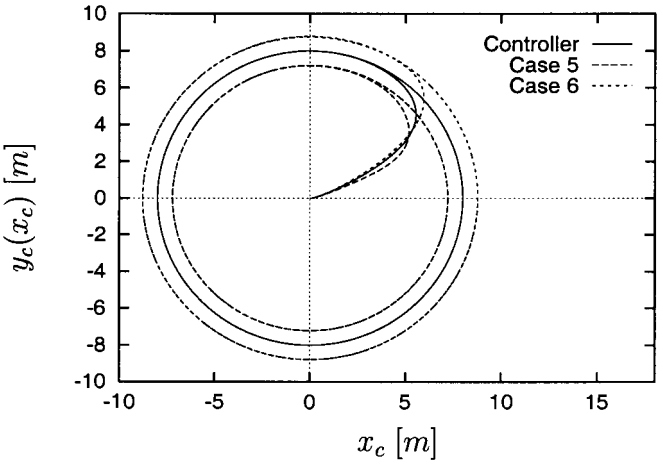

Figure 5.19: The values of y_c as a function of x_c. Variation of radius of disk considered - comparison of Case 5 and Case 6.

5.4 Conclusion and remarks

In this chapter the tracking controller designed in chapter 3 was examined for the effects that parametric uncertainties have on the performance of the controller. It was shown that the fundamental design of the controller does not take parametric uncertainties into account. The system obtained after applying the inverse dynamics control laws is neither linear nor is it decoupled as was the case in the absence of all uncerties.

The presence of the feedback control laws (5.9) - (5.11) was shown in a numerical study to improve the performance of the overall control strategy. The results obtained show that large uncertainties in the parameters result in relatively small deviations from the desired behavior of the system. Variations in the radius of the disk was shown (equation (5.14)) to cause proportional variations in the path followed by the point of contact between the disk and the plane. This was also demonstrated by the numerical study where very small deviations from the desired path was observed when the controller and the system had the same radius.

In practice the size and mass of the components can be expected to be measured to a high degree of accuracy. The results of this chapter shows that in the presence of small uncerties the controller will result in stable operation of the system and that the resultant behavior of the system will be close to the desired behavior. However, if the control strategy has to be implemented on different systems with different dimensions it will be necessary to change the parameters in each case to obtain results of high accuracy.

Chapter 6

Extended Inverse Dynamics Control

6.1 Introduction

In the previous chapters of this work inverse dynamics control has been used to create the control laws for the applied torques on the given system. The importance of inverse dynamics control for solving nonlinear control problems was discussed in chapter 1. In this chapter an extended inverse dynamics control is introduced, (see also [42] , which introduces the notion of extended inverse dynamics control) which is an extension of the basic theory of inverse dynamics control and is applicable to a larger class of control problems. An example concerning the constrained motion of an articulated crane is also solved here using extended inverse dynamics control.

Inverse dynamics control is applied to dynamical systems given by

$$\boldsymbol{M}(\boldsymbol{q})\frac{d^2\boldsymbol{q}}{dt^2} + \boldsymbol{f}(\boldsymbol{q},\boldsymbol{p}) = \boldsymbol{u}\ , \tag{6.1}$$

where $\boldsymbol{M}(\boldsymbol{q})$ is a given $n \times n$ matrix with $\det \boldsymbol{M}(\boldsymbol{q}) > 0$, $\forall\ \boldsymbol{q} \in D$. Here D is a given

open set in $\mathbb{R}^n$ and the inverse dynamics control will subsequently be defined on the set D . $\boldsymbol{f} : D \times D \rightarrow \mathbb{R}^n$ is a given vector function , and $\boldsymbol{u} = (u_1 , \ldots , u_n)^T$ represents the control vector of the system.

Note for example that equation (2.62) has this form and equation (3.6) has a form similar to (6.1) but higher order derivatives are present. See also for example [6] for inverse dynamics control applied to a different system also of the general form given by equation (6.1).

Consider a dynamical system given by the following equations

$$\boldsymbol{N}(\boldsymbol{q})\frac{d^2\boldsymbol{q'}}{dt^2} + \boldsymbol{f}(\boldsymbol{q},\boldsymbol{p}) = \boldsymbol{E}(\boldsymbol{q'})\,\boldsymbol{u} \ , \tag{6.2}$$

$$\frac{d^2\boldsymbol{q''}}{dt^2} = \sum_{i=1}^{m} \boldsymbol{H}_i(\boldsymbol{q})\frac{d^2 q_i}{dt^2} + \boldsymbol{G}(\boldsymbol{q},\boldsymbol{p}) \ , \tag{6.3}$$

where, in equation (6.2) , $\boldsymbol{q} = (q_1 , \ldots , q_n)^T$ is a vector of generalized coordinates; $\boldsymbol{p} = d\boldsymbol{q}/dt$; $\boldsymbol{q'} = (q_1 , \ldots , q_m)^T$, $m \leq n$. $\boldsymbol{N}(\boldsymbol{q})$ is is a given $m \times m$ matrix with $\det \boldsymbol{N}(\boldsymbol{q}) > 0$, $\forall\ \boldsymbol{q} \in D$ where D is a given open set in $\mathbb{R}^n$; $\boldsymbol{E}(\boldsymbol{q'})$ is a given $m \times m$ matrix with $\det \boldsymbol{E}(\boldsymbol{q'}) \neq 0$, $\forall\ \boldsymbol{q'} \in D_O$ where D_O is a given open set in $\mathbb{R}^m$. $\boldsymbol{f} : D \times D \rightarrow \mathbb{R}^m$ is a given vector function , and $\boldsymbol{u} = (u_1 , \ldots , u_m)^T$ is the vector of applied generalized forces on the system. Furthermore, in equation (6.3), $\boldsymbol{q''} = (q_{m+1} , \ldots , q_n)^T$; $\boldsymbol{H}_i$, $i = 1 , \ldots , m$, and $\boldsymbol{G}$ are given vector functions in $\mathbb{R}^{n-m}$.

Choose a control law in the form

$$\boldsymbol{E}(\boldsymbol{q'})\boldsymbol{u} = \boldsymbol{N}(\boldsymbol{q})\boldsymbol{v} + \boldsymbol{f}(\boldsymbol{q},\boldsymbol{p}) \ , \tag{6.4}$$

where $\boldsymbol{v} = (v_1 , \ldots , v_m)^T$ is an auxilary control vector. The above control law will be referred to here as an extended inverse dynamics control law. From equations (6.2) and (6.4) it follows that

$$\frac{d^2\boldsymbol{q}'}{dt^2} = \boldsymbol{v} \quad , \quad q \in D \, , \tag{6.5}$$

which is called a double integrator system. Furthermore, equations (6.3) and (6.5) yield

$$\frac{d^2\boldsymbol{q}''}{dt^2} = \sum_{i=1}^{m} \boldsymbol{H}_i(\boldsymbol{q})\, v_i + \boldsymbol{G}(\boldsymbol{q}, \boldsymbol{p}) \, , \tag{6.6}$$

which is a complementary nonlinear system.

In conclusion, a dynamical system given by equations (6.2) and (6.3) , can be partially linearized by using an extended inverse dynamics control law of the form given by equation (6.4). This leads to a representation of the system which consists of a double integrator system, equation (6.5) and a complementory nonlinear system given by equation (6.6). Furthermore, equation (6.5) is a decoupled linear system (double integrator system) which is completely controllable, [1].

Equation (6.6) can also be considered as representing the internal dynamics of the system given by equations (6.2) and (6.3). The internal dynamics of the system represents the part of the system which cannot be seen from the external input-output relationship given in this case by (6.5). The presence of an "unobservable" part of the system occurs when the number of controls, m , is less than the number of generalized coordinates, n. Different approaches have been used to handle the problem of internal dynamics, see for example [43] in which the internal dynamics of a system is shown to be bounded. The question of feedback stabilization of underactuated systems is examined in [44] using topological methods and general feedback design methods, explicit feedback laws are derived to stabilize a spacecraft with only two independent controls around an attractor.

However, in this chapter a different, and much simpler approach is taken. For a given control problem with a given a time interval $[0, t_f]$, $t_f > 0$, the control objectives is to choose the auxilary control vector $\boldsymbol{v}(\cdot)$ in such a manner that the following conditions are met:

(i) $\boldsymbol{q}'(t) \in D_O$ for all $t \in [0, t_f]$

(ii) $\boldsymbol{q}(t) \in D$ for all $t \in [0, t_f]$

(iii) The components of $\boldsymbol{q}(\cdot)$ will satisfy all the goals and constraints placed upon it for the specific problem under consideration.

Once these specifications and goals are met, then, by using the control law (6.4) , the values of the control vector $\boldsymbol{u}(\cdot)$ can be calculated from the values of $\boldsymbol{v}(\cdot)$. The constraints mentioned in point (iii) can be used to place bounds on $\boldsymbol{q}''(t)$ and its derivatives on the interval $[0, t_f]$, resulting in the stabilisation of the internal dynamics of the system.

6.2 Example

In this section a physical system is described which can be represented by equations (6.2) and (6.3) stated in the previous section. The dynamical model of the system is derived in the next section and the rest of the chapter deals with the control of this system, using extended inverse dynamics control.

The system (see figure 6.1 and also [45]) is composed of two identical uniform links of lenght l and mass $m = m_1 = m_2$. The upper ends of the links are freely pivoted at a joint O of mass m_0. The lower end of each link is freely pivoted to a disk which acts as a wheel. The two wheels, denoted by W_1 and W_2 respectively, are identical, with radius a and mass m_D. The controls are via the driving torques on the wheels, it is assumed that a torque u_1 is acting on wheel W_1 and a torque u_2 is acting on wheel W_2. A mass M is hanging from the point O on a rod of lenght L , $L < l$, which is freely pivoted from the point O. It is assumed in this work that the mass of this rod is negligible with respect to M. The motion of the system is confined to the $(X$, $Z)$ - plane, and it is furthermore assumed here that the motion of the wheels involves rolling

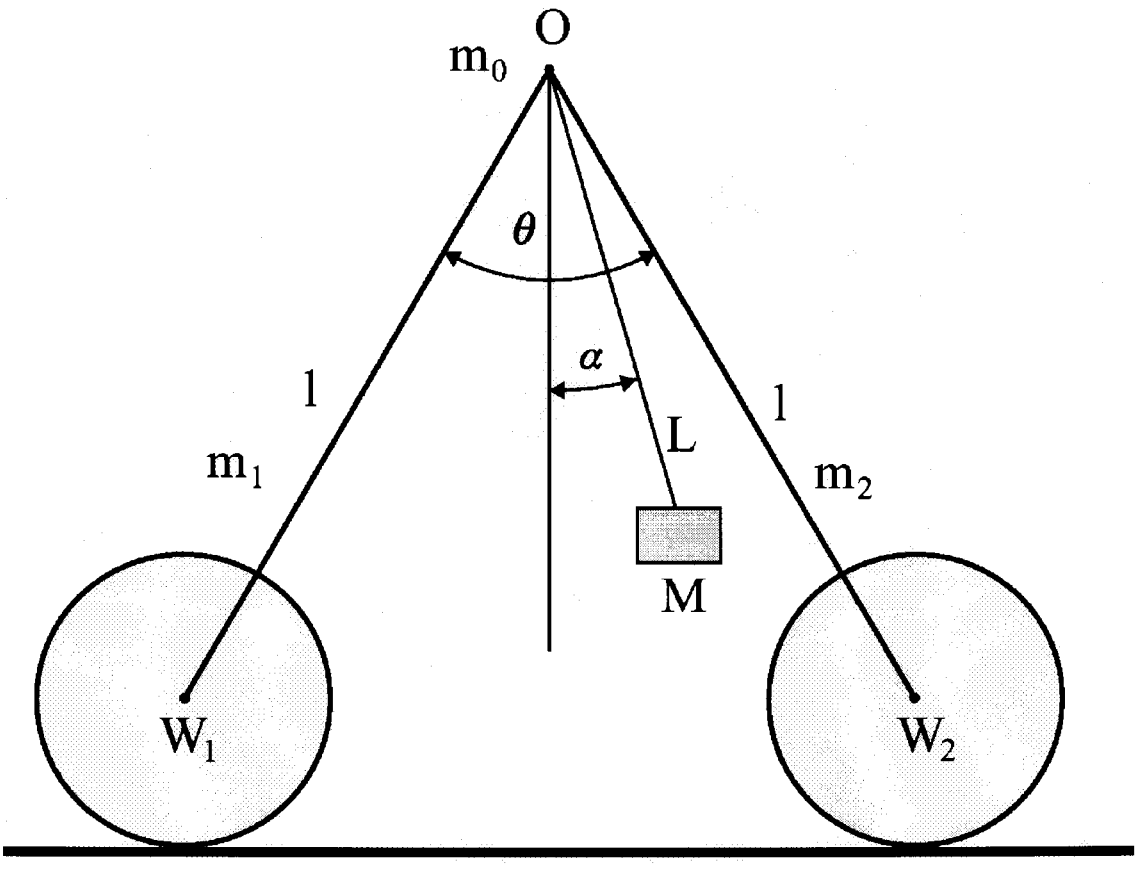

Figure 6.1: View of moving crane

without slipping.

6.3 Dynamical model

Let $(\boldsymbol{I}, \boldsymbol{J}, \boldsymbol{K})$ be an inertial frame of reference with the system constrained to move in the $(\boldsymbol{I}, \boldsymbol{K})$ - plane. The inertial frame of reference is furthermore chosen with the center of the wheels on the $\boldsymbol{I}$ - axis. The axis of both wheels is thus along the unit vector $\boldsymbol{J}$.

Denote by (x, z) the position of the point O in the $(\boldsymbol{I}, \boldsymbol{K})$ - plane. The coordinate z is given in terms of the angle between the two links, θ, by

$$z = l \cos \frac{\theta}{2} . \tag{6.7}$$

Denote by $\boldsymbol{r}_{D1}$ and $\boldsymbol{r}_{D2}$ the center of mass of wheel 1 and wheel 2 respectively,

$$\boldsymbol{r}_{D1} = (x - l \sin \frac{\theta}{2}) \, \boldsymbol{I} , \tag{6.8}$$

$$\boldsymbol{r}_{D2} = (x + l \sin \frac{\theta}{2}) \, \boldsymbol{I} . \tag{6.9}$$

Denote by $\boldsymbol{r}_1$ and $\boldsymbol{r}_2$ the center of mass of rod 1 and rod 2 respectively,

$$\boldsymbol{r}_1 = (x - l_{01} \sin \frac{\theta}{2}) \, \boldsymbol{I} + l_{01} \cos \frac{\theta}{2} \, \boldsymbol{K} , \tag{6.10}$$

$$\boldsymbol{r}_2 = (x + l_{01} \sin \frac{\theta}{2}) \, \boldsymbol{I} + l_{01} \cos \frac{\theta}{2} \, \boldsymbol{K} , \tag{6.11}$$

where $l_{01} = l/2$ has been used.

Let $\boldsymbol{r}_0$ denote the position of point O

$$\begin{aligned} \boldsymbol{r}_0 &= x \, \boldsymbol{I} + z \, \boldsymbol{K} \\ &= x \, \boldsymbol{I} + l \cos \frac{\theta}{2} \, \boldsymbol{K} . \end{aligned} \tag{6.12}$$

The angular velocity of wheel W_1 is denoted by $d\psi_1/dt$ and the angular velocity of wheel W_2 is denoted by $d\psi_2/dt$.

The condition that the motion of the wheels on the plane involves rolling without slipping leads to the following kinematical constraints

$$\frac{dx}{dt} - l_{01}\frac{d\theta}{dt}\cos\frac{\theta}{2} - a\frac{d\psi_1}{dt} = 0 \quad , \quad \frac{dx}{dt} + l_{01}\frac{d\theta}{dt}\cos\frac{\theta}{2} - a\frac{d\psi_2}{dt} = 0 \, . \tag{6.13}$$

Let I_D denote the moment of inertia of each of the wheels about its axis and let I_R denote the moment of inertia of each of the links about a vector in the $\boldsymbol{J}$ - direction located at the center of mass of the link.

The Lagrangian of the system is then given by

$$\begin{aligned}
\mathfrak{L} = \frac{1}{4}\Bigg[& 4\,g\,L\,M\,\cos\alpha - 8\,g\,l_{01}\,m\,\cos\frac{\theta}{2} - 8\,g\,l_{01}\,M\,\cos\frac{\theta}{2} \\
& - 8\,g\,l_{01}\,m_0\,\cos\frac{\theta}{2} + 2\,(2\,m + M + 2\,m_D + m_0)\left(\frac{dx}{dt}\right)^2 \\
& + 4\,L\,M\,\cos\alpha\,\frac{dx}{dt}\,\frac{d\alpha}{dt} + 2\,L^2\,M\left(\frac{d\alpha}{dt}\right)^2 - 4\,L\,l_{01}\,M\,\sin\alpha\,\sin\frac{\theta}{2}\,\frac{d\alpha}{dt}\,\frac{d\theta}{dt} \\
& + I_R\left(\frac{d\theta}{dt}\right)^2 + {l_{01}}^2\,m\left(\frac{d\theta}{dt}\right)^2 + {l_{01}}^2\,M\left(\frac{d\theta}{dt}\right)^2 + 2\,l_{01}^2\,m_D\left(\frac{d\theta}{dt}\right)^2 \\
& + l_{01}^2\,m_0\left(\frac{d\theta}{dt}\right)^2 - l_{01}^2\,M\,\cos\theta\left(\frac{d\theta}{dt}\right)^2 + 2\,l_{01}^2\,m_D\,\cos\theta\left(\frac{d\theta}{dt}\right)^2 \\
& - l_{01}^2\,m_0\,\cos\theta\left(\frac{d\theta}{dt}\right)^2 + 2\,I_D\left(\frac{d\psi_1}{dt}\right)^2 + 2\,I_D\left(\frac{d\psi_2}{dt}\right)^2\Bigg] \quad .
\end{aligned} \tag{6.14}$$

By applying the Lagrangian method, [4] , to the Lagrangian, $\mathfrak{L}$, together with the kinematical constraints, equations (6.13), the following dynamical model of the system was obtained after some algebraic manipulations. Note that the constraints given by equations (6.13) are integrable, but was used in kinematical form to simplify calculations.

$$\boldsymbol{N}(\boldsymbol{q})\frac{d^2\boldsymbol{q}'}{dt^2} + \boldsymbol{f}(\boldsymbol{q},\boldsymbol{p}) = \boldsymbol{E}(\boldsymbol{q}')\boldsymbol{u}\ , \tag{6.15}$$

$$\frac{d^2\boldsymbol{q}''}{dt^2} = \sum_{i=1}^{2} \boldsymbol{H}_i(\boldsymbol{q})\frac{d^2 q_i}{dt^2} + \boldsymbol{G}(\boldsymbol{q},\boldsymbol{p})\ , \tag{6.16}$$

where $\boldsymbol{q} = (x, \theta, \alpha)^T$, $\boldsymbol{q}' = (x, \theta)^T$, $\boldsymbol{q}'' = \alpha$ and $\boldsymbol{p} = d\boldsymbol{q}/dt$.

Denoting the components of $\boldsymbol{N}$ by N_{ij} , $i,j = 1,2$ and of $\boldsymbol{E}$ by E_{ij} , $i,j = 1,2$

$$N_{11} = m_0 + 2\,m + 2\,m_D + M\sin^2\alpha + 2\,\frac{I_D}{a^2} \quad ,$$

$$N_{12} = N_{21} = M l_{01}\sin\frac{\theta}{2}\sin\alpha\cos\alpha \quad ,$$

$$N_{22} = \frac{2}{3}\,m\,l_{01}^2 + 2\left(m_D + \frac{I_D}{a^2}\right) l_{01}^2\cos^2\frac{\theta}{2} + m_0\,l_{01}^2\sin^2\frac{\theta}{2} + M l_{01}^2\sin^2\frac{\theta}{2}\cos^2\alpha\ ,$$

and

$$E_{11} = E_{12} = a^{-1} \quad , \quad E_{21} = -\,E_{22} = -\,\frac{l_{01}}{a}\cos\frac{\theta}{2}\ .$$

The vector $\boldsymbol{f}$ is given by $\boldsymbol{f}(\boldsymbol{q},\boldsymbol{p}) = (f_1\ ,\ f_2)^T$ with

$$f_1 = h_1 - h_3\,\frac{\cos\alpha}{L} \quad , \quad f_2 = h_2 + h_3\,\frac{l_{01}}{L}\sin\frac{\theta}{2}\sin\alpha\ ,$$

where

$$h_1 = -\,ML\left(\frac{d\alpha}{dt}\right)^2\sin\alpha\ ,$$

$$h_2 = l_{01}\left(\frac{m_0}{2} + \frac{M}{2} - m_D - \frac{I_D}{a^2}\right)\left(\frac{d\theta}{dt}\right)^2\sin\frac{\theta}{2}\cos\frac{\theta}{2}$$
$$-\,g l_{01}(M + m + m_0)\sin\frac{\theta}{2} - ML l_{01}\left(\frac{d\alpha}{dt}\right)^2\sin\frac{\theta}{2}\cos\alpha\ ,$$

$$h_3 = -\,ML\left[\frac{l_{01}}{2}\left(\frac{d\theta}{dt}\right)^2\cos\frac{\theta}{2} - g\right]\sin\alpha\ .$$

Also, the functions used in equation (6.16) are given by

$$\boldsymbol{H}_1 = -\frac{1}{L}\cos\alpha \quad , \quad \boldsymbol{H}_2 = \frac{l_{01}}{L}\sin\frac{\theta}{2}\sin\alpha \, ,$$

$$\boldsymbol{G} = \left[\frac{l_{01}}{2}\left(\frac{d\theta}{dt}\right)^2\cos\frac{\theta}{2} - g\right]\frac{\sin\alpha}{L} \, .$$

Furthermore, it can be shown that

$$\det \boldsymbol{N}(\boldsymbol{q}) \geq I_1 N_{22}(\boldsymbol{q}) \quad \text{and} \quad \det \boldsymbol{E}(\boldsymbol{q}') = 2\frac{l_{01}}{a^2}\cos\frac{\theta}{2} \, . \tag{6.17}$$

The sets D and D_O in this example are therefore given by

$$D = \mathbb{R}^3 \quad \text{and} \quad D_O = \mathbb{R}^2 - (\mathbb{R} \times L) \, ,$$

where

$$L = \left\{(2k+1)\,\pi \;:\; k = 0\,,\, \pm 1\,,\, \pm 2\,,\, \ldots\right\} \, ,$$

is the set of values of θ for which the matrix $\boldsymbol{E}$ is not invertible ($\det \boldsymbol{E} = 0$).

The physical nature of the system also constitutes certain constraints on the system. The angle θ is constrained to remain between

$$\theta_s \leq \theta \leq \theta_o \, , \tag{6.18}$$

where the minimum angle θ_s is the angle where the wheels touch and the maximum angle θ_o is the angle where the suspended mass is touching the surface. These angles are given by the followng relations

$$\theta_s = 2\sin^{-1}\frac{a}{l} \quad , \quad \theta_o = 2\cos^{-1}\frac{L-a}{l} \, . \tag{6.19}$$

6.4 Inverse dynamics control

The control law given by equation (6.4) is now applied to the system described by equations (6.15) and (6.16). Equations (6.4) - (6.6) then reduce, for the system under consideration, to

$$\begin{pmatrix} u_1 \\ u_2 \end{pmatrix} = D^{-1} \begin{pmatrix} \frac{l_{01}}{a}\cos\frac{\theta}{2} & -\frac{1}{a} \\ \frac{l_{01}}{a}\cos\frac{\theta}{2} & \frac{1}{a} \end{pmatrix} \left[\begin{pmatrix} N_{11} & N_{12} \\ N_{21} & N_{22} \end{pmatrix} \begin{pmatrix} v_1 \\ v_2 \end{pmatrix} + \begin{pmatrix} f_1 \\ f_2 \end{pmatrix} \right] , \tag{6.20}$$

$$\begin{pmatrix} \frac{d^2x}{dt^2} \\ \frac{d^2\theta}{dt^2} \end{pmatrix} = \begin{pmatrix} v_1 \\ v_2 \end{pmatrix} , \tag{6.21}$$

$$\frac{d^2\alpha}{dt^2} = \boldsymbol{H}_1 v_1 + \boldsymbol{H}_2 v_2 + \boldsymbol{G} , \tag{6.22}$$

where

$$D = 2\frac{l_{01}}{a^2}\cos\frac{\theta}{2} .$$

The extended inverse dynamics control law, equation (6.20) enables the system given by equations (6.15) and (6.16) to be represented by a double integrator system given by equation (6.21) and a complementary nonlinear equation , equation (6.22) , together with (6.20) with which the applied torques can be calculated. In the rest of the chapter a constrained control problem is solved which illustrates the advantage of having the system representation in the form given by equations (6.20) - (6.22) .

6.5 Constrained control problem

In this section a constrained control problem for the system given by equations (6.15) and (6.16) is dealt with. As mentioned before, the solution of the problem will be carried out via equations (6.20) - (6.22). A command function $\boldsymbol{\delta} = (\delta_1, \delta_2)$ is introduced such that

$$\frac{dv_i(t)}{dt} = \frac{\delta_i(t) - v_i(t)}{\beta_i} \quad , \quad i = 1, 2 \, , \tag{6.23}$$

where β_1 and β_2 are positive real numbers to be specified later. The command functions δ_1 and δ_2 defined by equation (6.23) are added to equations (6.20) - (6.22) to ensure that the behaviour of $\boldsymbol{v}(\cdot)$ is smooth, and subsequently, that the behaviour of $\boldsymbol{u}(\cdot)$ is smooth, which in turn represent the torques applied to wheels. Define the vector $\boldsymbol{\eta}$ as

$$\boldsymbol{\eta}(t) = \left(x(t) \, , \, \frac{dx(t)}{dt} \, , \, \theta(t) \, , \, \frac{d\theta(t)}{dt} \, , \, \alpha(t) \, , \, \frac{d\alpha(t)}{dt} \, , \, v_1(t) \, , \, v_2(t) \right) \, ,$$

The control problem dealt with here can now be stated as follows: Given a final time t_f , $0 < t_f < \infty$, and an initial state of the system, $\boldsymbol{\eta}(0) \in \mathbb{R}^8$, find a command function $\boldsymbol{\delta}(t)$, $t \in [0, t_f]$ such that

(1) $\boldsymbol{\eta}(t_f) = \boldsymbol{\eta}_f$, where $\boldsymbol{\eta}_f$ is a given point in $\mathbb{R}^8$.

(2) During the time interval $[0, t_f]$ the motion of the system is subject to the following contraints $\theta_{min} \leq \theta(t) \leq \theta_{max}$, $|\alpha(t)| \leq \gamma_1$, $\left| \frac{d\alpha(t)}{dt} \right| \leq \gamma_2$, (6.24) where $\theta_{max} > \theta_{min} > 0$, $\gamma_1 > 0$ and $\gamma_2 > 0$ are given numbers, and $[\theta_{min} \, , \, \theta_{max}] \subset D_O$.

The contrained control problem posed above is solved here using the method of feasible command strategies, see for example [5] , [46] or [47]. Henceforward, we will only be interested in the motion of the system, during a time interval $[0, t_f]$ where $t_f > 0$ is a given number.

Let $0 = \tau_0 < \tau_1 < \tau_2 < \cdots < \tau_{N-1} = t_f$ be a partition of the interval $[0, t_f]$ such that $\tau_{i+1} - \tau_i = \Delta$, $i = 0, \ldots, N-2$. Denote by Λ the class of all command functions $\boldsymbol{\delta}_c = (\delta_1 \, , \, \delta_2) : [0, t_f] \to \mathbb{R}^2$ such that

$$\delta_1(t) = A_i(t) \, c_i + B_i(t) \, c_{i+1} \quad , \quad t \in [\tau_i \, , \, \tau_{i+1}] \, , \, i = 0, \ldots, N-2 \, , \tag{6.25}$$

$$\delta_2(t) = A_i(t)\, c_{N+i} + B_i(t)\, c_{N+i+1} \quad , \quad t \in [\tau_i\ ,\ \tau_{i+1}]\ ,\ i = 0, \ldots , N-2\ , \tag{6.26}$$

where

$$A_i(t) = (\tau_{i+1} - t)/\Delta \quad , \quad B_i(t) = (t - \tau_i)/\Delta \quad , \quad i = 0, \ldots , N-2\ . \tag{6.27}$$

That is, if $\boldsymbol{\delta} \in \Lambda$ then $\delta_i(t)$, $i = 1, 2$, is piecewise linear on the given partition $\{\tau_i\}_{i=0}^{N-1}$. Furthermore, the partition $\{\tau_i\}_{i=0}^{N-1}$, together with the $2N$ numbers $\{c_0\ ,\ \ldots\ ,\ c_{2N-1}\}$ completely define $\boldsymbol{\delta}$ via equations (6.25) - (6.27).

Let $\boldsymbol{\delta}_c$ be an element of Λ and denote by $\boldsymbol{\zeta}(t\ ,\ \boldsymbol{\eta}_0\ ;\ \boldsymbol{\delta}_c)$, $t \geq 0$ the solution to equations (6.21) and (6.22), together with equation (6.23), whenever it exists, such that $\boldsymbol{\zeta}(0\ ,\ \boldsymbol{\eta}_0\ ;\ \boldsymbol{\delta}_c) = \boldsymbol{\eta}_0$, $\boldsymbol{\eta}_0 \in \mathbb{R}^8$.

Define the following sets

$$A_p = \left\{ \boldsymbol{\eta} \in \mathbb{R}^8 : \theta_{min} \leq \eta_3 \leq \theta_{max}\ ,\ |\eta_5| \leq \gamma_1\ ,\ |\eta_6| \leq \gamma_2 \right\}\ , \tag{6.28}$$

$$A_f = \left\{ \boldsymbol{\eta} \in \mathbb{R}^8 : |\eta_1 - x_f| \leq \epsilon_1\ ,\ |\eta_2| \leq \epsilon_2\ ,\ |\eta_4| \leq \epsilon_4 \right\}\ , \tag{6.29}$$

where θ_{min} , θ_{max} , γ_1 , γ_2 , ϵ_i , $i = 1, 2, 4$ are given positive numbers and x_f is a given real number and the notation $\boldsymbol{\eta} = (\eta_1\ ,\ \eta_2\ ,\ \ldots\ ,\ \eta_8)^T$ was used.

Given a fixed time $t_f > 0$; a partition $\{\tau_i\}_{i=0}^{N-1}$ and an initial state $\boldsymbol{\eta}_0 \in A_p$. The problem dealt with here is to find a command strategy $\boldsymbol{\delta}_c \in \Lambda$ such that

$$\boldsymbol{\zeta}(t\ ,\ \boldsymbol{\eta}_0\ ;\ \boldsymbol{\delta}_c) \in A_p \quad , \quad t \in [0, t_f]\ , \tag{6.30}$$

and

$$\boldsymbol{\zeta}(t_f\ ,\ \boldsymbol{\eta}_0\ ;\ \boldsymbol{\delta}_c) \in A_f\ . \tag{6.31}$$

Equation (6.30) represents the path contraints placed upon the system during the time interval $[0, t_f]$ and equation (6.31) represents the boundary condition on system at the final time $t = t_f$. A command strategy $\boldsymbol{\delta}_c \in \Lambda$ for which equations (6.30) and (6.31) are satisfied will be called here a feasible command strategy.

6.6 Solution of the problem

Define the following functions

$$G(z, \lambda) = [\max(z - \lambda\ ,\ 0) + \min(z + \lambda\ ,\ 0)]^2 \quad , \quad \lambda > 0\ , \tag{6.32}$$

$$G_{12}(z, \lambda_1, \lambda_2) = [\max(z - \lambda_2\ ,\ 0) + \min(z - \lambda_1\ ,\ 0)]^2 \quad , \quad \lambda_2 > \lambda_1 > 0\ , \tag{6.33}$$

for all $z \in \mathbb{R}$. Let $\boldsymbol{c} = (c_0\ ,\ c_1\ ,\ \ldots\ ,\ c_{N-1}) \in \mathbb{R}^{2N}$, and let $\boldsymbol{\delta}_c \in \Lambda$ be defined by equations (6.25), (6.26) and (6.27). Note that the notation used here to describe the motion of the system is given by: $\zeta_1(t, \boldsymbol{\eta}_0\,;\, \boldsymbol{\delta}_c) = x(t)$, $\zeta_2(t, \boldsymbol{\eta}_0\,;\, \boldsymbol{\delta}_c) = dx(t)/dt$, $\zeta_3(t, \boldsymbol{\eta}_0\,;\, \boldsymbol{\delta}_c) = \theta(t)$, $\zeta_4(t, \boldsymbol{\eta}_0\,;\, \boldsymbol{\delta}_c) = d\theta(t)/dt$, $\zeta_5(t, \boldsymbol{\eta}_0\,;\, \boldsymbol{\delta}_c) = \alpha(t)$, $\zeta_6(t, \boldsymbol{\eta}_0\,;\, \boldsymbol{\delta}_c) = d\alpha(t)/dt$, $\zeta_7(t, \boldsymbol{\eta}_0\,;\, \boldsymbol{\delta}_c) = v_1(t)$, $\zeta_8(t, \boldsymbol{\eta}_0\,;\, \boldsymbol{\delta}_c) = v_2(t)$.

Define the following functional $F(\boldsymbol{c})$ by

$$\begin{aligned} F(\boldsymbol{c}) = {} & P_1\, G(\zeta_1(t, \boldsymbol{\eta}_0\,;\, \boldsymbol{\delta}_c) - x_f\ ,\ \epsilon_1)\ +\ P_2\, G(\zeta_2(t, \boldsymbol{\eta}_0\,;\, \boldsymbol{\delta}_c)\ ,\ \epsilon_2) \\ & + P_4\, G(\zeta_4(t, \boldsymbol{\eta}_0\,;\, \boldsymbol{\delta}_c)\ ,\ \epsilon_4)\ +\ P_9 \int_0^{t_f} G_{12}(\zeta_3(t, \boldsymbol{\eta}_0\,;\, \boldsymbol{\delta}_c)\ ,\ \theta_{min}\ ,\ \theta_{max})\ dt \\ & + P_{10} \int_0^{t_f} \Big[G(\zeta_5(t, \boldsymbol{\eta}_0\,;\, \boldsymbol{\delta}_c)\ ,\ \gamma_1) + G(\zeta_6(t, \boldsymbol{\eta}_0\,;\, \boldsymbol{\delta}_c)\ ,\ \gamma_2) \Big]\ dt \quad , \end{aligned} \tag{6.34}$$

where P_k , $k = 1, 2, 4, 9, 10$ are given positive numbers and the desired state at the final time is give by

$$\boldsymbol{\eta}_f = (x_f\ ,\ 0\ ,\ \theta_f\ ,\ 0\ ,\ \alpha_f\ ,\ \alpha_{df}\ ,\ v_{1D}\ ,\ v_{2D})^T\ .$$

In the problem dealt with here the numbers θ_f , α_f , α_{df} , v_{1D} and v_{2D} are unspecified. However, θ_f , α_f and α_{df} must still satisfy equation (6.24) , that is $\boldsymbol{\eta}_f \in A_p$, which follows from equation (6.34) .

The functional $F(\boldsymbol{c})$ is a sum of penalty functions which incorporates all the control and state constraints together with the required goals. An element $\boldsymbol{c}^0 \in \mathbb{R}^{2N}$ for which $F(\boldsymbol{c}^0) = 0$ will be called here a feasible command vector. A command strategy $\boldsymbol{\delta}^0$ which is the solution of equations (6.25) and (6.26) using $\boldsymbol{c} = \boldsymbol{c}^0$ will be called a feasible command strategy.

Thus, if a feasible command strategy, induced by a feasible command vector, is applied to the system, the solution of equations (6.20) - (6.22) and (6.23) , given by $\boldsymbol{\zeta}(t, \boldsymbol{\eta}_0\,;\,\boldsymbol{\delta}^0)$, will be such that equations (6.30) and (6.31) are satisfied. All the specifications and goals of the control problem posed here are then satisfied.

In this section the control problem considered can then be stated as follows: Find an element $\boldsymbol{c}^0 \in \mathbb{R}^{2N}$ such that $F(\boldsymbol{c}^0) = 0$. The computations of $\boldsymbol{c}^0$ was conducted by solving an unconstrained minimisation problem for $F(\boldsymbol{c})$ on $\mathbb{R}^{2N}$. The minimisation of the functional $F(\boldsymbol{c})$ was done by using the gradient method described in [48] and [49] and subsequently applying the gradient method described in [50](p. 104). At each step during the minimisation process the command function $\boldsymbol{\delta}(\cdot)$ was computed using equations (6.25) and (6.26) after which $F(\boldsymbol{c})$ was calculated by solving equations (6.20) - (6.23) on $[0, t_f]$. Finally, once $\boldsymbol{c}^0$ has been calculated then $\boldsymbol{u}(\cdot)$ can be calculated using equation (6.20) .

6.7 Numerical study

In this section an example is solved using the control strategy proposed in the previous section. The following set of parameters has been used

$$M = 1000 \text{ kg} \qquad m = 100 \text{ kg} \qquad m_0 = 50 \text{ kg}$$
$$m_D = 50 \text{ kg} \qquad l = 4 \text{ m} \qquad L = 2.5 \text{ m}$$
$$a = 0.5 \text{ m} \qquad \beta_1 = \beta_2 = 0.1 \qquad N = 11$$

The initial conditions used are given by

$$x(0) = 0 \text{ m} \qquad \frac{dx(0)}{dt} = 0 \text{ m/sec} \qquad \theta(0) = 1.45 \text{ rad}$$
$$\frac{d\theta(0)}{dt} = 0 \text{ rad/sec} \qquad \alpha(0) = 0 \text{ rad} \qquad \frac{d\alpha(0)}{dt} = 0 \text{ rad/sec}$$
$$v_1(0) = 0 \text{ m/sec}^2 \qquad v_2(0) = 0 \text{ rad/sec}^2$$

The parameters used in the penalty functional $F(\boldsymbol{c})$ are given by

$$x_f = 20 \text{ m} \qquad \epsilon_1 = 0.1 \text{ m} \qquad \epsilon_2 = 0.1 \text{ m/sec}$$
$$\epsilon_4 = \pi/60 \text{ rad} \qquad \theta_{min} = 0.3 \text{ rad} \qquad \theta_{max} = 2.0 \text{ rad}$$
$$\gamma_1 = 6 \text{ deg} \qquad \gamma_2 = 6 \text{ deg/sec} \qquad P_1 = P_4 = 10$$
$$P_2 = 10^2 \qquad P_9 = 5 \times 10^3 \qquad P_{10} = 5 \times 10^2$$

The calculation of equations (6.21) , (6.22) and (6.23) was done by using a Runge - Kutta order four algoritm with a stepsize $\Delta = 10^{-5}$ sec . Some of the results obtained are shown in figures (6.2) - (6.11)

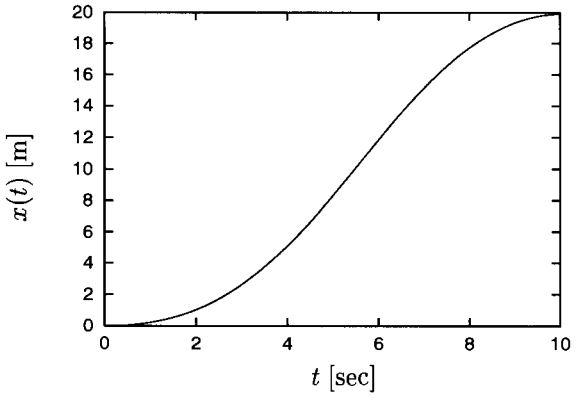

Figure 6.2: The values of $x(t)$, $t \in [0, t_f]$ in m

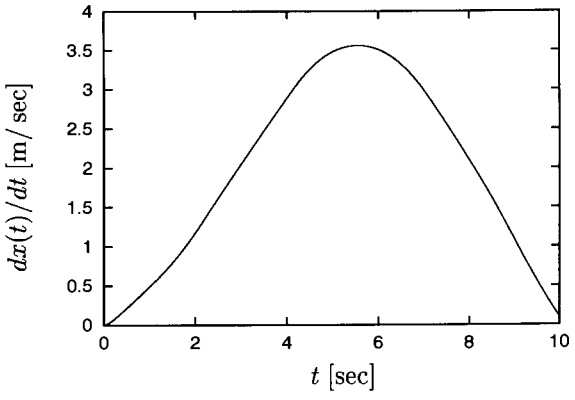

Figure 6.3: The values of $dx(t)/dt$, $t \in [0, t_f]$ in m/ sec

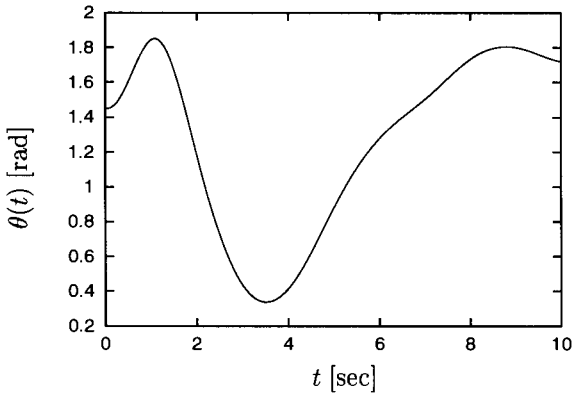

Figure 6.4: The values of $\theta(t)$, $t \in [0, t_f]$ in radians

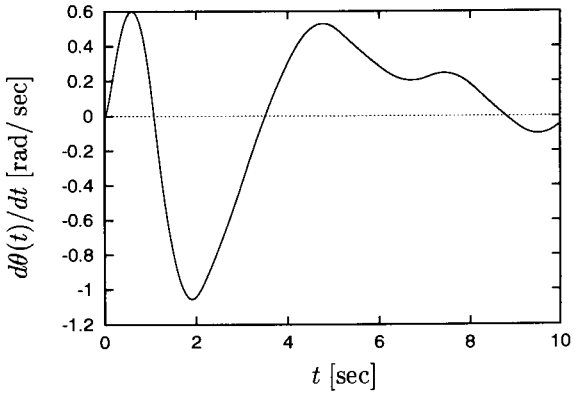

Figure 6.5: The values of $d\theta(t)/dt$, $t \in [0, t_f]$ in rad/ sec

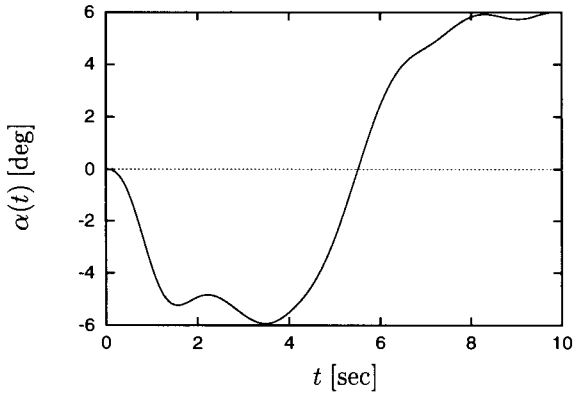

Figure 6.6: The values of $\alpha(t)$, $t \in [0, t_f]$ in degrees

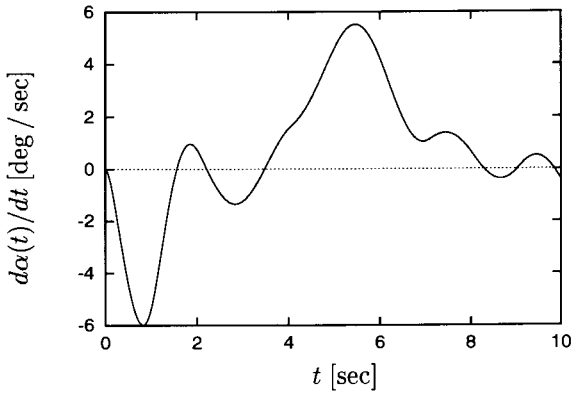

Figure 6.7: The values of $d\alpha(t)/dt$, $t \in [0, t_f]$ in deg/ sec

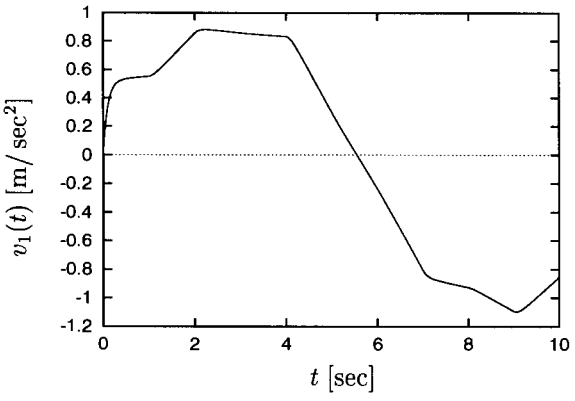

Figure 6.8: The values of $v_1(t), t \in [0, t_f]$ in m/sec^2

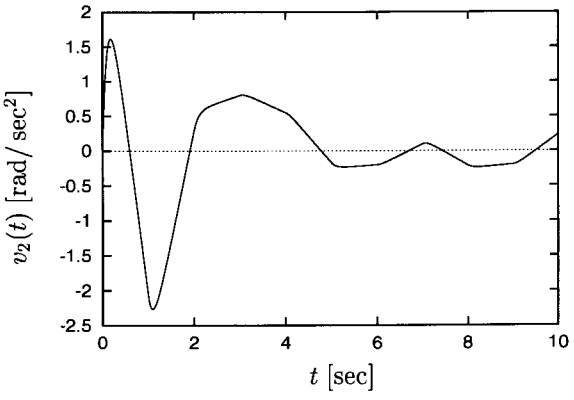

Figure 6.9: The values of $v_2(t), t \in [0, t_f]$ in rad/sec^2

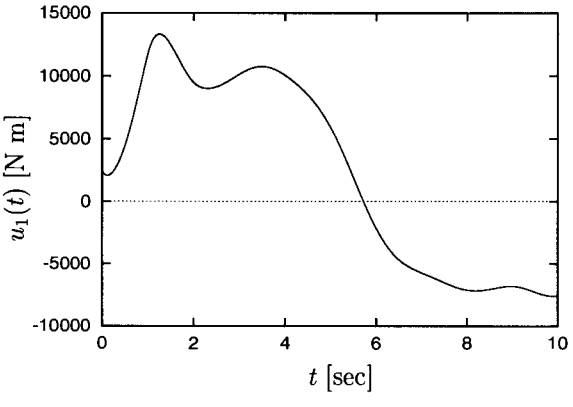

Figure 6.10: The values of $u_1(t)$, $t \in [0, t_f]$ in N·m

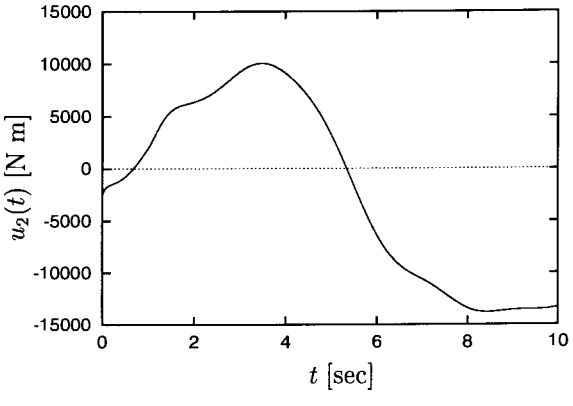

Figure 6.11: The values of $v_2(t)$, $t \in [0, t_f]$ in N·m

6.8 Conclusion and remarks

This chapter introduced the concept of extended inverse dynamics control and its application to systems of the form given by equations (6.2) and (6.3). It was shown that such a system can be represented by a double integrator system, equation (6.5), together with a complementory nonlinear part given by equation (6.6).

A problem concerning the constrained motion of an articulated crane is solved to demonstrate the effectiveness of extended inverse dynamics control. A feasible control strategy is developed to solve the problem by calculating a feasible open-loop trajectory in state space under which the internal dynamics of the system remains bounded and the motion of the crane reach its desired final position in the pre-specified time interval $[0, t_f]$.

Any gradient method, or search method can be applied for the solution of $F(\boldsymbol{c}) = 0$, $c \in \mathbb{R}^{2N}$. However, each step of the minimisation process involves the solution of the dynamics of the system on the interval $[0, t_f]$. This calculation takes most of the computation time. Using equations (6.5) and (6.6) is much less time consuming than using equations (6.2) and (6.3) directly.

Chapter 7

Conclusion

This work dealt with the control of nonlinear, nonholonomic systems. Inverse dynamics control formed the basis of the all the control strategies which were designed.

First a system configuration concerning a disk, a controlled rod and two overhead rotors was considered. It was shown that by applying two successive inverse dynamics control laws it is possible to separate the kinematics of the system from the dynamics of the system. This enables the design of control strategies which directly controls the motion of the system.

A feedback tracking controller was designed which stabilised the motion of the disk and asymptotically track any given smooth reference path. It was later shown that the controller was robust under small parametric variations. It was also shown that the system is path controllable and a controller was designed which stabilised the disk while moving it from any initial point to any final point in a given finite time interval.

Extended inverse dynamics control was introduced and an example concerning an articulated crane was solved. The crane system is underactuated and by applying an extended inverse dynamics control law the system was split into a completely controllable linear decoupled system together with a complementary nonlinear part which is

not independently controllable. A feasible control strategy was then used to calculate the control inputs which moved the crane from an initial to a final position in a given finite time interval while insuring that the uncontrollable variable remains within the problem specifications during the motion of the crane.

Three publications has resulted from this work. The tracking controller designed in chapter 3 was also dealt with in [32]. The work on path controllability presented in chapter 4 was described in more detail in [35]. The articulated crane as an application of extended inverse dynamics control (chapter 6) was dealt with in [45].

It was thus found that inverse dynamics control is a very effective method for the control of nonlinear, nonholonomic systems. Furthermore the method is theoretically simple and easy to apply and also works well on underactuated systems where only part of the system can be controlled.

Bibliography

[1] B. Friedland, *Control System Design*, McGraw-Hill, New York, N.Y., 1987.

[2] F.M. Callier and C.A. Desoer, *Linear System Theory*, Springer - Verlag, New York, 1991.

[3] H. Goldstein, *Classical Mechanics*, Addison-Wesley, second edition, 1980.

[4] E.T. Whittaker, *A Treatise on the Analytical Dynamics of Particles and Rigid bodies*, Cambridge University Press, Cambridge, UK, 1917.

[5] Y. Yavin and C. Frangos, "Open loop strategies for the control of a disk rolling on a horizontal plane," *Computer methods in applied mechanics and engineering*, vol. 127, pp. 227–240, 1995.

[6] Y. Yavin, G.W. Ehlers, and C. Frangos, "Closed-loop control of the motion of a sphere rolling on a moving horizontal plane," *Journal of Optimization Theory and Applications*, vol. 92, no. 2, pp. 377–391, 1997.

[7] Y. Yavin, "Open-loop control laws for a vehicle towing three trailers," *Mathematical and Computer Modelling*, vol. 30, pp. 199–209, 1999.

[8] I. Kolmanovsky and N.H. McClamroch, "Developments in nonholonomic control problems," *IEEE Control Systems*, vol. 15, no. 6, pp. 20–36, 1995.

[9] D.G. Luenberger, *Introduction to Dynamic Systems*, John Wiley & Sons, New York, 1979.

[10] W.J. Rugh, "Analytical framework for gain scheduling," *IEEE Control Systems*, vol. 11, no. 1, pp. 79–84, 1991.

[11] A.J. Krener, "On the equivalence of control systems and the linearization of nonlinear systems," *SIAM J. Control*, vol. 11, no. 4, pp. 670–676, 1973.

[12] L.R. Hunt, R. Su, and G. Meyer, "Global transformations of nonlinear systems," *IEEE Trans. Automat. Contr.*, vol. AC-28, no. 1, pp. 24–30, 1983.

[13] A. Isidori, *Nonlinear Control Systems*, Springer - Verlag, London, 1995.

[14] H. Nijmeijer and A.J. van der Schaft, *Nonlinear Control Systems*, Springer - Verlag, New York, 1990.

[15] C. Reboulet and C. Champetier, "A new method for linearizing non-linear systems: the pseudolinearization," *Int. J. Control*, vol. 40, no. 4, pp. 631–638, 1984.

[16] J. Wang and W.J. Rugh, "Feedback linearization families for nonlinear systems," *IEEE Trans. Automat. Contr.*, vol. AC-32, no. 10, pp. 935–940, 1987.

[17] M.W. McConley, "Computational complexity of Lyapunov stability analysis problems for a class of nonlinear systems," *SIAM J. Control Optim.*, vol. 36, no. 6, pp. 2176–2193, 1998.

[18] A.M. Bloch, M. Reyhanoglu, and N.H. McClamroch, "Control and stabilization of nonholonomic dynamic systems," *IEEE Trans. Automat. Contr.*, vol. 37, no. 11, pp. 1746–1757, 1992.

[19] C. Samson, "Control of chained systems application to path following and time-varying point-stabilization of mobile robots," *IEEE Trans. Automat. Contr.*, vol. 40, no. 1, pp. 64–77, 1995.

[20] J. Luo and P. Tsiotras, "Exponentially convergent control laws for nonholonomic systems in power form," *Systems Control Lett.*, vol. 35, pp. 87–95, 1998.

[21] J.A. Reeds and L.A. Shepp, "Optimal paths for a car that goes both forward and backwards," *Pacific J. Mathematics*, vol. 145, no. 2, pp. 367–393, 1990.

[22] J.P. Laumond, P.E. Jacobs, M. Taix, and R.M. Murray, "A motion planner for nonholonomic mobile robots," *IEEE Trans. Robotics Automat.*, vol. 10, no. 5, pp. 577–593, 1994.

[23] O.J. Sordalen, "Exponential control law for a mobile robot: Extension to path following," *IEEE Trans. Robotics Automat.*, vol. 9, no. 6, pp. 837–842, 1993.

[24] A.M. Bloch and P.E. Crouch, "Newton's law and integrability of nonholonomic systems," *SIAM J. Control Optim.*, vol. 36, no. 6, pp. 2020–2039, 1998.

[25] G.W. Ehlers, Y. Yavin, and C Frangos, "On the motion of a disk rolling on a horizontal plane: Path controllability and feedback control," *Computer methods in applied mechanics and engineering*, vol. 137, pp. 345–356, 1996.

[26] Y. Yavin, "Inclination control of the motion of a rolling disk by using a rotor," *Computer methods in applied mechanics and engineering*, vol. 146, pp. 253–263, 1997.

[27] Y. Yavin, "Inclination control of the motion of a rolling disk by using a rotor fixed along its axis," *Dynamics of Continuous, Discrete and Impulsive Systems*, vol. 4, no. 1, pp. 47–65, 1998.

[28] Y. Yavin, "Directional control of the motion of a rolling disk by using an overhead rotor," *Dynamics of Continuous, Discrete and Impulsive Systems*, in press.

[29] Y. Yavin and P.D. Kemp, "Modelling and control of the motion of a rolling disk: Effect of motor dynamics on the dynamical model," *Computer methods in applied mechanics and engineering*, vol. 188, pp. 613–624, 2000.

[30] Y. Yavin and C. Frangos, "Closed-loop control of the motion of a disk - rod system," *Journal of Optimization Theory and Applications*, vol. 96, no. 2, pp. 453–473, 1998.

[31] J. Mathews and R.L. Walker, *Mathematical methods of physics*, W.A. Benjamin, INC., New York, second edition, 1970.

[32] P.D. Kemp and Y. Yavin, "Stabilization and control of the motion of a rolling disk by using two overhead rotors," *Computers and Mathematics with Applications*, vol. 39, pp. 237–252, 2000.

[33] J.-J.E. Slotine and W. Li, *Applied nonlinear control*, Prentice-Hall, 1991.

[34] Y. Yavin, "Stabilization and control of the motion of a rolling disk," *Mathematical and Computer Modelling*, vol. 29, pp. 45–54, 1999.

[35] P.D. Kemp and Y. Yavin, "Stabilization and path controllability of the motion of a rolling disk by using two overhead rotors," *The Journal of The Franklin Institute*, vol. 337, pp. 147–169, 2000.

[36] G. Walsh, D. Tilbury, R. Murray, and J.P. Laumond, "Stabilization of trajectories for systems with nonholonomic constraints," *IEEE Trans. Automat. Contr.*, vol. 39, no. 1, pp. 216–222, 1994.

[37] S. Gutman and Z. Palmor, "Properties of min-max controllers in uncertain dynamical systems," *SIAM J. Control and Optim.*, vol. 20, no. 6, pp. 850–861, 1982.

[38] M.J. Corless and G. Leitmann, "Continuous state feedback guaranteeing uniform ultimate boundedness for uncertain dynamic systems," *IEEE Trans. Automat. Contr.*, vol. 26, no. 5, pp. 1139–1144, 1981.

[39] J.-J. E. Slotine, "Sliding controller design for non-linear systems," *Int. J. Control*, vol. 40, no. 2, pp. 421–434, 1984.

[40] J.-J. E. Slotine, "Adaptive sliding controller synthesis for non-linear systems," *Int. J. Control*, vol. 43, no. 6, pp. 1631–1651, 1986.

[41] D.G. Taylor et al., "Adaptive regulation of nonlinear systems with unmodeled dynamics," *IEEE Trans. Automat. Contr.*, vol. 34, no. 4, pp. 405–412, 1989.

[42] Y. Yavin, "An extended inverse dynamics control," *Applied Mathematics Letters*, vol. 12, pp. 59–62, 1999.

[43] Y. Yavin, "Control of a rotary inverted pendulum," *Applied Mathematics Letters*, vol. 12, pp. 131–134, 1999.

[44] C.I. Byrnes and A. Isidori, "On the attitude stabilization of rigid spacecraft," *Automatica*, vol. 27, no. 1, pp. 87–95, 1991.

[45] Y. Yavin and P.D. Kemp, "On the application of extended inverse dynamics control," *Computers and Mathematics with Applications*, vol. 40, pp. 669–677, 2000.

[46] Y. Yavin, C. Frangos, G. Zilman, and T. Miloh, "Computation of feasible command strategies for the navigation of a ship in a narrow zigzag channel," *Computers and Mathematics with Applications*, vol. 30, no. 10, pp. 79–101, 1995.

[47] Y. Yavin and C. Frangos, "On the control of a constrained multibody system," *Computer methods in applied mechanics and engineering*, vol. 167, pp. 119–126, 1998.

[48] J.A. Snyman, "A new and dynamic method for unconstrained minimization," *Appl. Math. Modelling*, vol. 6, pp. 449–462, 1982.

[49] J.A. Snyman, "An improved version of the original leap-frog dynamic method for unconstrained minimization: LFOP1(b)," *Appl. Math. Modelling*, vol. 7, pp. 216–218, 1983.

[50] Y. Yavin, C. Frangos, and T. Miloh, "Computation of feasible control trajectories for the navigation of a ship around an obstacle in the presence of a sea current," *Mathematical and Computer modelling*, vol. 21, no. 3, pp. 99–117, 1995.

Appendix A

The components of $\boldsymbol{h}(\boldsymbol{q},\boldsymbol{p})$ from equation (2.60) are given by

$$\begin{aligned} h_1(\boldsymbol{q},\boldsymbol{p}) = {} & I_{o1}^{(2)}\left(2\frac{d\theta}{dt}\frac{d\alpha_2}{dt}\sin\alpha_2\cos\alpha_2 + \frac{d\phi}{dt}\frac{d\alpha_2}{dt}\sin^2\alpha_2\cos\theta\right) \\ & + I_{o1}^{(2)}\left(\frac{d\theta}{dt}\frac{d\phi}{dt}\sin\theta\sin\alpha_2\cos\alpha_2 - \frac{d\phi}{dt}\frac{d\alpha_2}{dt}\cos\theta\cos^2\alpha_2\right) \\ & + ma^2\frac{d\phi}{dt}\sin\theta\left(\frac{d\psi_1}{dt} + \frac{d\phi}{dt}\cos\theta\right) - \frac{\partial\mathfrak{L}}{\partial\theta}\,, \end{aligned} \tag{A.1}$$

$$\begin{aligned} h_2(\boldsymbol{q},\boldsymbol{p}) = {} & 2\left(I_{D1} + I_{o1}^{(2)} - I_1 - I_{D3} - ma^2\right)\frac{d\phi}{dt}\frac{d\theta}{dt}\sin\theta\cos\theta \\ & - \left(I_{D3} + m_{o1}aL_{12} + m_{o2}aL_{13}\right)\frac{d\psi_1}{dt}\frac{d\theta}{dt}\sin\theta \\ & - 2I_{o1}^{(1)}\frac{d\phi}{dt}\left(\frac{d\theta}{dt} + \frac{d\alpha_1}{dt}\right)\cos(\theta+\alpha_1)\sin(\theta+\alpha_1) \\ & - 2I_{o1}^{(2)}\frac{d\theta}{dt}\frac{d\alpha_2}{dt}\cos\theta\cos^2\alpha_2 + I_{o1}^{(2)}\left(\frac{d\theta}{dt}\right)^2\sin\theta\sin\alpha_2\cos\alpha_2 \\ & - 2I_{o1}^{(2)}\frac{d\phi}{dt}\left(\frac{d\alpha_2}{dt}\cos^2\theta\sin\alpha_2\cos\alpha_2 + \frac{d\theta}{dt}\sin\theta\cos\theta\cos^2\alpha_2\right)\,, \end{aligned} \tag{A.2}$$

$$h_3(\boldsymbol{q},\boldsymbol{p}) = -\left(I_{D3} + m_{o1}aL_{12} + m_{o2}aL_{13} + 2ma^2\right)\frac{d\phi}{dt}\frac{d\theta}{dt}\sin\theta\,, \tag{A.3}$$

$$h_4(\boldsymbol{q},\boldsymbol{p}) = I_{o1}^{(1)}\left(\frac{d\phi}{dt}\right)^2\cos(\theta+\alpha_1)\sin(\theta+\alpha_1)\,, \tag{A.4}$$

$$
\begin{aligned}
h_5(\boldsymbol{q},\boldsymbol{p}) = & -I_{o1}^{(2)}\frac{d\phi}{dt}\frac{d\theta}{dt}\cos\theta \\
& - I_{o1}^{(2)}\left(\frac{d\theta}{dt}\sin\alpha_2 - \frac{d\phi}{dt}\cos\alpha_2\cos\theta\right) \\
& \times \left(\frac{d\theta}{dt}\cos\alpha_2 + \frac{d\phi}{dt}\sin\alpha_2\cos\theta\right),
\end{aligned} \tag{A.5}
$$

where

$$
\begin{aligned}
\frac{\partial \mathfrak{L}}{\partial\theta} = & (I_{D1} - I_1)\left(\frac{d\phi}{dt}\right)^2 \sin\theta\cos\theta \\
& - I_{D3}\frac{d\phi}{dt}\sin\theta\left(\frac{d\psi_1}{dt} + \frac{d\phi}{dt}\cos\theta\right) \\
& - (m_{o1}aL_{12} + m_{o2}aL_{13})\frac{d\phi}{dt}\frac{d\psi_1}{dt}\sin\theta \\
& - I_{o1}^{(1)}\left(\frac{d\phi}{dt}\right)^2 \sin(\theta+\alpha_1)\cos(\theta+\alpha_1) \\
& - I_{o1}^{(2)}\frac{d\phi}{dt}\cos\theta\left(\frac{d\alpha_2}{dt} - \frac{d\phi}{dt}\sin\theta\right) \\
& + I_{o1}^{(2)}\frac{d\phi}{dt}\sin\theta\cos\alpha_2\left(\frac{d\theta}{dt}\sin\alpha_2 - \frac{d\phi}{dt}\cos\theta\cos\alpha_2\right) \\
& - \big(a(m_D + m_R) + m_{o1}(a + L_{12}) + m_{o2}(a + L_{13})\big)g\cos\theta\,.
\end{aligned} \tag{A.6}
$$